

Synthesis and Study of a Persistent Selenenic Acid

&

Preliminary Studies of Thiol Oxidation

By

Nathalie Presseau

A thesis submitted to the Department of Chemistry
in conformity with the requirements for the degree of

Master's of Chemistry

University of Ottawa

Ottawa, Ontario, Canada

March 2014

© Nathalie Presseau, Ottawa, Canada, 2014

ABSTRACT

Selenenic acids and other organoselenium compounds are important both in organic and biochemistry. In organic chemistry, *syn*-elimination of selenoxides is used to prepare alkenes, giving a selenenic acid by-product. In biochemistry, selenocysteine is catalytically active in a variety of selenoenzymes, which have antioxidant properties, and is oxidized to a selenenic acid intermediate. For example, glutathione peroxidase (GPx) plays a role in fighting oxidative damage by catalyzing the reduction of hydroperoxides.

Previous studies have shown that the lighter chalcogen analogue of selenenic acid, sulfenic acid, is a powerful antioxidant and that the known antioxidant activity of garlic is attributable to the 2-propenesulfenic acid derived from the compound allicin. This has prompted questions concerning the role of selenenic acid in the antioxidant activity of organoselenium compounds. In order to study the physiochemical properties of selenenic acids—a functional group about which little is known—and to evaluate their potential as antioxidants, a persistent selenenic acid is needed. Herein, the model compound, 9-triptyceneselenenic acid, is prepared by a previously reported procedure and a new pathway is designed, such that its properties and reactivity can be studied.

The oxidation of thiols is important in cell signalling, leading to the disulfide bonds implicated in post-translational modification, among other biological roles. While this reaction is presumed to occur through the reaction of thiol with an oxidant that forms sulfenic acid, and from a subsequent reaction of sulfenic acid with another thiol, sulfenic acids are so reactive that they are not usually seen as intermediates. Given the stability of the 9-triptycenesulfenic acid previously synthesized, preliminary kinetic study of the oxidation of 9-triptycenesulfenic acid to its corresponding sulfenic acid is made possible.

ACKNOWLEDGEMENTS

Firstly, I am very grateful to Professor Derek Pratt for offering me a position in his group and for teaching me so much in these two years. Through many discussions, I observed, and learned from, his extraordinary intelligence, critical thinking and scientific integrity. I have been fortunate to work with him and to learn so much about chemistry from him.

My colleagues in the Pratt lab have been a big part of my life in these past two years. They have all been helpful, sharing some of their best chemistry tips and tricks. Through much time spent together and over many beers, they have also opened my eyes to many things and helped me clarify my goals. I am especially grateful to the close friends I've made in the department, Meghan Haycock, Melissa MacDonald and Kevin Stamplecoskie, have been unbelievably supportive when I was going through the worst and continue to motivate and encourage me. I am also indebted to Tito Scaiano, who gave me my start in chemistry, accepting me in his group as an honours student. He has always believed in me as a chemist and as a person. His continued encouragement and mentorship, even after I moved on from his lab, has been incredibly helpful and heart-warming.

My friends and family are the real superstars of this endeavour. I literally would not have made it to the end if it weren't for their unwavering support, at all hours of the day and night, through all kinds of problems. Marisa and Marika, I thank you both for tolerating and answering countless email, text and phone call rants. You both mean the world to me; when I needed you most you were there, helping me in every way you could. Mom and Dad, you have been the perfect supporters as

always. I cannot even begin to thank you enough for everything you do. From wake-up calls to lovingly made Sunday dinners, your encouragement and constant reminders of your love and faith in me you've helped me in every way. Finally, to all my other friends, teammates, and family members who have supported and stood by me through this experience, thank you for the welcome reminders of life outside the lab and of how good and kind people can be.

STATEMENT OF ORIGINALITY

I hereby certify that all of the work described within this thesis is the original work of the author, with the following exceptions: Synthesis of the 9-triptycenesulfenic acid and 9-triptycenesulfonic acid used for studies described in Chapter 4 was performed by undergraduate students Andrew Ingold and Jazmin Bansagi respectively; EPR experiments were carried out by Charles O'Neil-Crites, a graduate student in Dr. Scaiano's research group; and additional EPR and inhibited autoxidation experiments were conducted by Dr. Luca Valgimigli at the University of Bologna.

Nathalie Presseau

2014

TABLE OF CONTENTS

Abstract	II
Acknowledgements	III
Statement of Originality	V
Table of Contents	VI
List of Schemes	IX
List of Figures	XII
List of Abbreviations	XVIII
Chapter 1 - Introduction to Oxidation, Sulfenic and Selenenic Acids	1
1.1 Reactive Oxygen Species and Lipid Peroxidation	1
1.2 Antioxidants	4
1.3 Sulfenic Acids.....	9
1.3.1 Thiosulfinates from Alliums	9
1.3.2 Sulfenic Acid Stability	12
1.4 Selenenic Acids.....	14
1.4.1 Selenenic Acids in Organic Synthesis.....	17
1.4.2 Selenenic Acid Stability.....	18
1.5 Hydrogen Atom Transfer	29
1.6 Research Objectives	24
1.7 References.....	25

Chapter 2 – Synthesis of a Persistent Selenenic Acid	29
2.1 Introduction	29
2.2 Results and Discussion	35
2.2.1 Attempts to Repeat the Ishii 9-triptyceneselenenic Acid Synthesis.....	35
2.2.2 New Synthetic Approach to 9-triptyceneselenenic Acid.....	41
2.2.3 Study of 9-triptycene(phenethyl)selenoxide <i>syn</i> -elimination	49
2.3 Conclusion.....	55
2.4 Experimental Procedures.....	56
2.5 References.....	63
Chapter 3 – Study of a Persistent Selenenic Acid	65
3.1 Introduction	65
3.2 Results and Discussion	66
3.2.1 Electrochemistry.....	66
3.2.2 Electron Paramagnetic Resonance	71
3.2.3 Antioxidant Activity.....	74
3.3 Conclusion.....	86
3.4 Experimental Procedures.....	88
3.5 References.....	90

Chapter 4 – Preliminary Studies of Thiol Oxidation	93
4.1 Introduction	93
4.2 Results and Discussion	97
4.2.1 Preliminary Data on the Oxidation of 9-Triptycenethiol	97
4.2.2 Oxidation in Basic Methanol Buffers	101
4.2.3 Reaction Profiles Monitored by LC/MS.....	111
4.3 Conclusion.....	116
4.4 Experimental Procedures.....	117
4.5 References.....	119

LIST OF SCHEMES

Scheme 1.1 Degradation of superoxide to other ROS.....	1
Scheme 1.2 General mechanism of hydrocarbon autoxidation.....	2
Scheme 1.3 Conversion of non-proteogenic amino acid, alliin to the thiosulfinate allicin and sulfenic acid.....	10
Scheme 1.4 Mechanism of radical trapping as proposed by Okada (A) ²⁰ and Pratt (B) ²¹	11
Scheme 1.5 Solvent effects A) allicin decomposition to sulfenic acid prevented by hydrogen bonding to HFIP and B) radical-trapping slowed by hydrogen bonding of sulfenic acid to MeCN.....	12
Scheme 1.6 Reaction of two sulfenic acids, one acting as nucleophile, the other as electrophile, to form a thiosulfinate.....	13
Scheme 1.7 Catalytic cycle of glutathione peroxidase.....	16
Scheme 1.8 General procedure for preparation of alkenes using selenoxide <i>syn</i> - elimination.....	17
Scheme 1.9 Proton-coupled electron transfer mechanism vs. hydrogen atom transfer mechanism for reaction of selenenic acid with peroxy radical.....	23
Scheme 2.1 Reactions of selenenic acid that may contribute to its lack of persistence; oxidation (2.1), disproportionation (2.2), and self-condensation (2.3).	29
Scheme 2.2 Persistent areneselenenic acids. ⁴ ,	30
Scheme 2.3 2,4,6- <i>tri-tert</i> -butylbenzeneselenenic acid and the equilibrium between selenoseleninate and selenenic acid demonstrated by formation of methylselenenate (Ar = 2,4,6- <i>tri-tert</i> -butylphenyl). ⁷	31

Scheme 2.4 Novel Bmt (bowl-type) selenenic acid and its regeneration cycle from selenol and thioselenide. Reprinted with permission from Goto, K.; Nagahama, M.; Mizushima, T.; Shimada, K.; Kawashima, T.; Okazaki, R. <i>Org. Lett.</i> 2001, 3, 3569–3572. . Copyright 2001 American Chemical Society. ⁹	33
Scheme 2.5 A) GPx Selenocysteine oxidation to an aliphatic selenenic acid by hydrogen peroxide, B) target aliphatic selenenic acid, 2,2-dimethylbenzoylethylselenenic acid , C) product selenoseleninate. ⁴	34
Scheme 2.6 9-Triptyceneselenenic acid synthesis as reported by Ishii <i>et al.</i> ¹⁰	36
Scheme 2.7 Synthesis of 9-bromotriptycene.....	36
Scheme 2.8 Mechanism for formation of benzyne and cycloaddition to anthracene to form triptycene.....	37
Scheme 2.9 Synthesis of <i>bis</i> -triptycenetriselenide	37
Scheme 2.10 Radical mechanism for formation of triptycene (Trp) initiated by reaction of 9-lithiumtriptycene with elemental selenium (Se ₈)	39
Scheme 2.11 Reported synthesis of 9-triptycene(<i>n</i> -butyl)selenide.....	40
Scheme 2.12 New retrosynthetic approach to TrpSeOH.....	42
Scheme 2.13 Synthesis of <i>bis</i> -phenethyl diselenide.....	43
Scheme 2.14 Synthesis of 9-triptycene(phenethyl)selenide.....	44
Scheme 2.15 Oxidation and <i>syn</i> -elimination of styrene and TrpSeOH from selenoxide.	45
Scheme 2.16 New synthesis of TrpSeOH.....	48
Scheme 2.17 Selenoxide (SeOx) <i>syn</i> -elimination reaction	50

Scheme 2.18 ^1H NMR (Top) and ^{13}C NMR (bottom) of 9-triptycene(phenethyl) selenide	83
Scheme 2.19 ^1H NMR (Top) and ^{13}C NMR (Bottom) of 9- triptycene(phenethyl)selenoxide	84
Scheme 3.1 Oxidation of either TrpSeOH or TrpSOH produces a radical cation species, which rapidly undergoes further chemistry, precluding reduction back to the original species.	68
Scheme 3.2 REqEPR of TrpSeOH with BHT to determine SeO-H BDE from K_{eq} Equation for BDE (TrpSeOH) is dependant on the assumption that the entropy change for the radical equilibration is negligible.	71
Scheme 3.3 Inhibition of radical autoxidation by phenolic antioxidant.....	75
Scheme 4.4 Possible reaction of TrpSOH and TrpSH to 1,2-di-9-triptycenedisulfide	96
Scheme 4.1 Unlikely equilibrium between triptycenesulfenic acid and hydrogen peroxide, and triptycenesulfenic acid and water. Bond strengths of S-H, O-O, S-O and O-H bonds needing to be broken for the equilibrium	105
Scheme 4.2 Possible mechanism of amine base reaction with sulfenic acid.....	106
Scheme 4.3 Reaction of peroxy carbonate with TrpSH.....	109
Scheme 4.4 Reaction of deprotonated triptycene thiol and sulfenic acid with H_2O_2	116

LIST OF FIGURES

Figure 1.1 Two possible mechanism by which antioxidants inhibit free radical autoxidation, adapted from the Encyclopedia of Radicals in Chemistry, Biology and Materials	4
Figure 1.2 Inhibition by phenolic antioxidants through radical trapping, and termination.....	6
Figure 1.3 Representation of a typical profile of oxygen-uptake during uninhibited autoxidation (1); a modest antioxidant (2); and autoxidation in the presence of a strong antioxidant where τ indicates the time of full antioxidant depletion(3); adapted from the Encyclopedia of Radicals in Chemistry, Biology and Materials ¹⁰	7
Figure 1.4 Oxidation states of protein cysteine thiols <i>in vivo</i> . ¹⁴	8
Figure 1.5 Formation of disulfide bond by ROS such as H ₂ O ₂ through sulfenic acid intermediate.	9
Figure 1.6 Examples of persistent sulfenic acids. ^{25,26,27,28,29}	14
Figure 1.7 Examples of the many GPx mimics divided in three categories. ⁴²	17
Figure 1.8 Examples of persistent selenenic acids. ^{45,46}	18
Figure 1.9 Benzyl/toluene (left): (A) the geometry and (B) the SOMO at the HAT transition structure. Phenoxy/phenol (right): (A) geometry of the hydrogen-bonded complex, (B) the geometry and (C) the SOMO at the PCET transition structure. Reproduced with permission from Mayer, J.M.; Hrovat, D.A.; Thomas, J.L.; Borden, W.T., <i>J. Am. Chem. Soc.</i> , 2002, 124, 11142-11147. Copyright 2002 American Chemical Society. ⁴⁸	19

Figure 1.10 Structure of the cis and trans transition states of the *tert*-butylperoxyl/phenol couple with their respective HOMO and SOMO. The oxygen lone pair-ring π -orbital net bonding overlap in the cisoid TS allows the H exchange to proceed by a multi-center PCET mechanism. Reprinted with permission from DiLabio, G.A.; Johnson, E.R., *J. Am. Chem. Soc.*, 2007, 129, 6199-6203. Copyright 2007 American Chemical Society.....20

Figure 1.11 a) Cisoid and b) transoid transition-state structures for the HSOH/ \bullet OOH reaction c) The four highest occupied molecular orbitals of the structure in (a) showing the overlap between the sulfenic acid S atom and the internal peroxy O atom. Reprinted with permission from Vaidya, V.; Ingold, K.U.; Pratt, D.A., *Angew. Chem. Intl. Ed.*, 2009, 48, 157-160. Copyright 2009 Wiley.²¹.....22

Figure 2.1 Stable selenenic acid, 1,4-bridgedcalix[6]arene selenenic acid and its X-Ray crystal structure indicating the selenenic acid moiety buried in the bulky bowl-type structure. Reprinted with permission from Goto, K.; Saiki, T.; Okazaki, R. *Phosphorus, Sulfur Silicon Relat. Elem.* 1998, 136:1, 475-487. Copyright 1998 Taylor and Francis. ⁸.....32

Figure 2.2 9-Triptyceneselenenic acid and its X-Ray crystal structure. Reprinted with permission from Ishii, A.; Matsubayashi, S.; Takahashi, T.; Nakayama, J. *J. Org. Chem.* 1999, 64, 1084-1085. Copyright 1999 American Chemical Society.¹⁰.....35

Figure 2.3 Kinetic ¹H NMR of 10 mM selenoxide (δ 5.03 ppm, SeOx) *syn*-elimination of selenenic acid (δ 5.17 ppm, SeOH) and condensation to selenoseleninate (δ

5.15 & 5.20 ppm, SeOSe), in d_6 -benzene at 25°C monitored by integration of characteristic bridgehead protons. The signal at δ 5.21 ppm represents an unknown and unchanging impurity in the reaction.....	46
Figure 2.4 ^1H NMR (300 MHz, CDCl_3) of TrpSeOx (δ 5.36 ppm) as the major product with TrpSeOH (δ 5.42 ppm) and styrene (δ 5.25 & 5.76 ppm) in a 2:1:1 ratio. Solvent (CH_2Cl_2 , δ 5.30 ppm) is still present in this sample, along with unknown impurities at δ 5.41 ppm and δ 5.37 ppm.....	48
Figure 2.5 First order decay of TrpSeOx <i>syn</i> -elimination of TrpSeOH and self-condensation to selenoseleninate in d_6 -benzene. Monitored by ^1H NMR with bridgehead protons, TrpSeOx 5.03 ppm, TrpSeOH 5.17 ppm, selenoseleninate 5.15 and 5.20 ppm.....	51
Figure 2.6 First order decay of selenoxide <i>syn</i> -elimination of selenenic acid and self-condensation to selenoseleninate in d_3 -chloroform. Monitored by ^1H NMR with bridgehead protons, TrpSeOx 5.37 ppm, TrpSeOH 5.42 ppm, selenoseleninate 5.48 and 5.49 ppm.....	53
Figure 2.7 First order decay of selenoxide <i>syn</i> -elimination of selenenic acid and self-condensation to selenoseleninate in d_3 -acetonitrile	54
Figure 3.1 Cyclic voltammogram corresponding to the oxidation of TrpSeOH (generated <i>in situ</i> from a 5.0 mM solution of TrpSeOX) acetonitrile containing 0.1 M Bu_4PF_6 as supporting electrolyte at a scan rate of 100 mV/s.....	67
Figure 3.2 Cyclic voltammograms corresponding to the oxidation of TrpSeOH (generated <i>in situ</i> from a 5.0 mM solution of TrpSeOX) in acetonitrile containing	

0.1 M Bu ₄ PF ₆ as supporting electrolyte and (left) 2.5 mM Bu ₄ NOH at a scan rate of 100 mV/s and (right) 10 mM Bu ₄ NOH at a scan rate of 100 mV/s.....	69
Figure 3.3 Cyclic voltammograms corresponding to the oxidation of 5 mM TrpSOH in MeCN containing 0.1 M Bu ₄ PF ₆ as supporting electrolyte and no additive (black), (b) 30 mM CF ₃ SO ₃ H (red), or (c) 5 mM Bu ₄ NOH (blue) at a scan rate of 100 mV/s. Reprinted with permission from McGrath, A.J.; Garrett, G.E.; Valgimigli, L.; Pratt, D.A., <i>J. Am. Chem. Soc.</i> 2010, 132, 16759-16761. Copyright 2010 American Chemical Society. ¹	70
Figure 3.4 EPR spectrum of TrpSO• from irradiation of TrpSOH with 10% v/v di- <i>tert</i> -butylperoxide in the absence of O ₂ . g value = 2.01199.	73
Figure 3.6 Illustration of energy diagrams of the orbitals involved in photoinduced electron transfer mechanism, the HOMO and LUMO of the fluorophore (* indicates excited state) and the HOMO of the donor quenched and fluorescent modes. Reprinted with permission from Schaferling, M.; Grogel, D. B. M.; Schreml, S. <i>Microchimica Acta</i> 2011, 174, 1. Copyright 2011 Springer.	77
Figure 3.7 Illustration of liposomes bilayers made from egg phosphatidylcholine with hydrophilic (A) or hydrophobic (B) radical initiators.	79
Figure 3.7 Fluorescence (at 520 nm) intensity–time profiles from MeOAMVN-mediated (0.2 mM) oxidations of egg phosphatidylcholine liposomes (1 mM) containing 0.15 mM H ₂ B-PMHC and increasing concentrations of 9-triptycenesulfenic acid (C) or PMHC (D). Reprinted with permission from Zheng, F.; Pratt, D.A., <i>Chem. Commun.</i> , 2013, 49, 8181-8183. Copyright 2013 American Chemical Society.	81

Figure 3.8 Fluorescence intensity–time profiles recorded in 1 mM egg phosphatidylcholine liposomes with increasing concentrations of TrpSeOx and ABAP (top), or MeOAMVN (bottom), showing no inhibition period.....	82
Figure 3.9 Fluorescence intensity–time profiles recorded in 1 mM egg phosphatidylcholine liposomes with increasing concentrations of TrpSeEtPh and ABAP (top), or MeOAMVN (bottom), showing no inhibition period.....	84
Figure 3.10 Fluorescence intensity–time profiles recorded in 1 mM egg phosphatidylcholine liposomes with increasing concentrations of TrpSeOH and ABAP (top), or MeOAMVN (bottom), showing no inhibition period.....	85
Figure 4.1 Possible reaction pathways for oxidation of protein cysteine thiols in vivo. Adapted with permission from Paulsen, C. E.; Carroll, K.S., ACS Chem. Biol., 2010, 5, 1, 47-62. Copyright 2010 American Chemical Society. ⁵	94
Figure 4.2 Strategies for detecting sulfenic acids in proteins using either dimedone- based affinity probes or fluorescent-tagged reagents. Reproduced from Seo, Y.H.; Carroll, K.S., <i>Proc. Natl. Acad. Sci.</i> , 2009, 61, 16163-16168. Copyright 2009 The National Academy of Science. ⁶	95
Figure 4.3 AM1 energy minimized structure of <i>bis</i> -tritycenedisulfide showing C-S- S-C bond angle of 180° and adverse interaction of peri hydrogens.	97
Figure 4.4 ¹ H NMR (300 MHz) of thiol oxidation (50 mM) by H ₂ O ₂ -urea complex (50 mM) in <i>d</i> ₃ -MeOH at 25°C. Decay of TrpSH and growth of TrpSOH and TrpSO ₃ H is monitored by their respective bridgehead protons at time zero (A), 30 minutes (B), 5 hours (C) and 3 days (D).....	98

Figure 4.5 Reaction of TrpSH with 2 equivalents (top) and 10 equivalents (bottom) of H₂O₂ (30% in water) in MeOH containing 20 mM Et₃N buffer at 25°C over the course of a day. Initial rate for reaction with 2 equivalents (top) d[TrpSH]/dt = 2.7 x 10⁻⁵ mM/s and d[TrpSOH]/dt = 3.4 x 10⁻⁵ x 10 mM/s. Initial rate for reaction with 10 equivalents (bottom) d[TrpSH]/dt = 8.9 x 10⁻⁵ mM/s and d[TrpSOH]/dt = 4.0 x 10⁻⁵ x 10 mM/s..... 102

Figure 4.6 Reaction of TrpSH with 2 equivalents of H₂O₂ (30% in water) MeOH containing 20 mM TMP at 25°C over a period of 5 hours..... 103

Figure 4.7 Reaction of TrpSOH with Et₃N (20 mM) in MeOH at 25 °C. Initial rate for TrpSOH decay = 3.96 x 10⁻⁶ mM/s and for TrpSH growth = 2.05 x 10⁻⁶ x 10 mM/s..... 106

Figure 4.8 Reaction of sulfenic acid with TMP (20 mM) in MeOH at 25 °C. Initial rate for TrpSOH decay = 8.36 x 10⁻⁶ mM/s and for TrpSH growth = 1.94 x 10⁻⁶ x 10 mM/s..... 107

Figure 4.9 Reaction of TrpSH with 10 equivalents of peroxy carbonate (H₂O₂ + NaHCO₃) in MeOH. Initial rate for TrpSH decay = 3.15 x 10⁻⁶ mM/s and for TrpSOH growth = 8.14 x 10⁻⁷ x 10 mM/s..... 110

Figure 4.10 Mass spectral chromatograms of the products of a TrpSH oxidation: TrpSO₃H (top), TrpSO₂H (2nd from top), TrpSOH (3rd from top), and starting material TrpSH (bottom) from LC/MS analysis with 20% H₂O/MeOH mobile phase, flow rate 0.2 mL/min, Acquity C₁₈ 1.7µm 2.1 x 50 mm column and MS detection (ESI⁻) at m/z of 333, 317, 301, and 285..... 112

Figure 4.11 Standard curve for TrpSH using the internal standard phenol, for TrpSH sample concentrations from 10 to 30 μM	112
Figure 4.12 Standard curve TrpSOH using the internal standard phenol, or TrpSOH sample concentrations from 10 to 30 μM	113
Figure 4.13 Standard curves for TrpSO ₃ H using the internal standard phenol, for TrpSO ₃ H sample concentrations from 10 to 30 μM	113
Figure 4.15 Reaction of TrpSH with 10 equivalents of peroxy carbonate ($\text{H}_2\text{O}_2 + \text{K}_2\text{CO}_3$) in MeOH showing decay of TrpSH and growth of TrpSOH and TrpSO ₃ H. TrpSO ₂ H was also produced but could not be plotted because no authentic material has been synthesised in order to generate a standard curve.	114

LIST OF ABBREVIATIONS

α -TOH	α -tocopherol
ABAP	2,2'-azobis(2- amidinopropane)monohydrochloride
BDE	Bond Dissociation Enthalpy
BHT	2,6-di- <i>tert</i> -butyl-4-methylphenol
Bmt	4- <i>t</i> -butyl-2,6- <i>bis</i> [2,2'',6,6''-tetramethyl]phenyl
CV	Cyclic Voltammetry
DCE	1,2-dichloroethane
DMDO	Dimethyldioxirane
DMF	Dimethylformamide
EggPC	L- α -phosphocholine
EPR	Electron Paramagnetic Resonance
GPx	Glutathione peroxidase

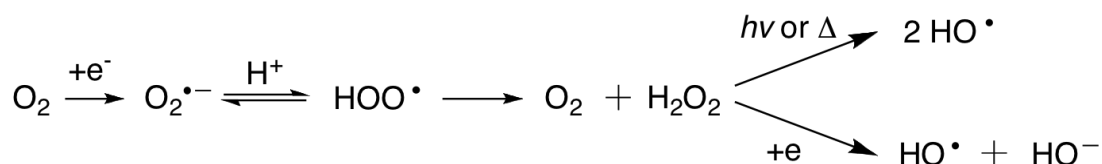
GSH	Glutathione
HAT	Hydrogen Atom Transfer
HFIP	Hexa fluoro isopropanol
HPLC	High Pressure Liquid Chromatography
LAH	Lithium Aluminium Hydride
<i>m</i> CPBA	<i>meta</i> -chloroperbenzoic acid
MeOAMVN	2,2'-azobis(4-methoxy-2,4-dimethyl valeronitrile)
OUA	Oxygen Uptake Apparatus
PCET	Proton Coupled Electron Transfer
PET	Photoinduced Electron Transfer
PMHC	2,2,5,6,7-pentamethyl-6-hydroxychromanol
REqEPR	Radical Equilibrium Electron Paramagnetic Resonance
ROS	Reactive Oxygen Species
SeOSe	<i>bis</i> -9-triptyceneselenoseleninate
Trp	Triptycene
TrpSeOx	9-triptyene phenethyl selenoxide

CHAPTER 1

INTRODUCTION

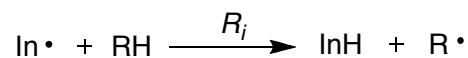
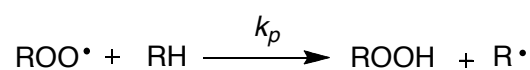
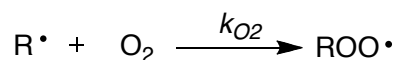
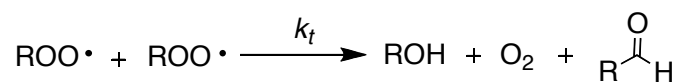
1.1 Reactive Oxygen Species and Lipid Peroxidation

Free radicals derived from oxygen, which are reactive oxygen species (ROS), arise naturally in the body as a product of aerobic respiration via the incomplete reduction of molecular oxygen, and also external sources such as ionizing radiation. They play both positive and negative roles in biological systems:¹ while they are implicated in cell signalling and the body's defence against pathogens, it is also believed that they contribute to the pathogenesis of degenerative diseases and to aging overall.² ROS formation generally begins with the formation of superoxide ($O_2^{\bullet-}$) from the one-electron reduction of molecular oxygen, which can lead to other ROS such as hydroperoxyl (HOO^{\bullet}), hydrogen peroxide (H_2O_2) and subsequently hydroxyl radicals (HO^{\bullet}) as in Scheme 1.1. These and other ROS can become too numerous and exceed an organism's antioxidant defence mechanism, causing oxidative stress to occur.



Scheme 1.1 Degradation of superoxide to other ROS

Hydroxyl and hydroperoxyl radicals can initiate radical chain reaction, such as the autoxidation of hydrocarbons illustrated in Scheme 1.2. Here, HO• or HOO• could be the initiating radical, In•, which abstracts a hydrogen atom from a hydrocarbon, leaving a carbon centred radical that reacts rapidly with molecular oxygen to form a peroxy radical. The peroxy radical subsequently abstracts a hydrogen atom from another hydrocarbon propagating the chain until a termination reaction occurs by the reaction of two radicals. As long as the rate of propagation is at least equal to, or greater than, the rate of termination the chain will continue to consume hydrocarbons and yield hydroperoxides.

Initiation*Propagation**Termination*

Scheme 1.2 General mechanism of hydrocarbon autoxidation³

Polyunsaturated fatty acids are especially susceptible to autoxidation due to their labile allylic or bisallylic hydrogen atoms, which can easily be abstracted by free radicals such as HOO• or HO• to initiate a radical chain,⁴ or lipid peroxy radicals, to propagate a chain. The lipid hydroperoxides resulting from this process are important in some biological processes. For example, the cyclooxygenase and

lipoxygenase controlled formations of prostaglandins and leukotrienes are essential in cell signalling and in mediating pain, inflammation and fever.⁵

However, spurious and/or excess production of random lipid hydroperoxides can have severely detrimental effects on cell health. Because of their prominent role in the cell membrane, lipids, if they become oxidized, can significantly alter the constitution of the lipid bilayer and its function. The lipid oxidation products can change the fluidity of the membrane and its permeability to compounds which otherwise would not transfer except by proper channels. The negative impact of lipid peroxidation in the bilayer is increased by the large quantities of lipids in close proximity, which provide an ideal environment for the propagation of lengthy radical chains and a rapid deterioration of the cell membrane.

Lipid peroxidation products have a greater negative effect in cells that either do not, or are slow to regenerate, such as those of the brain and heart tissues, making these organs more susceptible to damage by ROS. Oxidative damage has been linked to Alzheimer's disease, Parkinson's disease and other neurodegenerative diseases. Lipid peroxidation is also implicated in atherosclerosis, which is the primary cause of cardiovascular disease, and in diabetes, in liver and kidney diseases and in carcinogenesis.⁶ Electrophilic carbonyls, such as reactive α,β -unsaturated aldehydes like 4-hydroxynonenal (4-HNE), are oxidative cleavage products of lipid peroxidation, and can cause further damage by reaction with DNA causing replication errors, and with proteins, inducing protein misfolding.^{7,8}

1.2 Antioxidants

Aerobic organisms are equipped with defence mechanisms to protect themselves from damage by ROS. So called antioxidants are classified in two categories: they are either *preventative*, as they slow the initiation of radical chains by eliminating the initiating radical or precursor thereof, or they are *chain-breaking*, as they quench the propagating radicals to end a radical chain.⁹

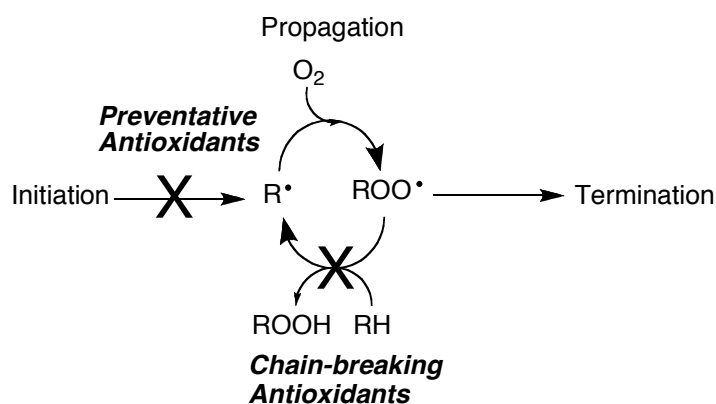
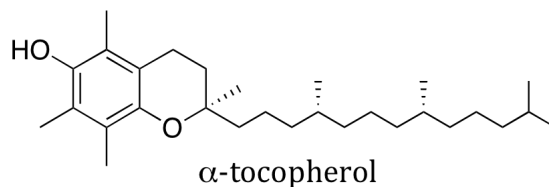


Figure 1.1 Two possible mechanism by which antioxidants inhibit free radical autoxidation, adapted from the Encyclopedia of Radicals in Chemistry, Biology and Materials¹⁰

Arguably the most important antioxidants in the body are enzymatic, such as the family of superoxide dismutases, which act as preventative antioxidants by quenching superoxide while forming H_2O_2 and water, and catalase, which converts H_2O_2 to harmless O_2 and water.¹¹ Other enzymatic antioxidants include glutathione peroxidases (GPx), discussed in more detail later in this chapter, which reduce hydrogen peroxide and/or lipid hydroperoxides using glutathione (GSH) as a cofactor.

The primary chain-breaking antioxidant in the body is vitamin E, a collection of 8 compounds, the most biologically active of which is α -tocopherol, (α -TOH).¹² These and other phenolic antioxidants act by donating a hydrogen atom to peroxy radicals (*cf.* Figure 1.2) with a given inhibition rate constant, k_{inh} . In order for these antioxidant to effectively break the radical chain propagation k_{inh} must be greater than the propagation rate constant, k_p , such that $ROO\bullet$ reacts preferentially with $ArOH$ over another RH . This depends on a facile hydrogen atom transfer, which requires the phenolic antioxidant to have a low O-H bond dissociation enthalpy (O-H BDE). α -TOH has k_{inh} of $3.2 \times 10^6 \text{ M}^{-1}\text{s}^{-1}$ and an O-H BDE of 78.23 kcal/mol,¹³ these favourable properties are due to delocalization of the radical on the phenol ring and the electron donating substituents.



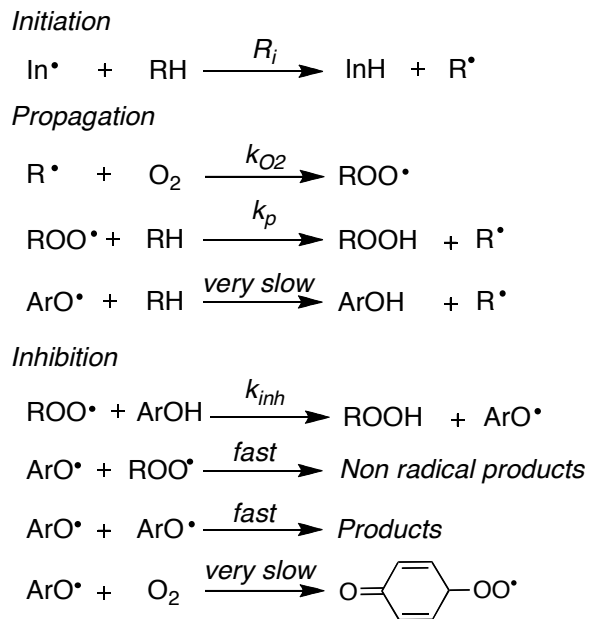


Figure 1.2 Inhibition by phenolic antioxidants through radical trapping, and termination

In inhibited autoxidations monitored by O₂ consumption, strong antioxidants are characterized by complete inhibition of lipid peroxidation until they are depleted and autoxidation resumes. The time at which the antioxidant is fully consumed is indicated as τ in the model oxygen uptake plot in Figure 1.3.

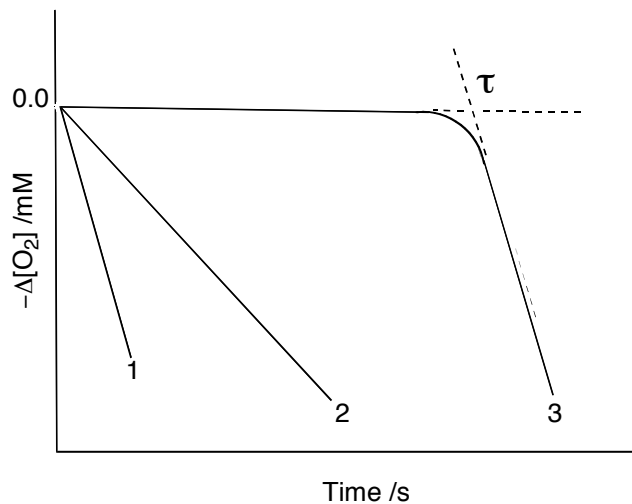


Figure 1.3 Representation of a typical profile of oxygen-uptake during uninhibited autoxidation (1); a modest antioxidant (2); and autoxidation in the presence of a strong antioxidant where τ indicates the time of full antioxidant depletion(3); adapted from the Encyclopedia of Radicals in Chemistry, Biology and Materials¹⁰

1.3 Sulfenic Acids

The most oxidizable amino acid residue is cysteine, which reacts with ROS to yield a multitude of products, including, thiols, disulfides, sulfinic and sulfonic acids as shown in Figure 1.4, all of which are believed to be formed via the intermediacy of a cysteine sulfenic acid.¹⁴ Sulfenic acids are important intermediates in cell signal transduction and they have recently been found to possess potent antioxidant properties.^{14,15}

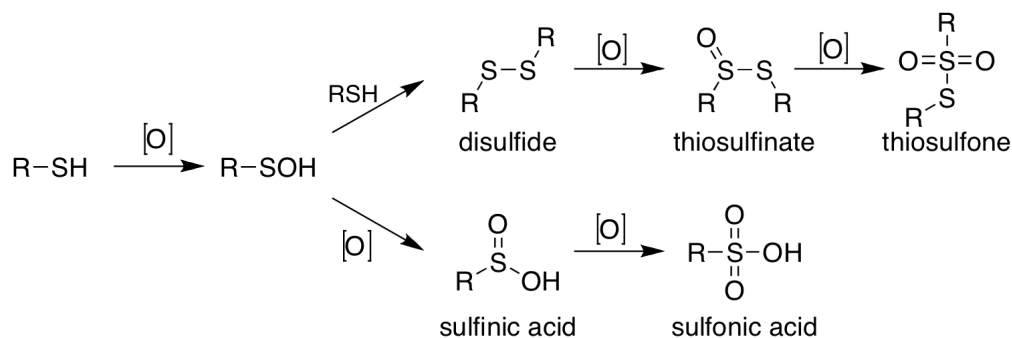


Figure 1.4 Oxidation states of protein cysteine thiols *in vivo*.¹⁴

Hydrogen peroxide, as discussed above, is a ROS generated through aerobic respiration, and responsible for oxidative stress disease states. Hydrogen peroxide, through its oxidation of cysteine residues on proteins, can modulate cell function and post-translational modifications of proteins, by oxidizing thiol to sulfenic acid, which rapidly forms either an intra-molecular disulfide bond with a neighbouring thiol residue (*cf.* Figure 1.5) or an inter-molecular disulfide bond with another thiol. The example shown in Figure 1.6 shows a model of this ROS signalling in the redox-regulation of cardiac hypertrophy, thickening of the arterial walls, by HDAC4. This enzyme is responsible for repressing the expression of genes involved in hypertrophy, and is localized in the nucleus by a multi-protein complex. The disulfide bonds formed in the presence of H_2O_2 stimulate dissociation and export of the complex, which can be reversed by reduction of the disulfide bonds.¹⁴

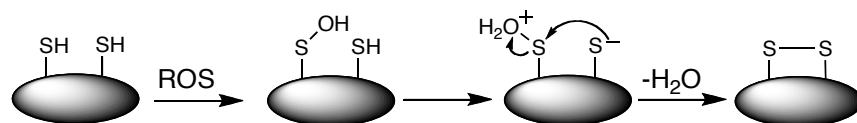
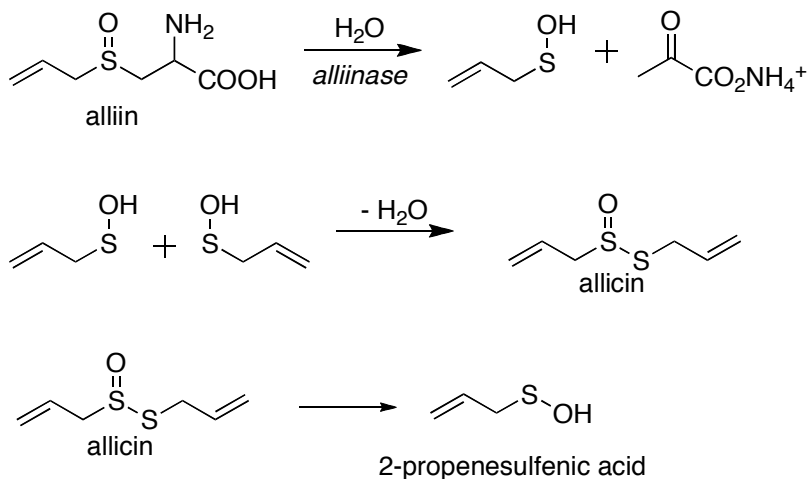


Figure 1.5 Formation of disulfide bond by ROS such as H₂O₂ through sulfenic acid intermediate.

Hydrogen peroxide is believed to oxidize cysteine thiols to sulfenic acids,^{16,17} which can then take one of several pathways: reaction with glutathione, a small molecule thiol, in what is known as S-glutathionation to form a disulfide, or reaction with another cysteine to form an intramolecular disulfide bond. This reaction remains reversible, and the products can be returned to their original thiol state through the action of glutathione reductase or thioredoxin reductase. In the absence of a thiol to react with the sulfenic acid, it may be further oxidized by hydrogen peroxide to sulfinic or sulfonic acids, in an irreversible process. Sulfonic acid has been used as a biomarker for oxidative stress in diseases such as cancer, diabetes, and cardiovascular and neurodegenerative diseases¹⁴ as it arises when the concentration of ROS overwhelms the organism's capacity to reduce sulfenic acid.

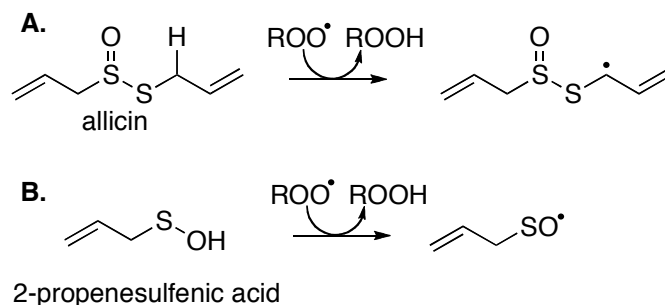
1.3.1 Thiosulfinates from Alliums

Garlic and other members of the *Allium* genus; onions, shallots and peteveria, have long been known as beneficial to health and have been used historically for their medicinal properties by ancient Egyptians and Greeks and in Chinese medicine.¹⁸ Today, garlic is known to help in the prevention of stroke, coronary thrombosis and atherosclerosis.¹⁹ The prevention of these and other diseases are attributed to the antioxidant activity inherent in garlic.



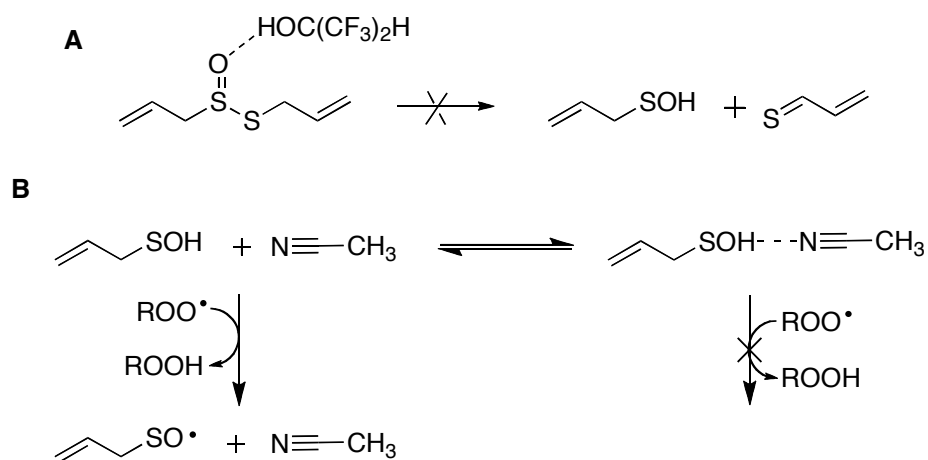
Scheme 1.3 Conversion of non-proteogenic amino acid, alliin to the thiosulfinate allicin and sulfenic acid

Garlic's antioxidant activity has been attributed to allicin, the compound which gives garlic its characteristic odour and flavour. Allicin is formed upon cutting or crushing garlic, which activates alliinase, the pyridoxine-dependent enzyme responsible for cleaving one of the C-S bonds in the non-proteinogenic amino acid derivative, S-allyl cysteine sulfoxide known as alliin. The products of alliinase's action on alliin are 2-propenesulfenic acid and ammonium pyruvate. Two molecules of the sulfenic acids, thus formed, condense to form the thiosulfinate allicin. Allicin was shown to be a powerful antioxidant in inhibited autoxidations of methyl linoleate and cumene, reported by Okada and coworkers.²⁰ They reported inhibition rate constants of 1.6×10^5 and $2.6 \times 10^3 \text{ M}^{-1} \text{ s}^{-1}$ respectively and proposed a mechanism of peroxy radical trapping by abstraction of the allylic hydrogen of allicin, shown in Scheme 1.4 A.



Scheme 1. 4 Mechanism of radical trapping as proposed by Okada (**A**)²⁰ and Pratt (**B**)²¹

Subsequently it was suggested by our group that the active antioxidant is not allicin itself, but the 2-propenesulfenic acid (Scheme 1.4 B) generated from allicin by Cope elimination.²¹ In fact, the rate constants reported by Okada were higher than would be expected for H-atom abstraction from allylic hydrocarbons ($1 \text{ M}^{-1}\text{s}^{-1}$)²² and the resulting carbon centred radical would readily trap oxygen to form a new peroxy radical, thus continuing the chain propagation and no inhibition should be observed. By contrast, the explanation that sulfenic acids are trapping peroxy radicals is supported by low calculated O-H BDEs for sulfenic acids ($\sim 68 \text{ kcal/mol}$) as compared to hydroperoxides ($\sim 86 \text{ kcal/mol}$), shown in Table 1.1.²¹ Furthermore, no inhibition period was observed when the Cope elimination was blocked by hydrogen bonding to hexafluoroisopropanol (HFIP), or when the sulfenic acid is protected by hydrogen bonding to acetonitrile (MeCN)³¹ (*cf.* Scheme 1.5).



Scheme 1.5 Solvent effects A) alliin decomposition to sulfenic acid prevented by hydrogen bonding to HFIP and B) radical-trapping slowed by hydrogen bonding of sulfenic acid to MeCN

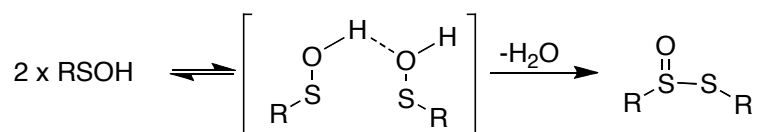
Table 1.1 Calculated O-H BDEs (kcal/mol) for some sulfenic acids and hydroperoxides using CBS-QB3 level of theory.²¹

Sulfenic Acids	O-H BDE	Hydroperoxides	O-H BDE
HSO-H	73.1	HOO-H	87.3
MeSO-H	68.4	MeOO-H	86.2
EtSO-H	68.6	EtOO-H	86.2
<i>t</i> BuSO-H	68.6	<i>t</i> BuOO-H	84.8
C ₆ H ₅ CH ₂ SO-H	68.6	C ₆ H ₅ CH ₂ OO-H	86.1

1.3.2 Sulfenic Acid Stability

Despite their prevalence *in vivo*, sulfenic acids are not very persistent under most conditions. There are many favourable avenues by which they can react, since they are both highly nucleophilic and highly electrophilic in nature. Among the most

common reactions are with thiols, such as cysteine, to yield disulfides, self-condensation to form the corresponding thiosulfinate equivalent, or disproportionation to give a disulfide, sulfenic acid and water. Sulfenic acids are also sensitive to oxidation, which will produce first a sulfinic acid, which can be further oxidized to a sulfonic acid.^{23,24}



Scheme 1.6 Reaction of two sulfenic acids, one acting as nucleophile, the other as electrophile, to form a thiosulfinate

Because of the instability of sulfenic acids, few examples are known that persist long enough to be either observed in solution or isolated. The first such example was reported in 1913 by Fries; his 1-anthraquinonesulfenic acid was stabilized by H-bonding of the OH group to the adjacent carbonyl.²⁵ Other isolable examples include 1,4-anthraquinone disulfenic acid (1957),²⁶ *trans*-decalin-9-sulfenic acid (1992),²⁷ 9-triptycenesulfenic acid (1983),²⁸ calix[6]arenesulfenic acid²⁹ and other sulfenic acids also protected by large bulky groups placing it in a protected cavity.³⁰

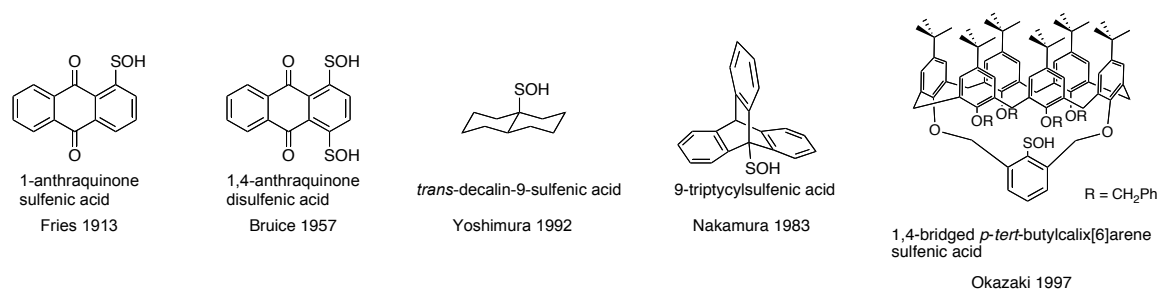


Figure 1.6 Examples of persistent sulfenic acids.^{25,26,27,28,29}

Most of the stable sulfenic acids are arenesulfenic acids, such as Fries' anthraquinones and the calix[6]arenes; however, *in vivo*, sulfenic acids, which are largely results of cysteine oxidation, would be alkylsulfenic acids. Therefore, an ideal model for understanding the reactions of cysteine would be an alkylsulfenic acid. To that end, our group has recently made use of 9-triptycenesulfenic acid in order to provide some support for our suggestion that sulfenic acids are key to the antioxidant activity of garlic and petiveria.³¹ In fact, our group was able to measure a sulfenic acid O-H BDE (71.9 kcal/mol), as well as a sulfenic acid pK_a (12.5) and redox potential (0.74 V) for the first time.¹⁵ With this compound in hand, our group has also been able to study sulfenic acid-peroxyl radical reactions directly – in both homogenous solution ($k_{inh} = 3.0 \times 10^6 \text{ M}^{-1}\text{s}^{-1}$)³² and liposomes.³³

1.4 Selenenic Acids

Like sulfenic acids, selenenic acids are believed to play important roles in biological systems. Selenium being a group VI member like sulfur, has similar properties and can in some cases “replace” sulfur, as in the case of selenocysteine and selenomethionine, the selenium amino acid equivalents to cysteine and

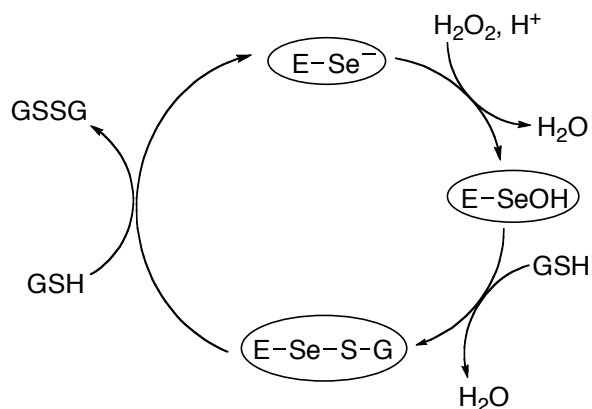
methionine. These selenoamino acids are integrated into selenoproteins, which are largely characterized as belonging to one of three main families: glutathione peroxidases, thioredoxin reductases or deiodonases.³⁴

Because of its incorporation into these selenoenzymes, selenium is an important dietary nutrient. This was discovered, along with selenium's involvement in antioxidant activities, due to the resemblance of the symptoms associated to selenium deficiency in animals to the symptoms of Vitamin E deficiency.³⁵ Furthermore, selenium intake was shown to improve the symptoms caused by Vitamin E deficiency, indicating a common antioxidant role of these two compounds.

Glutathione peroxidase (GPx) was discovered in 1957,³⁶ ironically the same year that selenium was found to be a trace element for mammals.³⁷ In 1973, Rotruck *et al.* found that selenium is present in, and plays a role in the activity of, GPx.³⁸ Glutathione peroxidases act as antioxidants by converting hydrogen peroxide and other hydroperoxides to water or their corresponding alcohols thus preventing the hydrogen peroxide from causing oxidative damage (*vide supra*). Selenocysteine is incorporated in the active site of GPx, as part of a catalytic triad, which also comprises glutamine and tryptophan. Among the family of glutathione peroxidase, phospholipid hydroperoxide glutathione peroxidase (PHGPx)³⁹ acts as protective agents in the cell membrane by reducing phospholipid hydroperoxides to alcohols.

In its resting state, the selenocysteine in GPx is deprotonated to its selenyl anion, which makes it very easily oxidized by hydrogen peroxide to yield a selenenic acid and the reduction products: water or alcohol. The enzyme is then reduced back to its original state by the co-factor glutathione, a first equivalent will react with the

selenenic acid to produce a selenylsulfide that is further reduced to its resting state by another glutathione forming a disulfide with the first, (*cf.* catalytic cycle in Scheme 1.7).³⁴



Scheme 1.7 Catalytic cycle of glutathione peroxidase.

A synthetic organoselenium compound, Ebselen, was reported in 1984 to exhibit GPx like activity.^{40,41} Ebselen was found in initial screening studies due to its anti-inflammatory properties and has been shown to reduce oxidants such as H_2O_2 and peroxynitrite, retard lipid peroxidation and protect against oxidative damage post ischemia in rabbit livers. This has prompted the synthesis of a series of small-molecule organoselenium compounds that act as GPx mimics *in vitro* and *in vivo*, examples of which are illustrated in Figure 1.7.⁴²

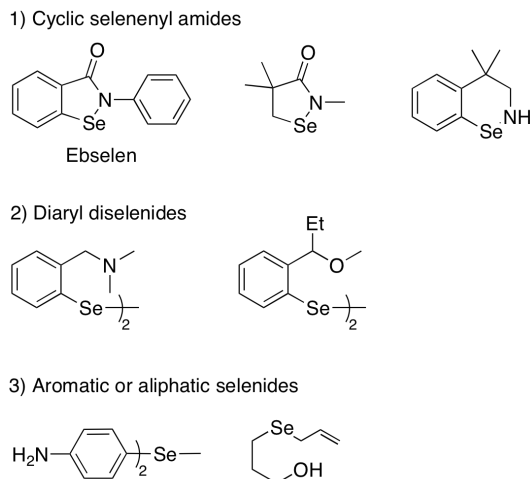
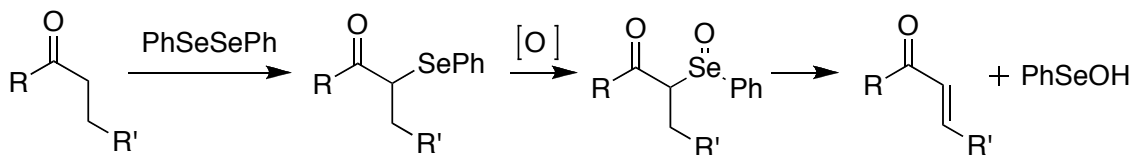


Figure 1.7 Examples of the many GPx mimics divided in three categories.⁴²

1.4.1 Selenenic Acids In Organic Synthesis

Beyond their role in biology, selenenic acids have received little attention. It should be noted that they are formed as a byproduct in selenoxide eliminations, a common method for preparing alkenes in organic synthesis. This method, illustrated in Scheme 1.8, is commonly used in the formation of α,β -unsaturated carbonyl compounds.⁴³



Scheme 1.8 General procedure for preparation of alkenes using selenoxide *syn*-elimination.⁴⁴

1.4.2 Selenenic Acid Stability

Despite their relevance in biological systems, little is known about the selenenic acid functional group owing to the fact that they are not very persistent. As discussed above in the case of the chalcogenic analogue sulfenic acids, selenenic acids rapidly disproportionate to diselenide, seleninic acid and water and self-condense to selenoseleninate.

Some persistent selenenic acids, as shown below, have been synthesized and either observed in solution or isolated,^{45,46} (these are discussed more thoroughly in Chapter 2). In most cases these are areneselenenic acids either stabilized by electron-withdrawing *ortho* substituents or by very large sterically protecting groups and often do not show sufficient persistence for extensive study. As such, much remains unknown about selenenic acids and the synthesis and study of a persistent or stable selenenic acid is a significant objective.

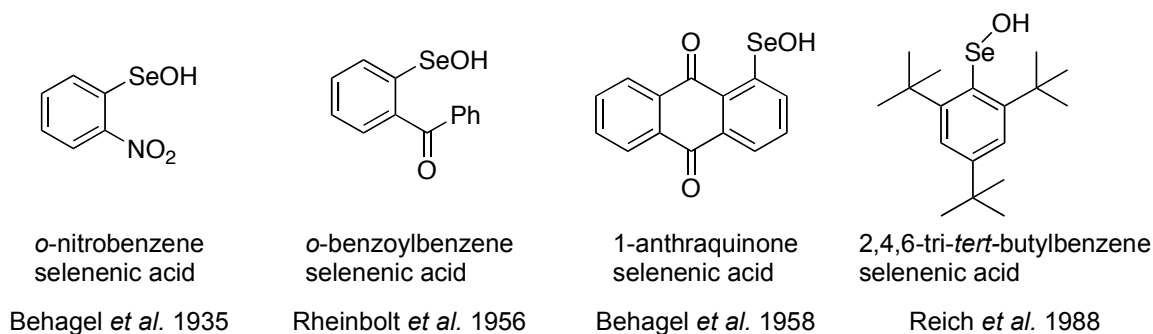


Figure 1.8 Examples of persistent selenenic acids.^{45,46}

1.5 Hydrogen Atom Transfer

Chain-breaking antioxidants, as discussed above, act by donating a hydrogen atom to the chain propagating peroxy radical, yielding both a more stable and more persistent radical that will not propagate the chain, but rather terminate it by reacting with another radical. This formal transfer of a hydrogen atom can occur by multiple mechanisms, including a direct hydrogen atom transfer (HAT) and a proton-coupled electron transfer (PCET).

In the HAT mechanism the proton and electron involved are transferred together. As shown by the reaction of a benzyl radical with toluene (Figure 1.9 – left), the donor loses one proton and one electron from the C-H σ -bond. This is in contrast to the PCET mechanism, where the electron being transferred does not come from the bond involving the H atom in question.

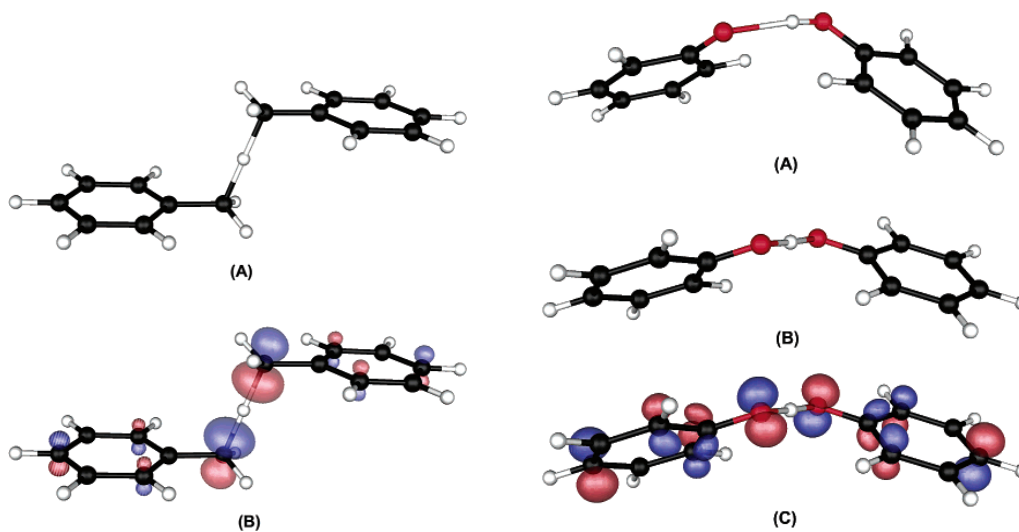


Figure 1.9 Benzyl/toluene (left): (A) the geometry and (B) the SOMO at the HAT transition structure. Phenoxy/phenol (right): (A) geometry of the hydrogen-bonded complex, (B) the geometry and (C) the SOMO at the PCET transition structure. Reproduced with permission from Mayer, J.M.; Hrovat, D.A.; Thomas, J.L.; Borden, W.T., *J. Am. Chem. Soc.*, 2002, 124, 11142-11147. Copyright 2002 American Chemical Society.⁴⁸

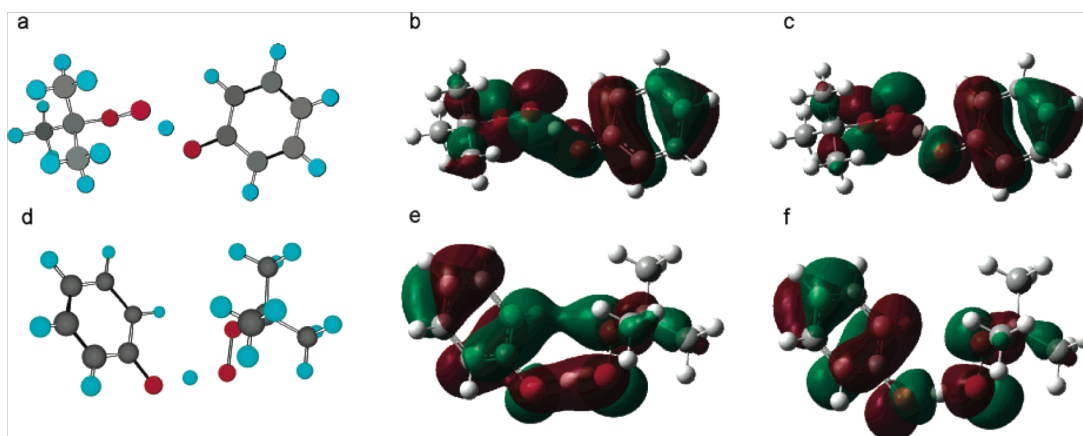


Figure 1.10 Structure of the cis and trans transition states of the *tert*-butylperoxyl/phenol couple with their respective HOMO and SOMO. The oxygen lone pair-ring π -orbital net bonding overlap in the cisoid TS allows the H exchange to proceed by a multi-center PCET mechanism. Reprinted with permission from DiLabio, G.A.; Johnson, E.R., *J. Am. Chem. Soc.*, 2007, 129, 6199-6203. Copyright 2007 American Chemical Society.⁴⁷

In the proton-coupled electron transfer (PCET) mechanism, the proton and the electron involved in the reaction are transferred from different orbitals on the donor to different orbitals on the acceptor. In the reaction between a phenoxy radical and a phenol (Figure 1.9 – right), the electron is transferred from the doubly occupied π orbital on the oxygen of the phenol to the singly occupied π orbital on the oxygen of the phenoxy radical while the proton is transferred from its σ -bond to the lone pair of the phenoxy radical.⁴⁸ However, the transition structure reported by Borden depicted in Figure 1.8 is not the correct position for PCET to occur. A subsequent report by DiLabio showed that the transition structure for the reaction of *tert*-butyl peroxy radical and phenol by PCET is *cis*, allowing orbital overlap between the lone pair of the oxygen and the π -orbital, as shown in Figure 1.11.⁴⁷

The report by DiLabio also showed that PCET is not restricted to two aromatic rings, but can also involve heteroatom lone pairs. This suggests that PCET is a plausible mechanism for the reaction of sulfenic acids with peroxy radicals, since both players have heteroatom lone pairs that can overlap for electron transfer, on the sulfur in the case of sulfenic acid, and on the internal oxygen of the peroxy radical. It is important to note that the difference between HAT and PCET has only been shown computationally and that no experimental data has been able to differentiate the two.

In light of the impressive radical-trapping antioxidant activity observed in sulfenic acids, one might expect the heavier chalcogen analogue, selenenic acid to have similar properties. Computational studies were carried out on a model selenenic acid to compare to the results obtained for sulfenic acids.²¹ Two aspects were compared for sulfenic and selenenic acids, first their respective O-H BDEs and second the activation energy for both of their reactions with peroxy radicals. Interestingly, despite the higher calculated O-H BDEs of selenenic acid as compared to sulfenic acids, by *ca.* 13 kcal/mol (Table 1.2), the calculated activation energy for the reaction of selenenic acid with peroxy radical was found to be lower than that for the same sulfenic acid, by *ca.* 1.5 kcal/mol, (Table 1.3).⁴⁹

Table 1.2 Calculated O-H BDEs (kcal/mol) for selected selenenic and sulfenic acids using CBS-QB3 level of theory.⁴⁹

Selenenic Acid	O-H BDE	Sulfenic Acid	O-H BDE
HSeO-H	86.5	HSO-H	73.1
MeSeO-H	81.9	MeSO-H	68.4

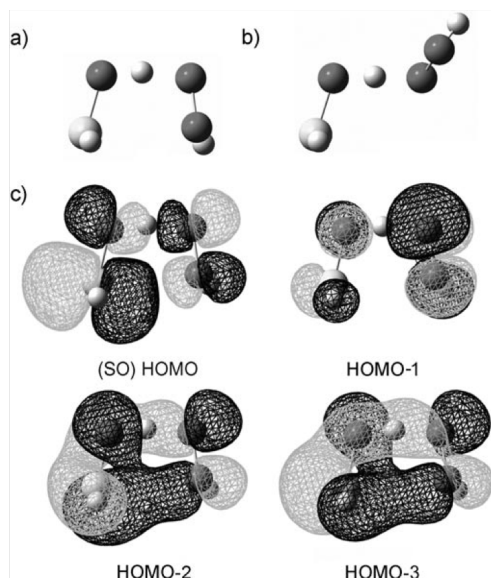
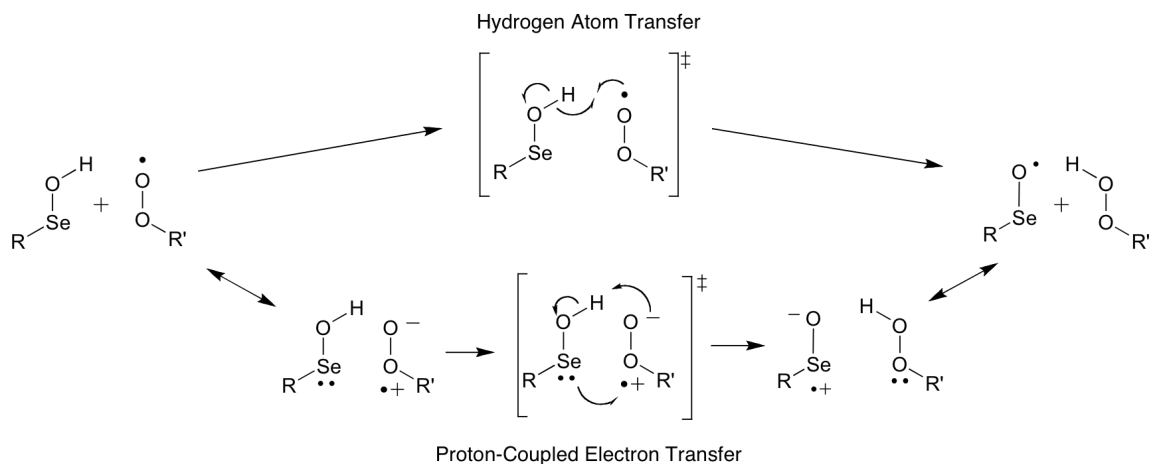


Figure 1.11 a) Cisoid and b) transoid transition-state structures for the HSOH/•OOH reaction c) The four highest occupied molecular orbitals of the structure in (a) showing the overlap between the sulfenic acid S atom and the internal peroxy O atom. Reprinted with permission from Vaidya, V.; Ingold, K.U.; Pratt, D.A., *Angew. Chem. Intl. Ed.*, 2009, 48, 157-160. Copyright 2009 Wiley.²¹

Table 1.3 Calculated activation energies (kcal/mol) for H-atom transfers from methylselenenic acid and methylsulfenic acid to peroxy radicals using CBS-QB3 level of theory.⁴⁹

Selenenic or Sulfenic Acid/ Peroxyl Radical Pair	E_a (<i>cis</i> TS)	E_a (<i>trans</i> TS)
MeSeO-H/ •OOME	3.0	15.1
MeSO-H/ •OOME	4.6	11.0



Scheme 1.9 Proton-coupled electron transfer mechanism vs. hydrogen atom transfer mechanism for reaction of selenenic acid with peroxy radical.

The higher O-H BDE in the case of HAT would necessarily lead to a higher activation energy for selenenic acid's reaction with peroxy radicals, and would then indicate the selenenic acids would not have greater potential as antioxidants than sulfenic acids. However, the lower activation energy in the *syn* transition state for selenenic acid suggests that an electron is being transferred from the Se atom to the internal O atom of the peroxy, separately from the proton being transferred, in conformity with the PCET mechanism (*cf.* Scheme 1.9). This reaction would be more favourable in the case of selenenic acid, due to the larger radius of the Se atom as compared to the S atom and thus its greater orbital overlap with the oxygen receiving the electron, making selenenic acids more powerful antioxidants than sulfenic acids.

The results presented in Tables 1.2 and 1.3 continue to support the intervention of a PCET mechanism for formal HAT reactions between entities possessing acidic H-atoms and adjacent heteroatoms or π orbitals. More

interestingly, it provides a testable hypothesis that would provide insight into the mechanism. This being based on computation study of small model compounds, it is necessary to further investigate experimentally using the actually compounds synthesis in this and previous work.

1.6 Research objectives

The relevance of selenenic acids in the catalytic cycle of GPx, involved in the enzymatic protection against oxidative damage in the body, has given rise to interest in the study of the properties and reactivity of this functional group. Any study of selenenic acids is made extremely difficult by the high reactivity of selenenic acids and their tendency to self-condense, disproportionate and oxidize. The primary objective of this thesis is to synthesize a persistent model selenenic acid, 9-triptycylselenenic acid, purify and characterize it, and develop conditions for its storage and use in experiments. With 9-triptycylselenenic acid in hand, the subsequent goals of this work are to study its stability as well as the persistence of its corresponding selenenyl radical and to study its reaction with peroxy radicals to quantify its antioxidant activity.

Finally, this thesis will study the oxidation of 9-triptycenethiol in an effort to contribute to further understanding the reactivity of sulfenic acid as an intermediate in the oxidation of thiol to disulfide, as well as to gain more understanding of the oxidation reactions of sulfenic acid to sulfinic and sulfonic acids. In the hopes of observing and characterizing the kinetics of the direct oxidation of thiol to sulfenic

acid by H₂O₂, previously reported persistent sulfenic acid, 9-triptycenesulfenic acid and its parent thiol, 9-triptycenedithiol, will be used in these studies.

1.7 References

- ¹ Niki, E., *Free Radical Res.*, **2000**, 33, 693-704.
- ² Harman, D. J. *Gerontol.*, **1956**, 11, 298-300.
- ³ Porter, N.A., *Acc. Chem. Res.*, **1986**, 19, 262-268.
- ⁴ Kagan, V.E.; Quinn, P.J., *Antiox. Redox Signal.*, **2004**, 6, 199-202.
- ⁵ Voet, J.G.; Voet D. *Biochimie*, 2^e edition; de Boeck: Bruxelles, 2004.
- ⁶ Negre-Salavayre, A.; Auge, N.; Alaya, V.; Basaga, H.; Boada, J.; Brenke, R.; Capple, S.; Cohen, G.; Feher, J.; Grune, T.; Lengyel, G.; Mann, G.E.; Pamplona, R.; Poli, G.; Portero-Otin, M.; Riah, Y.; Salavayre, R.; Sasson, S.; Serrano, J.; Shamn, O.; Siems, W.; Siow, R.C.M.; Wiswedel, I.; Zarkovic, K.; Zarkovic, N. *Free Radical Res.*, **2010**, 44, 1125-1171.
- ⁷ Yau, T. M. *Mech. Ageing Dev.*, **1979**, 11, 137-144.
- ⁸ Tanel, A.; Averill-Bates, D. A. *Free Radical Biology and Medicine* 2007, 42, 798-810.
- ⁹ Burton, G.W.; Ingold, K.U., *Acc. Chem. Res.*, **1986**, 19, 194-201.
- ¹⁰ Valgimigli, L.; Pratt, D.A., Antioxidants in Chemistry and Biology. *Encyclopedia of Radicals in Chemistry, Biology and Materials*; Wiley: New York, 2012; Vol.56, p. 1623-1677.
- ¹¹ Halliwell, B.; Gutteridge, J. M. C., *Free Radic. Biol. Med.*; 3rd ed.; Oxford University Press Inc: New York, 1999.
- ¹² Burton, G.W.; Ingold, K.U., *J. Am. Chem. Soc.*, **1981**, 103, 6471-6477.

- ¹³ Burton, G.W.; Doba, T.; Gabe, E.J.; Hughes, L.; Lee, F.L.; Pasad, L.; Ingold, K.U., *J. Am. Chem. Soc.*, **1985**, 107, 7053-7065.
- ¹⁴ Paulsen, C. E.; Carroll, K.S., *ACS Chem. Biol.* **2010**, 5, 1, 47-62.
- ¹⁵ McGrath, A.J.; Garrett, G.E.; Valgimigli, L.; Pratt, D.A., *J. Am. Chem. Soc.*, **2010**, 132, 16759-16761.
- ¹⁶ Luo, D.; Smith, S.W.; Anderson, B.D., *J. Pharma. Sci.*, **2005**, 94, 304-316.
- ¹⁷ Allison, W.S., *Acc. Chem. Res.*, **1976**, 9, 293-299.
- ¹⁸ Rivlin, R.S., *J. Nutr.*, **2001**, 131, 951S-954S.
- ¹⁹ Block, E., *Sci. Am.*, **1985**, 252, 114-119.
- ²⁰ Okada, Y.; Tanaka, K.; Fujita, I.; Sato, E.; Okajima, H., *Redox Rep.*, **2005**, 10, 96-102.
- ²¹ Vaidya, V.; Ingold, K.U.; Pratt, D.A., *Angew. Chem. Intl. Ed.*, **2009**, 48, 157-160.
- ²² Amorati, R.; Pedulli, G.F., *Org. Biomol. Chem.*, **2008**, 6, 1103-1107.
- ²³ Davis, F.A.; Jenkins, L.A.; Billmers, R.L., *J. Org. Chem.* **1986**, 51, 1033-1040.
- ²⁴ Claus, J.; Giles, G.I.; Giles, N.M.; Sies, H., *Angew. Chem. Intl. Ed.*, **2003**, 42, 4742-4758.
- ²⁵ Fries, K., *Ber. Dtsch. Chem. Ges.*, **1912**, 45, 2965-2973.
- ²⁶ Bruice, T.C.; Markiw, R.T., *J. Am. Chem. Soc.* **1957**, 79, 3150-3153.
- ²⁷ Toshiaki Yoshimura, Eiichi Tsukurimichi, Satoru Yamazaki, Shinichi Soga, Choichiro Shimasaki and Kiyoshi Hasegawa, *J. Chem. Soc., Chem. Commun.*, **1992**, 1337-1338.
- ²⁸ Nakamura, N., *J. Am. Chem. Soc.*, **1983**, 105, 7172-7173.
- ²⁹ Saiki, T.; Goto, K.; Tokitoh, N.; Goto, M.; Okazaki, R., *J. Organomet. Chem.*, **2000**, 611, 146-157.

- ³⁰ Goto, K.; Holler, M.; Okazaki, R., *Phosphorus, Sulfur Silicon Rel. Elem.*, **1997**, 120, 325-326.
- ³¹ Philip T. Lynett, P.T.; Butts, K.; Vaidya, V.; Garrett, G.E.; Pratt, D.A., *Org. Biomol. Chem.*, **2011**, 9, 3320-3330
- ³² Amorati, R.; Lynett, P.T.; Valgimigli, L.; Pratt, D.A., *Chem. Eur. J.*, **2012**, 18, 6370-6379.
- ³³ Zheng, F., Pratt, D.A., *Chem. Commun.*, **2013**, 49, 8181-8183.
- ³⁴ Birringer, M.; Pilawa, S.; Flohé, L., *Nat. Prod. Rep.*, **2002**, 19, 693-718.
- ³⁵ Flohé, L.; Günzler, W.A.; Schock, H.H., *FEBS Letters*, **1973**, 32, 132-134.
- ³⁶ Mills, G.C., *J. Biol. Chem.*, **1957**, 229, 189-197.
- ³⁷ Schwarz, K.; Foltz, C.M., *J. Am. Chem. Soc.*, **1957**, 79, 3292-3293.
- ³⁸ Rotruck, J.T.; Pope, A.L.; Ganther, H.E.; Swanson, A.; Hafeman, D.G.; Hoekstra, W.G.; *Science*, **1973**, 179, 588-590.
- ³⁹ Ursini, F.; Maiorino, M.; Gregolin, C., *Biochim. Biophys. Acta* **1985**, 62-70.
- ⁴⁰ Müller, A.; Cadenas, E.; Graf, P.; Sies, H., *Biochem. Pharmacol.*, **1984**, 33, 3235-3239.
- ⁴¹ Wendel, A.; Fausel, M.; Safayhi, H.; Tiegs, G.; Otter, R., *Biochem. Pharmacol.*, **1984**, 33, 3241-3245.
- ⁴² Bhabak, K.P.; Mugesh, G., *Acc. Chem. Res.*, **2010**, 43, 1408-1419.
- ⁴³ Reich, H. J.; Wollowitz, S., *Org. React.*, **1993**, 44, 1-296.
- ⁴⁴ Reich, H.J.; Renga, J.M.; Reich, I.L., *J. Am. Chem. Soc.*, **1975**, 97, 5434-5447.
- ⁴⁵ Reich, H.J.; Hoeger, C.A.; Willis, W.W. Jr.; *Tetrahedron* **1985**, 41, 21, 4771-4779.

⁴⁶ Reich, H.J.; Jasperse, C.P., *J. Org. Chem.*, **1988**, 53, 2389-2390

⁴⁷ DiLabio, G.A.; Johnson, E.R., *J. Am. Chem. Soc.*, **2007**, 129, 6199-6203

⁴⁸ Mayer, J.M.; Hrovat, D.A.; Thomas, J.L.; Borden, W.T., *J. Am. Chem. Soc.*, **2002**, 124, 11142-11147.

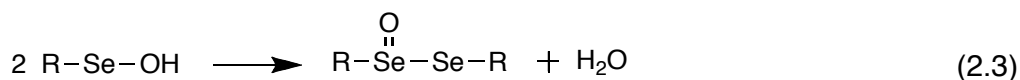
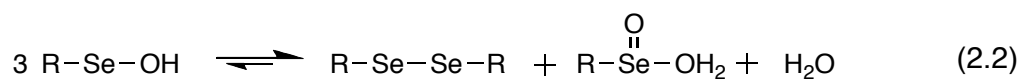
⁴⁹ McGrath, A.; Synthesis, Redox Chemistry and Antioxidant Activity of Sulfenic Acid. M.Sc. Thesis, Queen's University, Canada, 2010.

CHAPTER 2

SYNTHESIS OF A PERSISTENT SELENENIC ACID

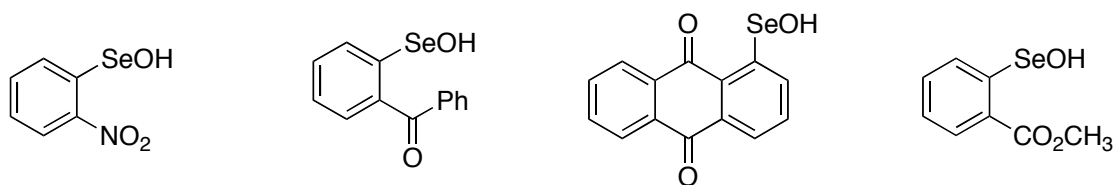
2.1 Introduction

Selenenic acids have been of great interest since the discovery, in the 1970s, that the important antioxidant enzyme, glutathione peroxidase, contains selenium as part of a selenocysteine residue in its active site¹ and the implication that the catalytic cycle of the enzyme involves a selenenic acid intermediate.² Selenenic acids also figure in organic synthesis as the by-product of the selenoxide *syn*-elimination reaction used to generate alkenes, generally in complex molecule synthesis.³ In fact, they are likely far more widespread than is currently appreciated, but their stabilities preclude their identification and/or isolation under most conditions. Indeed, little is known about the chemistry of this functional group, due to the ease with which selenenic acids are oxidized, disproportionate, and self-condense (*cf.* Equations 2.1, 2.2, and 2.3 respectively in Scheme 2.1). As such, few selenenic acids have been prepared or isolated which are persistent enough to be observed spectroscopically, let alone to be subject of detailed study.



Scheme 2.1 Reactions of selenenic acid that may contribute to its lack of persistence; oxidation (2.1), disproportionation (2.2), and self-condensation (2.3).

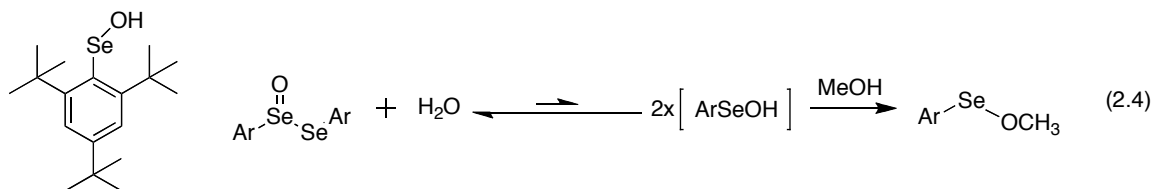
A few examples of persistent areneselenenic acids have been reported.⁴ These include *o*-nitrobenzeneselenenic acid, *o*-benzoylbenzeneselenenic acid and 1-anthraquinoneselenenic acid, which have been isolated and characterized or *o*-carbomethoxybenzeneselenenic acid, observed in solution. These areneselenenic owe their stability in part to the hydrogen bonding of the selenenic acid moiety to their *ortho* substituents. However, despite their increased persistence by comparison to most selenenic acids, these *ortho* substituted areneselenenic acids still undergo disproportionation to diselenides and seleninic acids, and remain difficult to study.



Scheme 2.2 Persistent areneselenenic acids.^{4,5,6}

Another approach towards persistent selenenic acids is using steric bulk to prevent disproportionation or condensation reactions. The bulky compound, 2,4,6-tri-*tert*-butylbenzeneselenenic acid was prepared and observed in solution.⁷ Despite the very large *ortho* substituents on this areneselenenic acid, it was still found to undergo disproportionation. It decomposed completely within 2 hours at 25°C in D₂O/CD₃CN. With the increased persistence afforded by the tri-*tert*-butylphenyl substituent, some insight was gained into the reactivity of selenenic acids; the condensation reaction was found to be reversible, albeit strongly

favouring the condensation products. No selenenic acid was detected at equilibrium, but when the mixture was treated with methanol the product corresponding to reaction with selenenic acid, methylselenenate, was observed (*cf.* Scheme 2.2).



Scheme 2.3 2,4,6-*tri-tert*-butylbenzeneselenenic acid and the equilibrium between selenoseleninate and selenenic acid demonstrated by formation of methylselenenate (Ar = 2,4,6-*tri-tert*-butylphenyl).⁷

The attempts at stabilizing selenenic acids with steric bulk were continued by Okazaki *et al.* with the use of the 1,4-bridged calix[6]arene structure previously used with sulfenic acids.⁸ The 1,4-bridged calix[6]arene selenenic acid was found to be resistant to disproportionation even after 5 hours at 120 degrees, a significant improvement over 2,4,6-*tri-tert*-butylbenzeneselenenic acid. This is explained, as expected, by its X-ray crystallographic structure (Figure 2.1) that shows that the selenenic acid moiety is buried in the bowl shape of this molecule, and that the selenenic acids of two molecules would be unable to meet in the disproportionation reactions. Despite the protection against disproportionation afforded by the large calix[6]arene, the selenenic acid retains some of its reactivity, it undergoes oxidation by *m*CPBA with a 88% yield and reaction with 1-butanethiol to afford the selenanyl sulfide in 78% yield.⁸

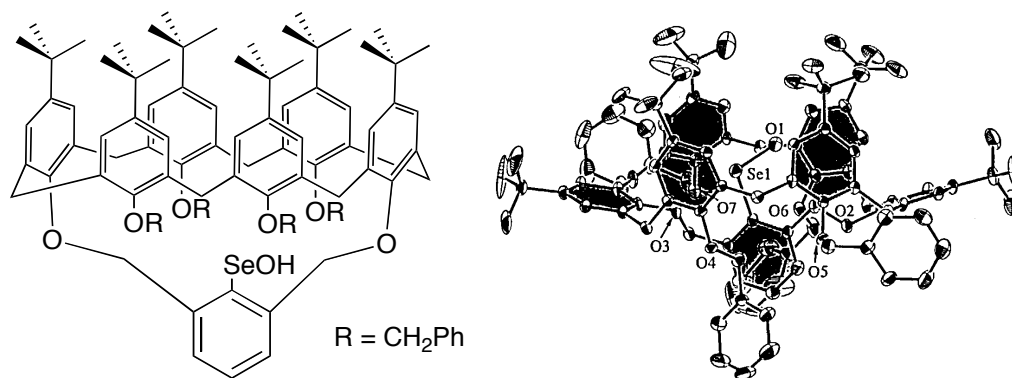
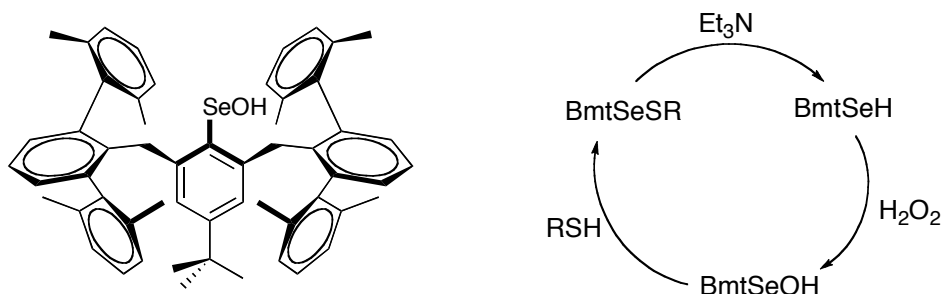


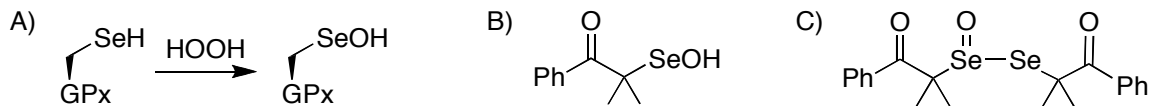
Figure 2.1 Stable selenenic acid, 1,4-bridgedcalix[6]arene selenenic acid and its X-Ray crystal structure indicating the selenenic acid moiety buried in the bulky bowl-type structure. Reprinted with permission from Goto, K.; Saiki, T.; Okazaki, R. *Phosphorus, Sulfur Silicon Relat. Elem.* 1998, 136:1, 475-487. Copyright 1998 Taylor and Francis.⁸

Another stable selenenic acid was reported in 2001 by Okazaki, this one stabilized by Bmt (4-*t*-butyl-2,6-bis[2,2'',6,6''-tetramethyl]phenyl), a novel bowl-type substituent illustrated in Scheme 2.3.⁹ This was the first example of a selenenic acid generated by direct oxidation of its corresponding selenol rather than the previous examples, which came from *syn*-elimination from a selenoxide, hydrolysis of selenenates or oxidations of selenenyl sulfides and diselenides.



Scheme 2.4 Novel Bmt (bowl-type) selenenic acid and its regeneration cycle from selenol and thioselenide. Reprinted with permission from Goto, K.; Nagahama, M.; Mizushima, T.; Shimada, K.; Kawashima, T.; Okazaki, R. *Org. Lett.* 2001, 3, 3569–3572. . Copyright 2001 American Chemical Society.⁹

Despite the growing number of persistent selenenic acids with bulky substituents, all are examples of areneselenenic acids. Given that a significant point of interest for the study of selenenic acid is to better understand the mechanism of glutathione peroxidase and its mimics, which contain aliphatic carbon-selenium bonds and thus implicate aliphatic selenenic acids among their intermediates, it stands to reason that the ideal models would be aliphatic selenenic acids. First attempts at synthesizing aliphatic selenenic acids were made in 1985 by Reich *et al.* with the target selenenic acid, 2,2-dimethyl-benzoyl ethylselenenic acid chosen in the hopes that the steric hinderance and nearby polar group would protect the selenenic acid from disproportionation and that the nearby carbonyl group would coordinate the selenenic acid affording it extra persistence.⁴ However efforts to prepare this compound were unsuccessful, only the corresponding selenoseleninate was observed (Scheme 2.4)



Scheme 2.5 A) GPx Selenocysteine oxidation to an aliphatic selenenic acid by hydrogen peroxide, B) target aliphatic selenenic acid, 2,2-dimethyl-benzoyl ethylselenenic acid , C) product selenoseleninate.⁴

Ishii et al. reported the first persistent alkane selenenic acid in 1999.¹⁰ The propeller-like triptycene moiety, which has been used to increase the persistence of sulfenic acid to the point of being isolable,¹¹ successfully improved the persistence of the selenenic acid as well. The group was able to synthesize, isolate and characterize the first example of a persistent alkane selenenic acid, including its X-ray crystallographic structure (Figure 2.2). Although fully characterized, no further studies were undertaken with this persistent selenenic acid, which prompted us to further this work by first reproducing the reported synthesis of 9-triptyceneselenenic acid (TrpSeOH) and subsequently studying its redox properties.

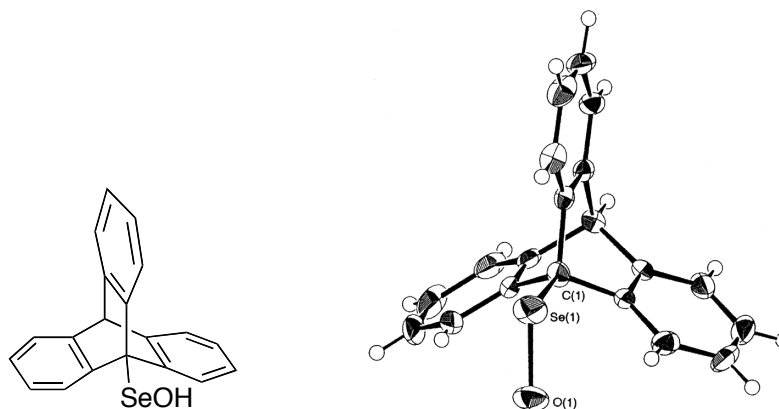
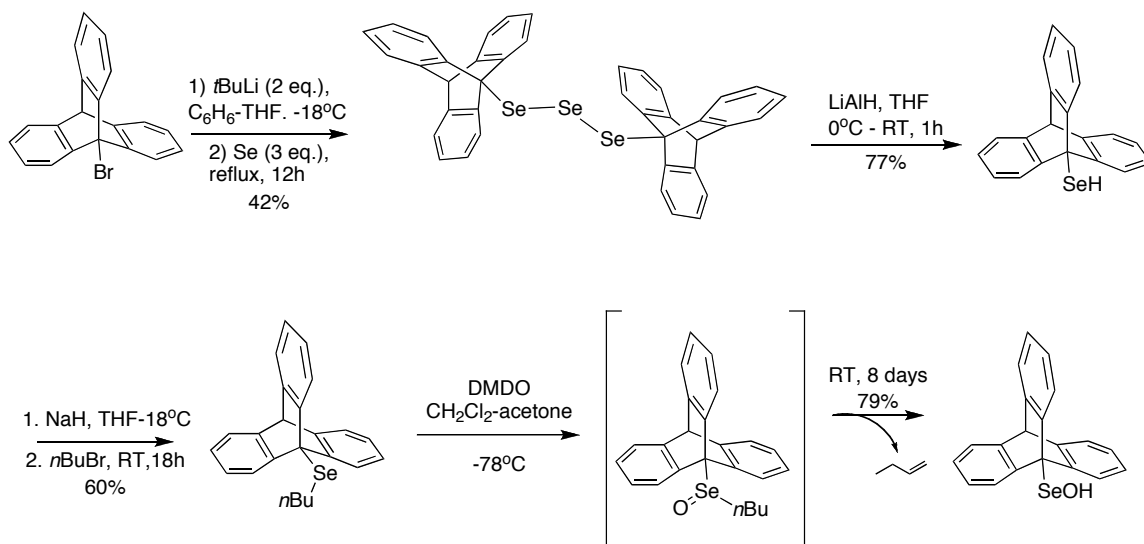


Figure 2.2 9-Triptyceneselenenic acid and its X-Ray crystal structure. Reprinted with permission from Ishii, A.; Matsubayashi, S.; Takahashi, T.; Nakayama, J. *J. Org. Chem.* 1999, 64, 1084-1085. Copyright 1999 American Chemical Society.¹⁰

2.2 Results and Discussion

2.2.1 Attempts to repeat the Ishii 9-triptyceneselenenic acid synthesis

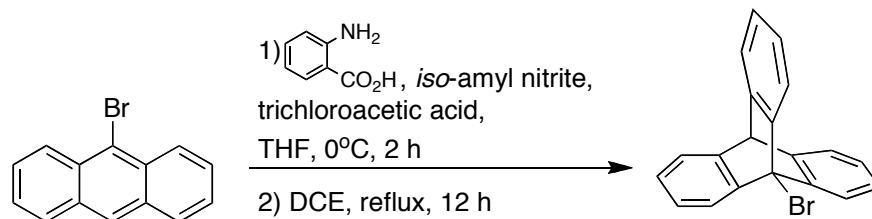
The four-step synthesis (Scheme 2.5) begins from 9-bromotriptycene, which is prepared by the cycloaddition of benzyne and 9-bromoanthracene.¹² The 9-bromotriptycene is then subjected to lithium-halogen exchange using *tert*-butyl lithium and quenching of the resulting 9-triptycenellithium with elemental selenium to produce a *bis*(triptycene) triselenide as the major product. The triselenide is then reduced with LiAlH_4 to yield 9-triptyceneselenol, which is subsequently alkylated with 1-bromobutane. The final step consists of oxidation of 9-triptycene(*n*-butyl)selenenide with dimethyldioxirane (DMDO) to yield the corresponding selenoxide, which undergoes *syn*-elimination of 1-butene to produce the desired 9-triptyceneselenenic acid.



Scheme 2.6 9-Triptyceneselenenic acid synthesis as reported by Ishii *et al.*¹⁰

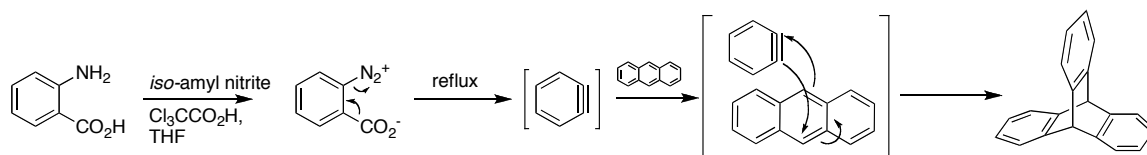
As reported by Ishii, this synthesis produces TrpSeOH in moderate yield with the only apparent disadvantage being the six-day reaction time for the final elimination step from the selenoxide. The intermediates (*bis*-triptyceneselenide, 9-triptycene(*n*-butyl)selenide, and 9-triptyceneselenoxide) were reported to be stable and easy to handle, 9-triptyceneselenol was not isolated.

Synthesis of the Triptycene Backbone



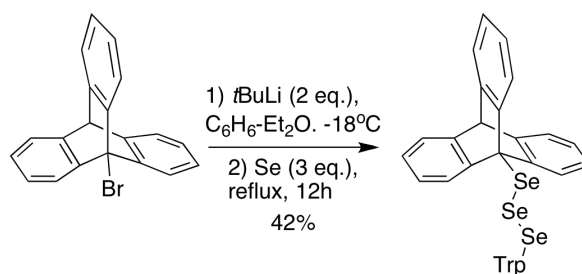
Scheme 2.7 Synthesis of 9-bromotriptycene

The reported synthesis begins with bromotriptycene, a known compound made from the cycloaddition of a benzyne on 9-bromoanthracene (Scheme 2.6). This step is also central to the synthesis of 9-triptycenesulfenic acid which was reported by Pratt *et al.* in 2010 in the cycloaddition of benzyne onto 9-(*tert*-butylthio)-anthracene,¹³ so the same conditions were used only substituting 9-bromoanthracene for the thio compound. The procedure consists of preparing a diazonium salt from the inexpensive starting materials anthranilic acid and isoamyl nitrite and heating the salt in the presence of the benzyne acceptor, 9-bromoanthracene. The salt undergoes loss of CO₂ and N₂ gases to generate the benzyne *in situ*, which adds to 9-bromotriptycene. This reaction proceeded as reported, with relatively simple purification by column chromatography and in moderate yields (~70%).



Scheme 2.8 Mechanism for formation of benzyne and cycloaddition to anthracene to form triptycene

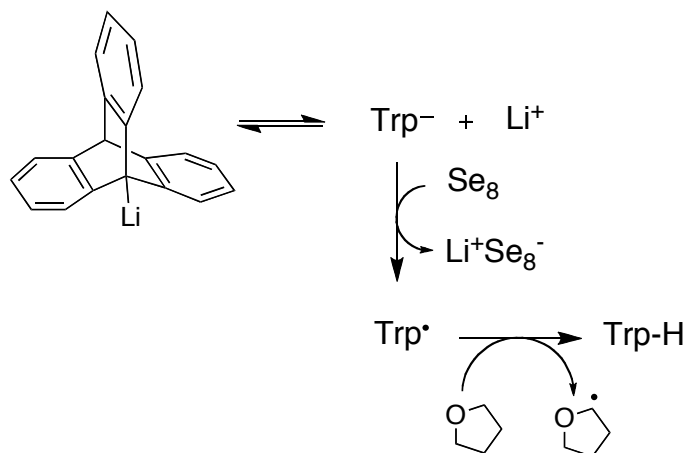
Addition of Selenium onto Triptycene



Scheme 2.9 Synthesis of *bis*-triptyceneselenide

With the starting material, 9-bromotriptycene, in hand the first step of the Ishii synthesis, formation of the *bis*-triptyceneselenide, could be attempted. The triselenide compound is made by addition of elemental selenium onto the 9-bromotriptycene through a 9-lithiumtriptycene intermediate. As reported by Ishii *et al.*, two equivalents of *t*-BuLi are used in a 1:2 ratio of benzene and THF to perform lithium-halogen exchange on the 9-bromotriptycene followed by addition of three equivalents of elemental selenium powder to form *bis*-triptyceneselenide in a 42% yield (*cf.* Scheme 2.9). In our attempts at reproducing this step the major product recovered from this reaction was almost always, with the exception of one successful reaction among over a dozen, unsubstituted triptycene.

At first we suspected that the 9-lithiumtriptycene was abstracting a proton from moisture in the system, however the same result was obtained even when extra care was taken with air and moisture free techniques. We also suspected that the elemental selenium may have been the source of moisture in the reaction mixture and so it was dried under vacuum over P₂O₅ overnight and subsequently stored in a glove box. Even with the use of dry selenium, only unsubstituted triptycene was obtained as a product. This points to the possibility that the hydrogen was being abstracted from the solvent THF through the radical mechanism shown in Scheme 2.10.¹⁴

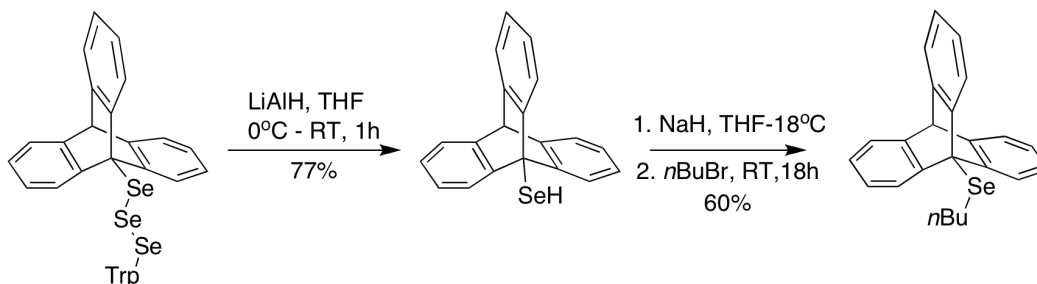


Scheme 2.10 Radical mechanism for formation of triptycene (Trp) initiated by reaction of 9-lithiumtriptycene with elemental selenium (Se_8)

To minimise the risk of abstracting a hydrogen atom from the solvent THF, we attempted the reaction in conditions reported by Hayashi *et al.* in 2009, which used the same ratio of benzene to an ether solvent, but replaced this solvent mixture with only benzene after formation of the 9-triptycenylium.¹⁵ In this method, once the lithium-halogen exchange has taken place and is complete by TLC, stirring of the reaction mixture was stopped and the 9-lithiumtriptycene precipitates as a white solid allowing the solvent mixture to be cannulated off and replaced by only benzene before the addition of elemental selenium. Therefore, if selenium oxidizes the organolithium, leaving a 1-triptycyl radical available for reaction with the solvent, benzene has been substituted as the solvent before the introduction of selenium, and does not offer a labile hydrogen. However, the desired product still was not formed and only unsubstituted triptycene and unreacted selenium were

recovered. The same result was observed a 1:2 mixture of methyl *t*-butyl ether and benzene was used as the solvent for this step. This prompted the search for an alternative synthetic approach to avoid this challenging step (*vide infra*).

Reduction of triselenide, alkylation and oxidation



Scheme 2.11 Reported synthesis of 9-triptycene(*n*-butyl)selenide

With the *bis*(triptycene)triselenide material that was made on the few occasions that the previous step worked, the subsequent reduction and alkylation were attempted as shown in Scheme 2.11. In these steps, however, we continued to encounter difficulties in repeating the previously reported work. The reduction to the selenol was only successful once out of four attempts. In all other attempts, the reduction of the triselenide could not be brought to completion using less than the 2.8 equivalents of LiAlH₄ used in the reported synthesis; however this quantity over reduced the compound and only unsubstituted triptycene and black/red selenium powder were recovered.

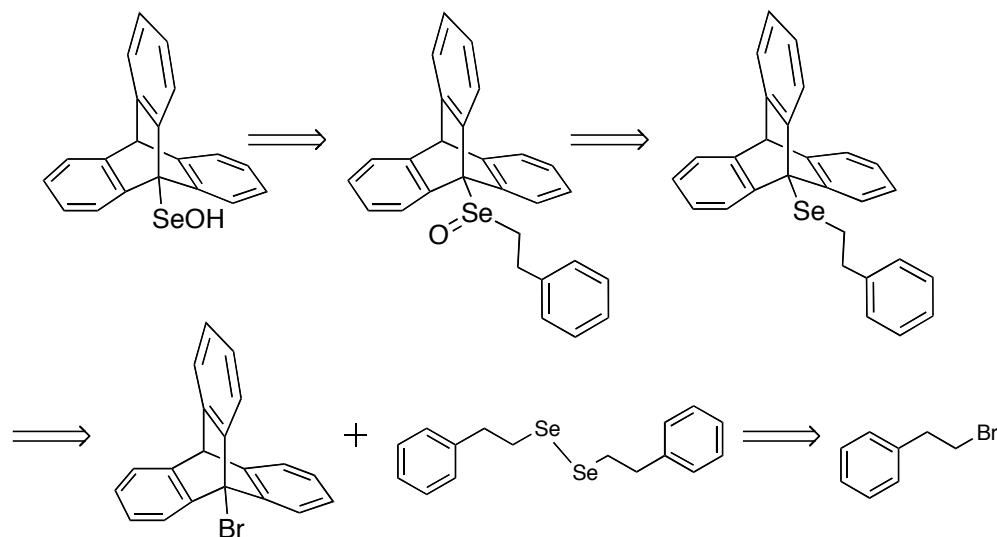
The alkylation was only attempted once, on the 9-triptyceneselenol material obtained from the sole successful reduction. Fortunately this alkylation reaction proceeded as expected and the 9-triptycene(*n*-butyl)selenide was subjected to

oxidation by DMDO. The oxidation reaction showed complete conversion from selenide to selenoxide by TLC almost immediately and was left to stir at room temperature for the six days reported to allow *syn*-elimination of selenenic acid. Formation of selenenic acid was observed by TLC, however selenoseleninate was also observed and was the only product remaining once the *syn*-elimination was complete by TLC.

Given the difficulties we faced in reproducing the synthesis of 9-triptyceneselenenic acid that was reported by Ishii *et al.*, loss of product in the selenium addition step, over-reduction of the product in the alkylation step and by-products in the final oxidation step, we chose to investigate a new synthetic approach to the desired target selenenic acid, which might eliminate these problems and possibly find a way to improve the limitations of the previous Ishii synthesis; such as low yields (42%) in the selenium addition step, the lengthy final *syn*-elimination step and difficulty reproducing the synthesis.

2.2.2 New synthetic approach to 9-triptyceneselenenic acid

The new approach to the synthesis of 9-triptyceneselenenic acid is shown in the retrosynthesis in Scheme 2.12. This synthesis is accomplished in three steps from 9-bromotriptycene; lithium-halogen exchange and addition of *bis*-phenethyldiselenide; oxidation of the resulting 9-(phenethylselenyl)triptycene; and *syn*-elimination yielding the desired selenenic acid. This new synthesis approach is shorter than the Ishii synthesis and should result in an improved overall yield.

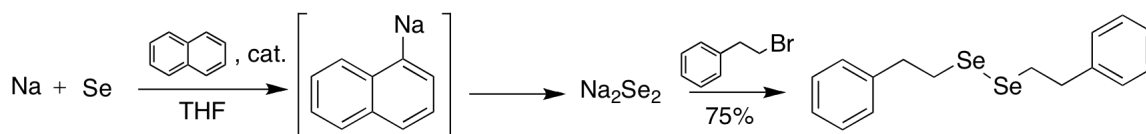


Scheme 2.12 New retrosynthetic approach to TrpSeOH

The use of the *bis*-phenethyl diselenide as the source of the selenium functionality onto the triptycene backbone rather than addition of elemental selenium reduces the total number of steps required in the synthesis by introducing both the selenium and the necessary side chain in one step rather than the three required in the Ishii synthesis (selenination, reduction, and alkylation). Because of the side chain used in this new approach, phenethyl rather than *n*-butyl, in the final step, the *syn*-elimination from the triptycene selenoxide should proceed much faster when eliminating styrene in this synthesis than the six days necessary for the elimination of 1-butene in the Ishii synthesis.

Preparing the diselenide

The starting materials for the new synthetic route to 9-triptyceneselenenic acid are 9-bromotriptycene, which is made from 9-bromoanthracene and benzyne by the method described above for the previously reported synthesis, and *bis*-phenethyl diselenide which is prepared by reaction of elemental selenium and phenethylbromide. The *bis*-phenethyl diselenide compound was prepared from sodium perselenide, which was prepared from elemental selenium and sodium naphthalide. This Na₂Se₂ salt is then reacted with phenethyl bromide to give the desired product as described by Thompson and Boudjouk.¹⁶



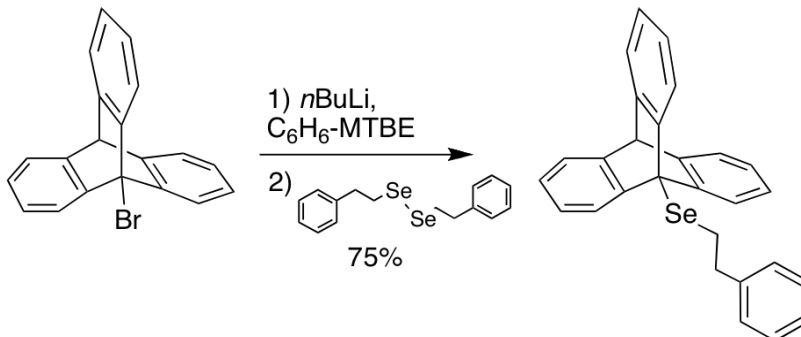
Scheme 2.13 Synthesis of *bis*-phenethyl diselenide

Triptycene substitution

In our attempts to reproduce the previously reported 9-triptyceneselenenic acid synthesis the reaction involved triptycene substitution with elemental selenium proved especially challenging. In our new approach, the same reaction must be performed using lithium-halogen exchange, but this time followed by reaction with the *bis*-phenethyl diselenide reagent described above. When the reaction was performed using the same conditions, two equivalents of *t*-BuLi in ether-benzene at -18°C followed by slow addition of the selenium-containing reagent, the major product of the reaction was again found to be unsubstituted triptycene. This was

also the case when the reaction was attempted using the two solvent system approach described above, ether-benzene for lithiation and only benzene for addition of selenium.

In order to avoid the reduction of the 9-lithiumtritycene species by hydrogen abstraction from the solvent, a 1:2 mixture of methyl *t*-butyl ether and benzene was used as the solvent for this step. The reaction proceeded easily to the desired 9-tritycene(phenethyl)selenide with greatly improved yield over the reported synthesis of *bis*-tritycene triselenide, 75% from 42% (Scheme 2.14).



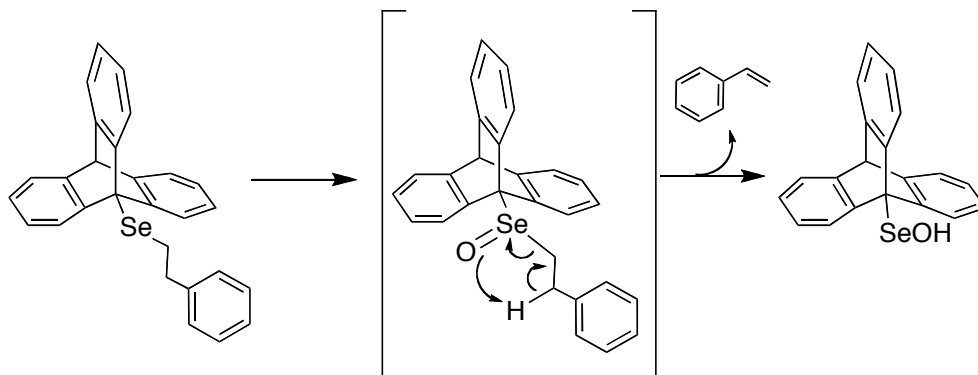
Scheme 2.14 Synthesis of 9-tritycene(phenethyl)selenide

Oxidation

With the phenethyl selenenyl triptycene intermediate in hand, the only remaining steps are the oxidation to the selenoxide intermediate and decomposition to triptycene selenenic acid (*cf.* Scheme 2.15). In an initial small-scale oxidation with DMDO done in an NMR tube and observed by NMR, the oxidation of the selenide to the selenoxide was complete within the minutes necessary to acquire the first spectrum. This successful small-scale experiment encouraged us to move on to preparative scale oxidation with DMDO. Oxidation was observed by TLC as

expected. Similar results were obtained when the oxidation was performed using *m*CPBA, eliminating the need for the complex and low yielding preparation of the more potent oxidant DMDO¹⁷ as required in the previously reported synthesis.

The *syn*-elimination from the selenoxide generated in the small-scale oxidation was also observed by NMR; the decay of the selenoxide bridgehead proton (δ 5.37 ppm) could be monitored, along with the growth of a signal corresponding to a new bridgehead proton (δ 5.42 ppm), consistent with the reported spectra for 9-triptyceneselenenic acid.¹⁰ The signals corresponding to styrene, the other elimination product, and to selenoseleninate, the product of selenenic acid self-condensation, were also observed. The spectra in Figure 2.3 show the evolution of the *syn*-elimination reaction in benzene of a sample of selenoxide prepared in the method described below.



Scheme 2.15 Oxidation and *syn*-elimination of styrene and TrpSeOH from selenoxide.

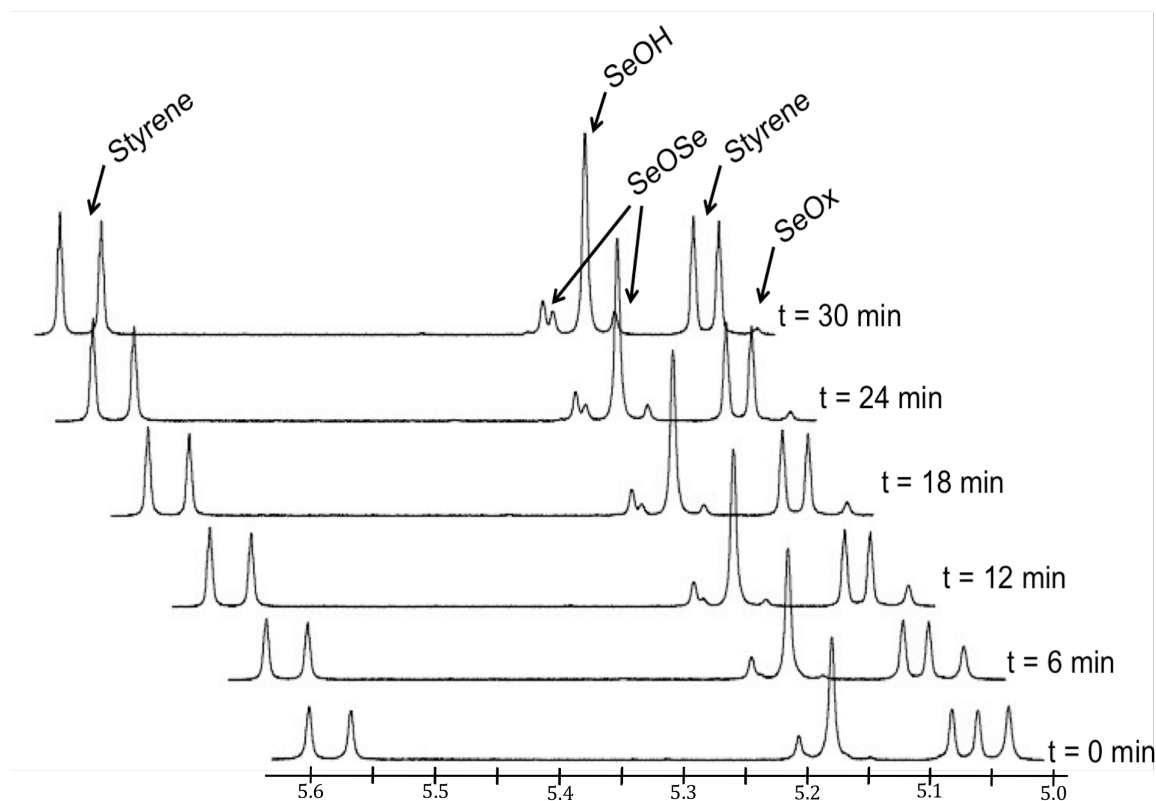


Figure 2.3 Kinetic ^1H NMR of 10 mM selenoxide (δ 5.03 ppm, SeOx) *syn*-elimination of selenenic acid (δ 5.17 ppm, SeOH) and condensation to selenoseleninate (δ 5.15 & 5.20 ppm, SeOSe), in d_6 -benzene at 25°C monitored by integration of characteristic bridgehead protons. The signal at δ 5.21 ppm represents an unknown and unchanging impurity in the reaction.

In all oxidations followed by *syn*-elimination of TrpSeOH , selenoseleninate was present in the NMR of the crude material after the reaction mixture had been concentrated *in vacuo*. This is explained by an increase in the rate of the self-condensation with increasing concentration of TrpSeOH as the solvent is being evaporated. Attempts at purifying the remaining TrpSeOH from the selenoseleninate and styrene present in the product by column chromatography were unsuccessful

because the same problem occurs when concentrating the sample of newly purified TrpSeOH.

Finally, it was decided to isolate the selenoxide rather than the selenenic acid. The selenoxide cannot self-condense and is thus less sensitive to being in an increasingly concentrated solution. The only concern is that at room temperature selenoxide eliminates styrene to give selenenic acid, which will then likely be lost to formation of selenoseleninate. Therefore it is necessary to concentrate the selenoxide while maintaining the solution below 0°C. The selenoxide was prepared by the same method of oxidation with *m*CPBA followed by a basic work up, done as quickly as possible with ice-cold water and solvents. The resulting solution of selenoxide was placed under high vacuum in a dry ice/acetone path and is concentrated over a period of several hours to give a white solid. Pure selenoxide was never observed by ¹H NMR, due to the formation of small amounts of selenenic acid during any attempt at handling the selenoxide, however that was minimized by maintaining a cold temperature as often as possible, and a mixture was observed by NMR which shows the major product to be selenoxide with selenenic acid and styrene (*cf.* Figure 2.4).

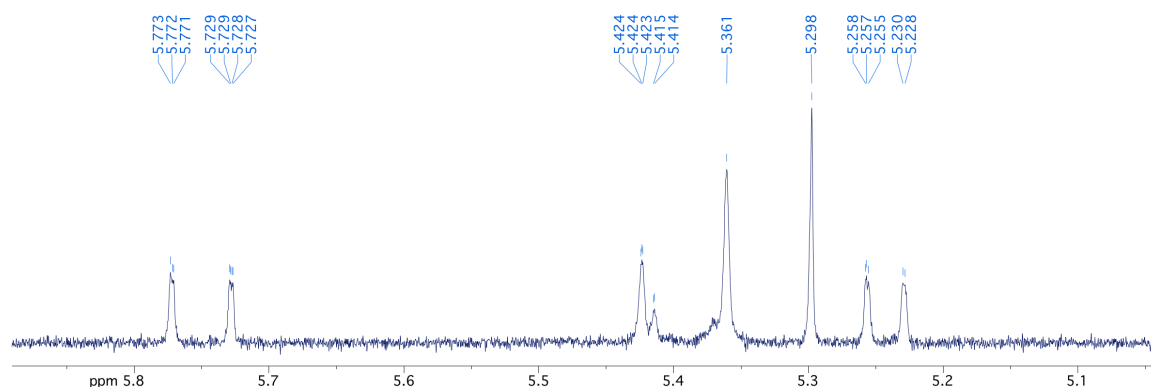
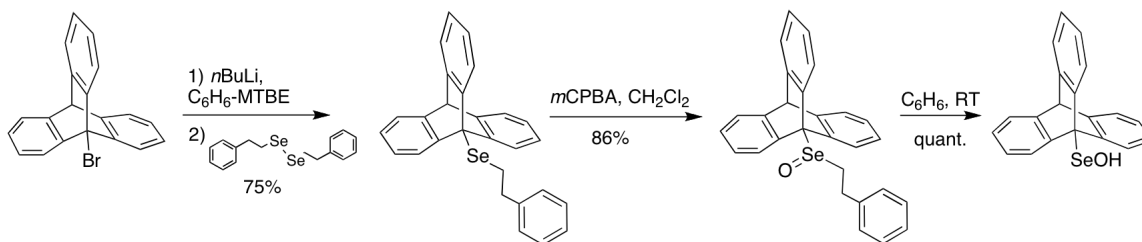


Figure 2.4 ^1H NMR (300 MHz, CDCl_3) of TrpSeOx (δ 5.36 ppm) as the major product with TrpSeOH (δ 5.42 ppm) and styrene (δ 5.25 & 5.76 ppm) in a 2:1:1 ratio. Solvent (CH_2Cl_2 , δ 5.30 ppm) is still present in this sample, along with unknown impurities at δ 5.41 ppm and δ 5.37 ppm.

The isolated selenoxide can be stored under argon in the freezer and used as needed in experiments by allowing it to decompose *in situ*. The decomposition of our compound, 9-triptycene(phenethyl)selenoxide was observed on the order of minutes by NMR (*vide infra*) rather than on the order of days as described for the 9-triptycene(*n*-butyl)selenoxide intermediate in the Ishii synthesis, making it rapid and convenient to generate selenenic acid *in situ* from our selenoxide.



Scheme 2.16 New synthesis of TrpSeOH

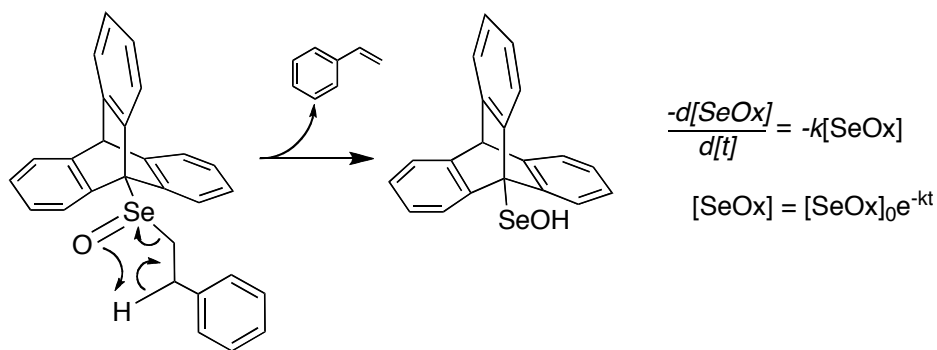
This new synthetic approach to TrpSeOH (*cf.* Scheme 2.16) is an improvement over the previously reported synthesis in that it is shorter, more reproducible and boasts better yields. It involves only two steps from the 9-bromotryptycene starting material, addition of phenethylselenide and oxidation, and both of these reactions could be carried out in higher yields than the corresponding addition of selenium and oxidation in the previously reported synthesis. Although isolation of the final product selenenic acid was not possible, an alternative method of isolating selenoxide and allowing it to decompose *in situ* to TrpSeOH for use in experiments was found and permitted the study of selenenic acid.

In comparing our results with those reported by Ishii, it is difficult to understand how their group was able to isolate TrpSeOH as a pure crystal for X-ray crystallography. In our efforts, pure TrpSeOH was never observed; styrene was always present and efforts to purify the compound only led to formation of selenoseleninate; we were also unable to crystallize the product as was reported. It is therefore unlikely that the final step of the Ishii synthesis--decomposition of the selenoxide at room temperature over six days followed by column chromatography--could be repeated with the information provided.

2.2.3 Study of 9-triptycene(phenethyl)selenoxide *syn*-elimination

In order to better understand the chemistry of the selenenic acid, and its precursor selenoxide, to be able to handle them efficiently for experiments, we set out to study the *syn*-elimination of selenenic acid from the selenoxide and the subsequent reactions undergone by selenenic acid. These studies were done using

proton NMR by following the characteristic bridgehead proton peaks of selenoxide (5.03 ppm), selenenic acid (5.17 ppm), and selenoseleninate (5.15 & 5.20 ppm). The kinetics of these reactions were monitored in d_3 -chloroform, as a comparable solvent to dichloromethane in which the oxidation and isolation of selenenic acid were previously attempted. As well as in d_6 -benzene and d_3 -acetonitrile, solvents in which we plan on performing experiments with selenenic acid and thus in which it would be helpful to understand the *syn*-elimination and self-condensation kinetics of these compounds. The relative integration of the bridgehead proton peak to the singlet of the internal standard DMF was used to determine the quantity of the products over time as the reaction progressed. Because the selenoxide elimination is a unimolecular process, we expect to see a first order exponential decay (*cf.* Scheme 2.18).



Scheme 2.17 Selenoxide (SeOx) *syn*-elimination reaction

Syn-elimination in d_6 -benzene

Selenoxide *syn*-elimination experiments were carried out in benzene, the solvent of choice for our anticipated EPR studies, discussed in Chapter 3. The starting material for this reaction, a mixture of selenoxide and selenenic acid, is

dissolved in d_6 -benzene and a small amount of DMF as an internal standard, and immediately inserted into the NMR instrument. Due to the time necessary to lock and shim the NMR instrument, the first data point can only be obtained after a few minutes of the start of the elimination reaction; the trend is extrapolated back to time zero to give an initial concentration of selenoxide.

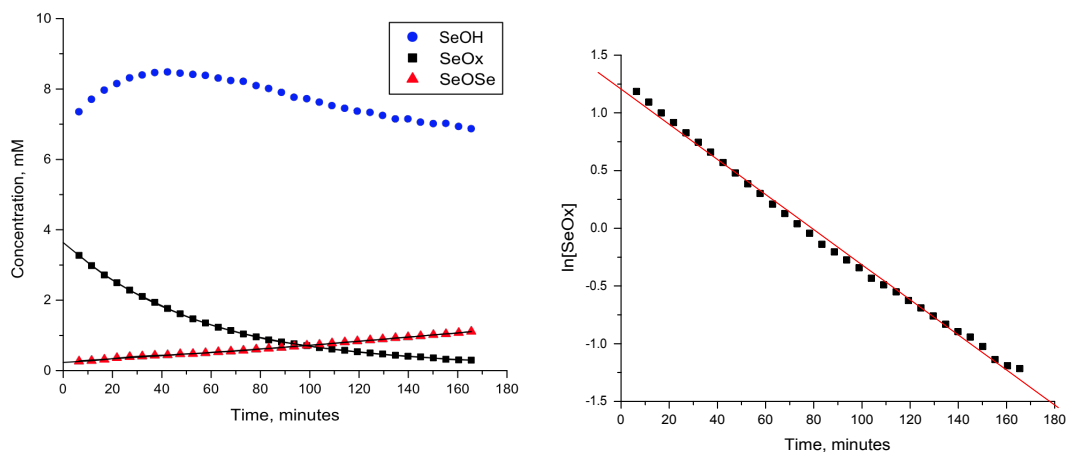


Figure 2.5 First order decay of TrpSeOx *syn*-elimination of TrpSeOH and self-condensation to selenoseleninate in d_6 -benzene. Monitored by ^1H NMR with bridgehead protons, TrpSeOx 5.03 ppm, TrpSeOH 5.17 ppm, selenoseleninate 5.15 and 5.20 ppm

In the reaction plots shown in Figure 2.5, the selenoxide follows a first order exponential decay with a rate constant of $2.5 \times 10^{-4} \text{ s}^{-1}$, which translates into a half-life of *ca.* 45 minutes. This rate appears to be initially matched by the growth of selenenic acid, for approximately the first half-life, 40 minutes, after which the selenenic acid concentration becomes too great, and it becomes vulnerable to self-condensation. At the same time, after the first half-life, considerably less selenenic

acid is being generated from selenoxide elimination, and so the net result is a decay of selenenic acid and formation of *bis*-trityceneselenoseleninate.

The results of the decomposition experiments in benzene are useful to us because they allow us to know the amount of time required for the majority of our selenoxide to undergo *syn*-elimination to give a solution of selenenic acid as major product, and thus ready to use for an experiment. With the rate constant calculated from these experiments we were able to prepare a solution of selenoxide at the desired concentration and use it soon thereafter as a solution of selenenic acid. The greatest disadvantage in this approach is that the concentration of selenenic acid is constantly changing, as seen in Figures 2.5-2.7, and we must assume the concentration of the selenenic acid solution based on the initial concentration of the selenoxide, which may not accurately represent the true concentration of selenenic acid at any given time.

However, the above experiments show that there was more selenenic acid than selenoxide in the starting material, and that there was no formation of selenoseleninate at this time. This suggests that selenoxide was undergoing decomposition in the solid state while being stored at -20°C; conditions which would not allow the bimolecular condensation reaction that leads to selenoseleninate.

Syn-elimination in d₃-chloroform

The rate of selenoxide elimination is significantly slower in chloroform than in benzene (*cf.* Figure 2.6), it proceeds with a rate constant of $4.51 \times 10^{-5} \text{ s}^{-1}$, ($t_{1/2}$ *ca.*

4.5 hours) approximately 20 times slower than in benzene. This is likely to be a result of hydrogen bonding chloroform, which stabilizes the starting material and greatly slows the Cope-type elimination, increasing the activation energy as a result. By comparison, the experiment in benzene showed a more rapid decomposition of the selenoxide, possibly because this solvent stabilizes the cyclic intermediate of the Cope-type elimination thus lowering the activation energy.

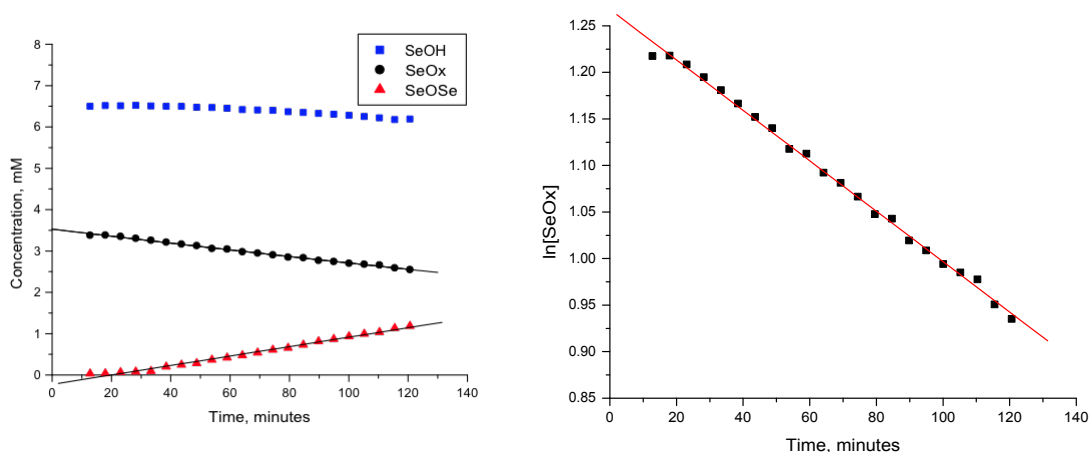


Figure 2.6 First order decay of selenoxide *syn*-elimination of selenenic acid and self-condensation to selenoseleninate in d_3 -chloroform. Monitored by ^1H NMR with bridgehead protons, TrpSeOx 5.37 ppm, TrpSeOH 5.42 ppm, selenoseleninate 5.48 and 5.49 ppm

Syn-elimination in d_3 -acetonitrile

Acetonitrile is the solvent of choice for electrochemistry studies we expect to carry out on the selenenic acid and it is necessary for this reason to understand the kinetics of the selenoxide *syn*-elimination reaction in acetonitrile, as we did in benzene and chloroform, in order to know the materials present in our samples.

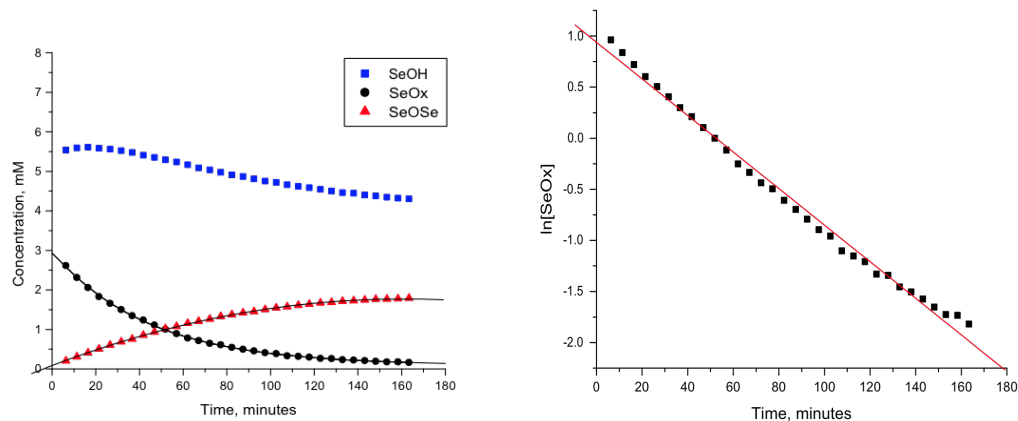


Figure 2.7 First order decay of selenoxide *syn*-elimination of selenenic acid and self-condensation to selenoseleninate in d_3 -acetonitrile

The *syn*-elimination reaction in acetonitrile (Figure 2.7) showed a rapid first order exponential decay of selenoxide as was also observed in benzene, and a faster loss of selenenic acid and growth in selenoseleninate. The decay of selenoxide occurs with a rate constant of $2.98 \times 10^{-4} \text{ s}^{-1}$, or a half-life of 39 minutes in acetonitrile. However, contrary to the results observed in benzene, the period of growth in selenenic acid doesn't last approximately one half life of the selenoxide, the concentration in selenenic acid begins to drop almost immediately and is of course accompanied by growth of selenoseleninate. This means that after approximately two hours, when the bulk of selenoxide has undergone *syn*-elimination, the mixture is not strictly the desired selenenic acid, but rather a 2.4:1 mixture of selenenic acid and selenoseleninate, which is likely to make precise electrochemical study more challenging.

Studies of selenoxide *syn*-elimination in benzene, chloroform and acetonitrile have yielded further knowledge of the formation of selenenic acid and the undesired by-product selenoseleninate and have shown that our approach to the synthesis of selenenic acid through selenoxide isolation affords better control of the reactivity of the final product. The initial concentrations in this experiment are especially interesting as they show a majority of TrpSeOH with no selenoseleninate present. This suggests that while TrpSeOH can be formed from decomposition of TrpSeOx either during the concentration of the product at -78°C or while stored in the solid state at -20°C, the condensation to selenoseleninate cannot occur under these conditions. This provides insight into a potential approach to isolating pure TrpSeOH, likely involving cold temperatures and maintaining the product either at low concentrations, which greatly reduce the rate of the bimolecular condensation reaction, or maintaining it in the solid state.

2.3 Conclusions

Our efforts towards the synthesis of TrpSeOH were more challenging than expected. We had significant difficulty repeating the previously reported synthesis as it was described, and were unable to obtain pure material as reported. Our new synthesis for TrpSeOH is shorter, higher yielding and more reproducible than the Ishii synthesis. The process of purifying and isolating TrpSeOH was more challenging than described by Ishii and co-workers, and prompted us to isolate TrpSeOx instead and to study its decomposition to TrpSeOH. These studies afforded insight into the reactivity of these compounds and should be helpful in future work.

Further efforts towards purification and full characterization of TrpSeOH are required and will hopefully make the subsequent experiments using the compound more facile and precise.

Note: Following the initial submission of this thesis, further experiments showed that decomposition of the selenoxide in the solid state over a period of two weeks yield pure selenenic acid.¹⁸

2.4 Experimental Procedures

General Procedures. All reagents were obtained from commercial sources and used without purification unless specified. Dry THF was obtained by distillation from sodium metal and benzophenone indicator. Selenium powder was dried over P₂O₅ under vacuum overnight and stored under argon. Methyl *tert*-butyl ether was purified by running through a column of alumina, followed by fractional distillation and was stored over sieves. Column chromatography was carried out using flash silica gel (60Å, 40-63 μ, 500 m²/g). ¹H and ¹³C NMR spectra were recorded on Bruker AVANCE 300 MHz and 400 MHz spectrometers at 298 K and referenced to CDCl₃ (δ 7.27 ppm and 77.36 ppm, respectively)

9-Bromotriptycene. To a suspension of anthranilic acid (9.17 g, 66.9 mmol) in THF (75.0 mL, 1.00 M) at 0°C was added trichloroacetic acid (508 mg, 3.11 mmol) followed by isoamyl nitrite (14.6 mL, 109 mmol) slowly. The reaction mixture was stirred in a melting ice bath for 1-2 hours until a tan precipitate formed. The

benzenediazonium-2-carboxylate was then collected by filtration with a fritted glass funnel and washed with cold THF until the washings were colourless and then DCE to displace the THF (note: care should be taken to avoid letting the salt become dry as it is known to detonate violently upon being heated or being scraped). The solvent-wet salt was washed with DCE (80.0 mL, 0.15 M) into a round bottom flask containing 9-bromoanthracene (4.00 g, 15.6 mmol) and equipped with a reflux condenser. The reaction mixture was heated to 60°C and a mildly exothermic reaction occurred after about 5-10 minutes, turning the reaction mixture from tan to black in colour. The reaction was then heated overnight and concentrated in vacuo. The product was purified by silica gel chromatography (eluent: 10-25 % methylene chloride/hexanes) to give 9-bromotriptycene (10.1 g, 65%). ¹H (CDCl₃, 400 MHz) δ ppm 5.44 (s, 1H), 7.05-7.10 (m, 6H), 7.37-7.41 (m, 3H), 7.78-7.82 (m, 3H) ¹³C (CDCl₃, 100 MHz) δ ppm 53.9, 71.6, 123.2, 124.0, 125.6, 126.5, 143.8, 144.5, HRMS (EI⁺) calculated (M) 332.0201, observed 332.0164.

Bis(2-phenethyl) diselenide. Dry selenium powder (3.50 g, 44.3 mmol), dry THF (100 mL), sodium chips (1.06 g, 44.2 mmol), and naphthalene (0.57 g, 4.45 mmol) were stirred overnight under argon in a flame-dried round-bottom flask. The mixture appeared dark purple and no sodium remained after ~12 hours, 2-bromoethylbenzene (6.03 mL, 44.0 mmol) was added drop-wise at room temperature with stirring. The mixture warmed slightly after addition. After 30 minutes of stirring the mixture changed color to a light orange. The mixture was stirred for an extra 30 min. The reaction mixture was filtered to remove a tan salt, and the filtrate was

concentrated *in vacuo*. The resulting orange oil was purified by column chromatography on silica gel, first with hexane and then an orange band was eluted with benzene and concentrated to obtain an orange oil product (7.77g, 91% yield). ^1H (CDCl_3 , 400 MHz) δ ppm 3.03-3.07 (m, 4H), 3.14-3.18 (m, 4H), 7.20-7.24 (m, 6H), 7.29-7.32 (m, 4H), ^{13}C (CDCl_3 , 100 MHz) δ ppm 30.7 37.5, 126.4, 128.5, 128.5, 140.8, HRMS (EI^+) calculated (M) 369.6739 observed 369.7735. The spectral characteristics are in good agreement with those presented in the literature.¹⁶

9-Triptycene(phenethyl)selenide. 9-Bromotriptycene (1.80 g, 5.42 mmol) was dissolved in dry benzene (100 mL) and dry methyl *tert*-butylether (70.0 mL) in a round bottom flask (flamed dried and cooled under argon), and cooled to -18°C . *n*-Butyllithium (3.80 mL, 5.44 mmol) was added dropwise. *Bis*-(phenethyl)-diselenide (2.10 g, 5.44 mmol) was suspended in a minimum amount of dry benzene and added dropwise to the reaction mixture at 0°C (slow addition of the diselenide was important in obtaining good yields). The reaction was stirred at room temperature overnight, quenched with water and extracted with ether, washed with a saturated NaCl solution, dried over MgSO_4 , and concentrated *in vacuo*. The resulting oily yellow solid was purified by silica gel chromatography (eluent: 5% dichloromethane/ hexanes) to yield an off white solid which was recrystallized from benzene/ ethanol to give 1.77 g, 75%). ^1H -NMR (400 MHz; CDCl_3) δ ppm 7.56-7.52 (m, 3H), 7.38-7.30 (m, 8H), 7.02-6.97 (m, 3H), 5.36 (s, 1H), 3.33-3.28 (m, 2H), 3.21-3.16 (m, 2H), ^{13}C (CDCl_3 , 100 MHz) δ ppm 25.6, 36.7, 54.1, 60.1, 123.2, 123.9, 124.9,

125.4, 126.5, 128.4, 128.5, 140.5, 145.0, 145.5, HRMS (EI⁺) calculated (M⁺) 438.0887, observed 438.0876. New compound (see Schemes 2.18).

9-Triptycene(phenethyl)selenoxide. *9-triptycene(phenethyl)selenide* (94 mg, 0.21 mmol) was weighed into a flame-dried flask, cooled under argon. Flask and product were placed under vacuum and refilled with argon three times. Dichloromethane (18 mL, from solvent purification system) was added to the flask and stirred at room temperature until the product was dissolved; the resulting clear reaction mixture was cooled to -78°C. *m*CPBA (77%, 48 mg, 0.21 mmol) was added slowly in 5.0 mL DCM. Reaction was checked by TLC (4:1 DCM/Hexanes), in most cases the reaction was complete immediately after addition of *m*CPBA. If not small portions (2.5 mg, 0.014 mmol) of *m*CPBA were added until no starting material remained on TLC. Once complete, the reaction mixture was worked up immediately by washing twice with 20 mL cold 0.7M KOH solution, followed by 20 mL ice water and 20 mL saturated NaCl solution. Organic phase was dried with MgSO₄, filtered and dried *in vacuo* while temperature remained at -78°C. A white or pale yellow solid was obtained (84 mg, 86% yield). The 9-triptycene(phenethyl)selenoxide was generally obtained as a mixture with 9-triptyceneselenenic acid and styrene; this can be minimized by keeping the sample cold throughout work up and concentration. ¹H NMR (300 MHz, CDCl₃) δ ppm 3.47-3.64 (m, 2H), 3.83-3.93 (m, 1H), 4.00-4.09 (m, 1H), 5.37 (s, 1H), 7.02-7.05 (m, 6H), 7.28-7.37 (m, 9H) 7.93-8.02 (m, 1H), 8.31-8.39 (m, 1H), ¹³C (CDCl₃, 100 MHz) δ ppm 29.8, 30.6, 48.8, 124.3, 126.1, 127.3, 128.9,

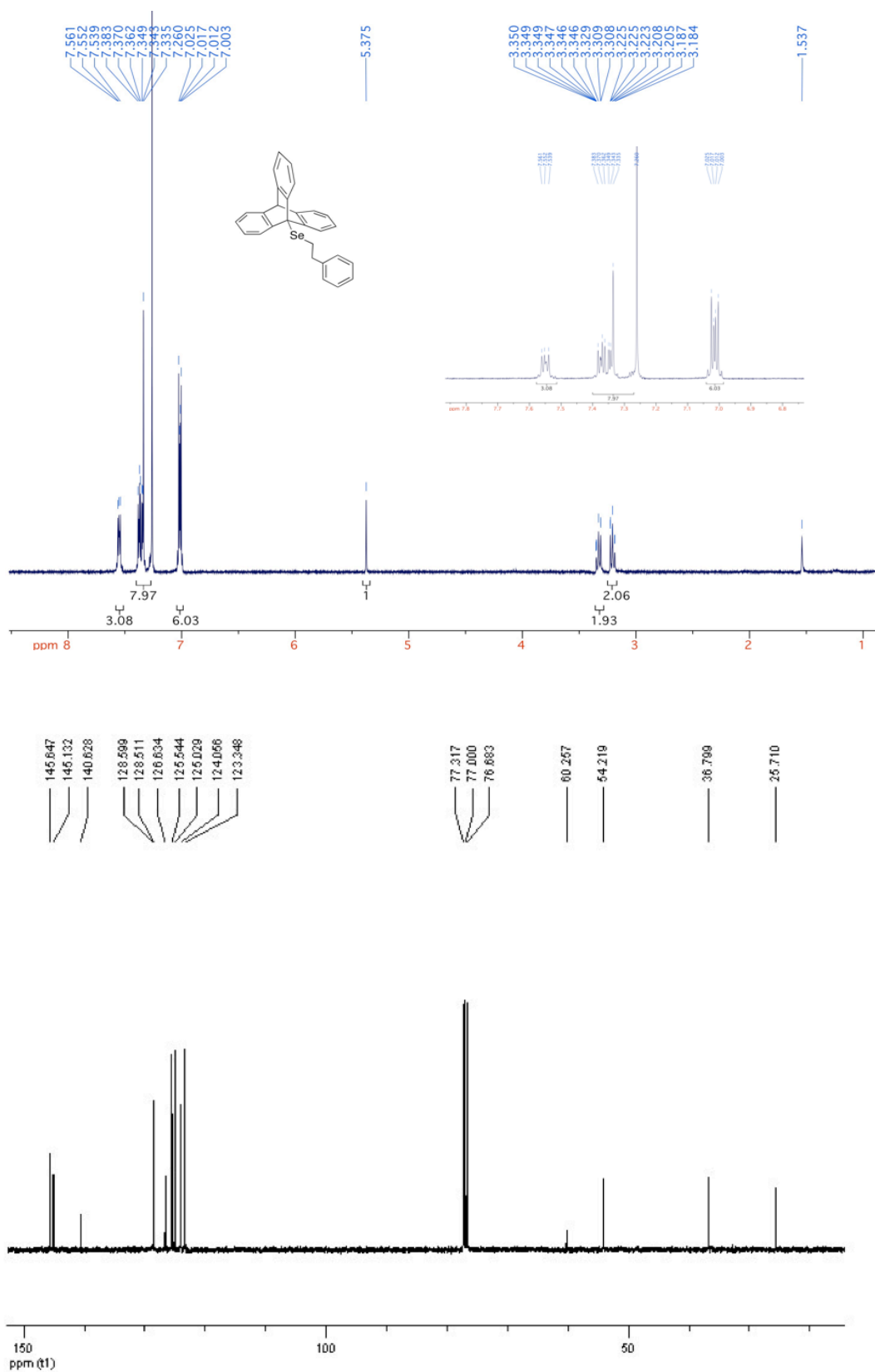
138.9, 144.4, 145.8, HRMS (EI⁺) calculated (M) 454.0834, observed 235.1 (triptycene), 189.1 (Se₂O₂), 104.1 (styrene). New compound (see Scheme 2.19).

9-Triptyceneselenenic acid. 9-triptycene(phenethyl)selenoxide (15 mg, 0.034 mmol) was dissolved in benzene (2.5 ml) and stirred at room temperature for 2 hours. The product was used as a solution in benzene. ¹H NMR (300 MHz, CDCl₃) δ ppm 5.42 (s, 1H), 7.02-7.05 (m, 6H), 7.41-7.44 (m, 6H), ¹³C (CDCl₃, 100 MHz) δ ppm 54.1, 123.0, 123.7, 125.3, 125.7, 144.3, 145.7 observed NMR as a mixture with styrene and *bis*-9-(phenethyltriptycene)selenoseleninate. Spectral characteristics are in good agreement with those presented in the literature.¹⁰

Styrene. ¹H NMR (300 MHz, CDCl₃) δ ppm 5.25 (dd, 1H), 5.76, (dd, 1H), 6.69 (q, 1H), 7.36 (m, 5H), ¹³C (400 MHz, CDCl₃) δ ppm 113.7, 126.2, 127.8, 128.5, 136.9.

***bis*-9-(Phenethyltriptycene)selenoseleninate.** Obtained as a yellow solid by-product in the synthesis of 9-triptyceneselenenic acid. ¹H NMR (300 MHz, CDCl₃) δ ppm 5.48 (s, 1H), 5.49 (s, 1H), 7.07-7.15 (m, 11H), 7.46-7.55 (m, 9H), 7.87-7.90 (m, 4H) observed by ¹H NMR as a mixture with 9-triptyceneselenenic acid. The spectral characteristics are in good agreement with those presented in the literature.¹⁰

NMR decomposition experiments. The starting material mixture of TrpSeO_x and TrpSeOH (5 mg) was dissolved in 0.6 mL of the deuterated solvent and DMF (0.001 mL, 0.013 mmol) in a NMR tube. Spectra of 16 scans were taken at 4 minute intervals using Bruker AVANCE 300 MHz spectrometer and integrated automatically using Bruker Topspin software.



Scheme 2.18 ¹H NMR (Top) and ¹³C NMR (bottom) of 9-triptycene(phenethyl) selenide

2.5 References

- ¹ Rotruck, J.T.; Pope, A.L.; Ganther, H.E.; Swanson, A.B.; Hafeman, D.G.; Hoekstra, W.G. *Science* **1973**, 179, 588-590.
- ² Stadtman, T.C. *J. Biol. Chem.* **1991**, 266, 16257-16260.
- ³ Back, T.G. in “Organoselenium Chemistry – A Practical Approach”, Oxford University Press, Oxford, **1999**, Chapter 2.
- ⁴ Reich, H.J; Hoeger, C.A.; Willis, W.W. Jr. *Tetrahedron* **1985**, 21, 4771-4779.
- ⁵ Behagel, O.; Müller, W. *Chem. Ber.* **1935**, 68, 1540-1548.
- ⁶ Rheinbolt, H.; Perrier, M. *Bull. Soc. Chem. Fr.* **1955**, 445-463.
- ⁷ Reich, H.J.; Jasperse, C.P. *J. Org. Chem.* **1988**, 53, 2389-2390
- ⁸ Goto, K.; Saiki, T.; Okazaki, R. *Phosphorus, Sulfur Silicon Relat. Elem.* **1998**, 136:1, 475-487.
- ⁹ Goto, K.; Nagahama, M.; Mizushima, T.; Shimada, K.; Kawashima, T.; Okazaki, R. *Org. Lett.* **2001**, 3, 3569–3572.
- ¹⁰ Ishii, A.; Matsubayashi, S.; Takahashi, T.; Nakayama, J. *J. Org. Chem.* **1999**, 64, 1084-1085.
- ¹¹ Nakamura, N. *J. Org. Chem.* **1983**, 105, 7173-7175.
- ¹² Friedman, L., Logullo, F.M. *J. Am. Chem. Soc.* **1963**, 85, 1549–1549.
- ¹³ McGrath, A.J.; Garrett, G.E.; Valgimigli, L.; Pratt, D.A. *J. Am. Chem. Soc.* **2010**, 132, 16759-16761.
- ¹⁴ Kawada, Y.; Iwamura, H. *J. Org. Chem.* **1981**, 46, 3357-3359.
- ¹⁵ Hayashi, S.; Nakamoto, T.; Minoura, M.; Nakanishi, W. *J. Org. Chem.* **2009**, 74, 4763-4771.

¹⁶ Thompson, D.P.; Boudjouk, P. *J. Org. Chem.* **1988**, 53, 2109-2112.

¹⁷ Murray, R.W.; Singh, M. *Org. Syn.*, **1997**, 74, 91-96.

¹⁸ Zielinski, Z.; Presseau, N.; Amorati, R.; Valgimigli, L.; Pratt, D.A., *J. Am. Chem. Soc.* **2014**, 136, 1570–1578

CHAPTER 3

STUDY OF A PERSISTENT SELENENIC ACID

3.1 Introduction

Determining the properties of selenenic acids is made difficult by their instability—in particular, their propensity to self-condense to selenoseleninates. Therefore, little is known about their chemistry. The synthesis of a persistent selenenic acid, 9-triptyceneselenenic acid (TrpSeOH), described in Chapter 2, has made it possible to conduct experiments with a selenenic acid. Of particular interest to the Pratt group are the redox properties of selenenic acids, *i.e.* the standard potential for oxidation of the selenenic acid and/or the selenenate ion— $E^\circ(\text{RSeOH}/\text{RSeOH}\cdot^+)$ and/or $E^\circ(\text{RSeO}^-/\text{RSeO}\cdot)$ —and the bond dissociation enthalpy (BDE) of the selenenic acid O-H bond, as well as the rate constants with which selenenic acids react with peroxy radicals.

Recent work by the Pratt group in the synthesis and study of a persistent sulfenic acid, reported the standard potential (E°): 0.74 V, the RSO-H BDE: 71.9 kcal/mol, the pK_a 12.5 and the k_{inh} : $3 \times 10^6 \text{ M}^{-1}\text{s}^{-1}$ of 9-triptycenesulfenic acid (TrpSOH).^{1,2} These results confirmed the prediction (made on the basis of quantum chemical calculations) that sulfenic acids have far lower O-H BDEs than their more common isoelectronic analogues, hydroperoxides (*ca.* 72 kcal/mol *vs.* *ca.* 88 kcal/mol).³ Likewise, inhibited autoxidations demonstrated that TrpSOH has a k_{inh} of $3 \times 10^6 \text{ M}^{-1}\text{s}^{-1}$, similar to the most reactive of radical-trapping antioxidants, and much greater than hydroperoxides (10^2 - $10^3 \text{ M}^{-1}\text{s}^{-1}$), despite the steric bulk associated with the triptycene moiety.⁴

Given that selenenic acids are the heavier chalcogen analogues of sulfenic acids and hydroperoxides, and have similar involvement in redox enzymes *in vivo*,⁵ it would be informative to compare experimental results to the analogous sulfenic acids and hydroperoxides, comparisons that have only been possible only by computational studies to date (*cf.* Chapter 1). The computed O-H BDEs have been higher for selenenic acids than for sulfenic acids (HSeOH 86.5 kcal/mol *vs.* HSOH 73.1 kcal/mol), computed E_a in the reaction of selenenic acids with peroxy radicals were lower than in the case of sulfenic acids (3.0 kcal/mol *vs.* 4.6 kcal/mol). For this reason, it would be interesting to be able to compare the experimental O-H BDEs and k_{inh} , and ideally, it would be of interest to also obtain redox (E°) and acid-base (pK_a) data with which we can compare to sulfenic acids and hydroperoxides in order to better understand the differences in the chemistry of the primary chalcogen oxyacids.

3.2 Results and Discussion

3.2.1 Electrochemistry

To provide insight into the redox behaviour of selenenic acids, cyclic voltammetry (CV) experiments were carried out on solutions of 9-triptyceneselenenic acid in acetonitrile. Since the selenenic acid is formed *in situ* by elimination from the corresponding selenoxide (see Chapter 2), it should be noted that the solutions contain a mixture of selenenic acid, selenoxide and styrene, as well as the supporting electrolyte (Bu_4PF_6). Voltammograms were referenced *vs.* NHE using the ferrocene/ferrocenium redox couple as a reference.⁶ A representative voltammogram obtained at 100 mV/s is shown in Figure 3.1. A single anodic (oxidation) peak is clear at ~ 1.0 V *vs.* NHE, but

there is no corresponding cathodic (reduction) peak. Faster scan rates, i.e. 200, 500 and 1000 mV/s were also investigated in an attempt to capture some of the $\text{TrpSeO}^{\bullet+}$ oxidation product before subsequent reactions could take place and observe some reversibility. However even at faster scan rates no cathodic peak was observed and the anodic peak became less clear and in some cases absent. Attempts were also made to observe the system through multiple scans of the same sample. Although these voltammograms were not very clear or reproducible, in occasional cases the anodic peak decreased after the first scan and was entirely gone after the second scan. Despite our efforts, no reversible, or quasi-reversible, voltammograms were obtained for TrpSeOH , implying that the radicals derived therefrom, i.e. $\text{TrpSeO}^{\bullet+}$ and/or TrpSeO^{\bullet} , undergo further chemistry on the timescale of the experiment.

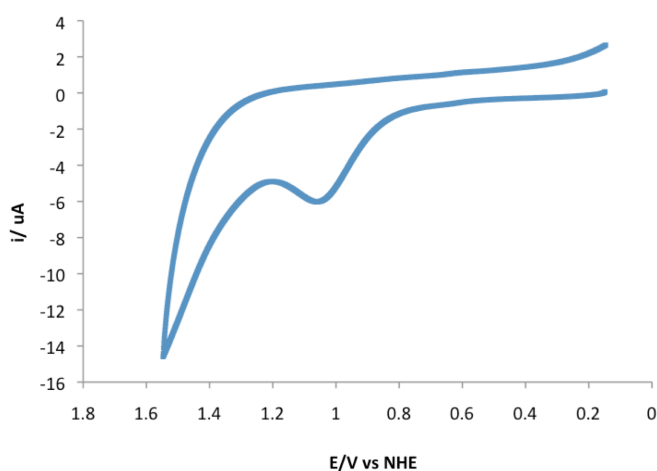
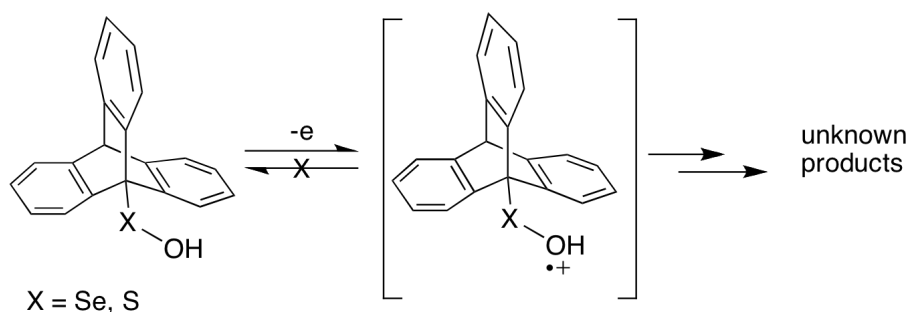


Figure 3.1 Cyclic voltammogram corresponding to the oxidation of TrpSeOH (generated *in situ* from a 5.0 mM solution of TrpSeOX) acetonitrile containing 0.1 M Bu_4PF_6 as supporting electrolyte at a scan rate of 100 mV/s.

Voltammograms obtained by our group on TrpSOH were also irreversible, suggesting that the $\text{TrpSOH}^{\bullet+}$ radical cation is unstable and undergoes further chemistry

before it can be reduced back to the starting species. The peak potential at 100 mV/s was $E_{pa} \sim 1.4 \text{ V vs NHE}$,¹ higher than the TrpSeOH $E_{pa} \sim 1.0 \text{ V vs NHE}$, suggesting that TrpSeOH is more easily oxidized than TrpSOH.



Scheme 3.1 Oxidation of either TrpSeOH or TrpSOH produces a radical cation species, which rapidly undergoes further chemistry, precluding reduction back to the original species.

Additional voltammograms were recorded in the presence of an organic base, (Bu_4NOH) to produce the $\text{RSeO}^-/\text{RSeO}^\bullet$ redox couple, precluding any concerns over the instability of the radical cation derived from TrpSeOH. The voltammograms obtained for the $\text{RSeO}^-/\text{RSeO}^\bullet$ redox couple were not always reproducible however two examples of are presented in Figure 3.2. Unfortunately, addition of the base, Bu_4NOH , did not produce a quasi-reversible cyclic voltammogram as was observed in the case of TrpSOH (*cf.* Figure 3.2). Instead with addition of 0.5 equivalents of base, the previously observed seemed to have shifted to a slightly higher voltage ($\sim 1.2 \text{ V vs NHE}$), and a new possible new anodic peak appeared at 0.7 V vs NHE . With addition of 2 equivalents of base, the voltammogram shows two clear anodic peaks at ~ 1.2 and 0.7 V vs NHE . The peak at 0.7

V vs NHE must be associated to the one-electron oxidation of the more electron rich TrpSeO^- anion to the TrpSeO^\bullet radical, and the peak at ~ 1.2 V vs NHE may be associated to oxidation of TrpSeOH , although this peak should not still appear with an excess of base, it did appear in other voltammograms with 1 or more equivalents of base.

Attempts were also made to record voltammograms of TrpSeOH in the presence of an acid ($\text{CF}_3\text{SO}_3\text{H}$), however no signal was observed. Similarly, no signal was observed in the voltammogram of selenoseleninate and so we propose that in the presence of acid, the condensation of TrpSeOH is fast and only selenoseleninate is present at the time of the measurement, giving no signal.

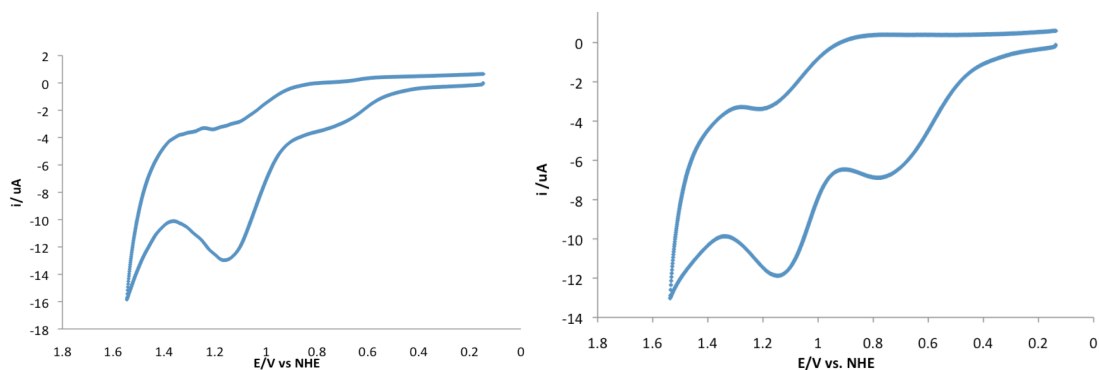


Figure 3.2 Cyclic voltammograms corresponding to the oxidation of TrpSeOH (generated *in situ* from a 5.0 mM solution of TrpSeOX) in acetonitrile containing 0.1 M Bu_4PF_6 as supporting electrolyte and (left) 2.5 mM Bu_4NOH at a scan rate of 100 mV/s and (right) 10 mM Bu_4NOH at a scan rate of 100 mV/s.

In a previously reported voltammogram of TrpSOH recorded in the presence of 1 equivalent of Bu_4NOH a cathodic peak was observed (Figure 3.3), indicating that TrpSO^\bullet is persistent in acetonitrile and allowing the calculation of $E^\circ = 0.74$ V vs NHE for the $\text{TrpSO}^-/\text{TrpSO}^\bullet$ redox couple.¹ Although we can safely conclude that both the selenenic acid and seleninate anion are more easily oxidized than the corresponding

sulfenic acid and sulfinate anion on the basis of the E_{pa} values that were determined for each, we cannot provide any accurate redox thermodynamics. This result shows that $\text{TrpSO}\cdot$ is more persistent than $\text{TrpSeO}\cdot$, because it has not undergone subsequent chemistry on the timescale of the experiment, unlike $\text{TrpSeO}\cdot$. This may be due to the combination of two $\text{TrpSeO}\cdot$ to form selenoseleninate. The equivalent reaction of two $\text{TrpSO}\cdot$ to form thiosulfinate is not possible because of increased steric hinderance due to the shorter S-S bond length, possibly explaining the difference in persistence between these two radicals.

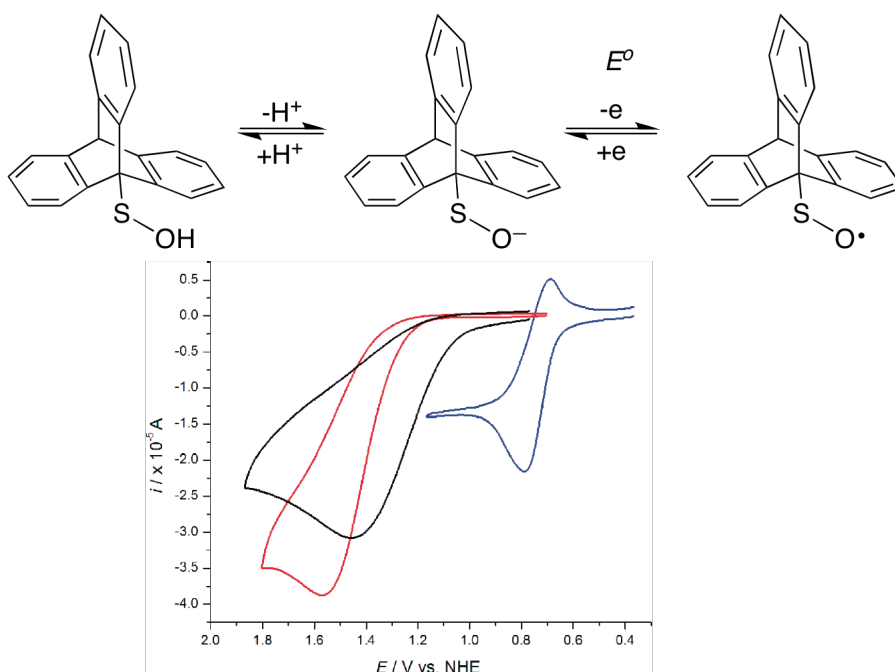
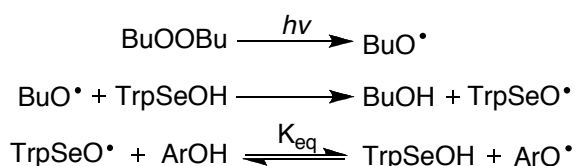


Figure 3.3 Cyclic voltammograms corresponding to the oxidation of 5 mM TrpSOH in MeCN containing 0.1 M Bu_4PF_6 as supporting electrolyte and no additive (black), (b) 30 mM $\text{CF}_3\text{SO}_3\text{H}$ (red), or (c) 5 mM Bu_4NOH (blue) at a scan rate of 100 mV/s. Reprinted with permission from McGrath, A.J.; Garrett, G.E.; Valgimigli, L.; Pratt, D.A., *J. Am. Chem. Soc.* 2010, 132, 16759-16761. Copyright 2010 American Chemical Society.¹

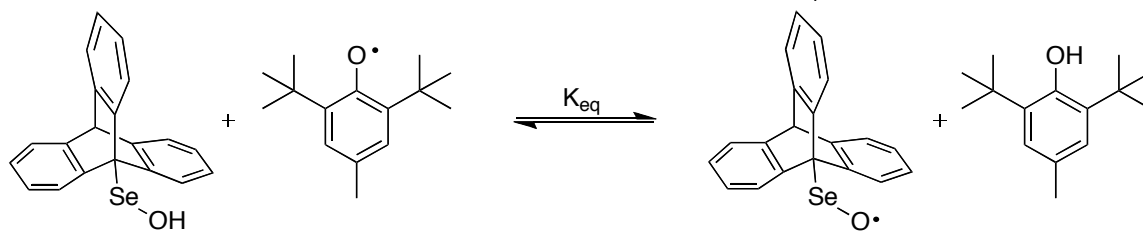
3.2.2 Electron Paramagnetic Resonance

Electron Paramagnetic Resonance (EPR) is a technique that allows the characterization of unpaired electrons, much in the same way that NMR allows the observation of nucleus such as ^1H and ^{13}C . It is also used in the favoured method for determining X-H BDEs;^{7,8} radical equilibration electron paramagnetic resonance (REqEPR). This process uses the equilibrium constant between two radicals, one of which is from a compound with a known BDE and acts as a reference, in order to calculate the unknown BDE (Scheme 3.1).



$$K_{\text{eq}} = \frac{[\text{TrpSeO}^\bullet][\text{ArO-H}]}{[\text{TrpSeOH}][\text{ArO}^\bullet]}$$

$$\text{BDE}(\text{TrpSeOH}) = \text{BDE}(\text{ArOH}) - RT/\ln K_{\text{eq}}$$



Scheme 3.2 REqEPR of TrpSeOH with BHT to determine SeO-H BDE from K_{eq} Equation for BDE (TrpSeOH) is dependant on the assumption that the entropy change for the radical equilibration is negligible.

In order to perform REqEPR, the reference compound chosen must have an O-H BDE that is within a few kcal/mol of TrpSeOH and must yield a persistent

radical on the EPR timescale (seconds to milliseconds on most conventional spectrometers). The computed BDE for MeSeO-H is 81.9 kcal/mol,² so 2,6-di-*tert*-butyl-4-methylphenol (BHT), with its O-H BDE of 81.02 kcal/mol,⁹ can be anticipated to be a good reference compound.

Before attempting EPR of TrpSeOH, instrument and conditions were tested using a sample of TrpSOH that has a known EPR spectrum. In fact, the EPR spectrum of the 9-tripycenesulfinyl radical (TrpSO•) was used in a REqEPR experiment with TEMPO to determine the O-H BDE in 9-triptycenesulfenic acid (71.9 ± 0.3 kcal/mol).¹ TrpSO• was obtained by irradiation of 10% v/v di-*tert*-butylperoxide, to generate *t*BuO•, to abstract H from TrpSOH, all done in the absence of O₂. The spectrum obtained (Figure 3.4) was in good agreement with the reported spectrum.¹

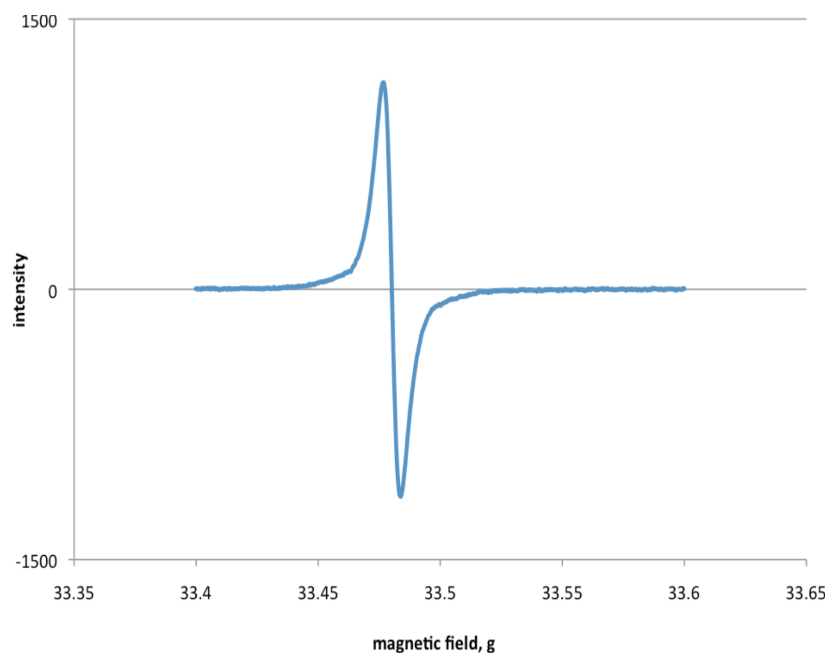


Figure 3.4 EPR spectrum of TrpSO• from irradiation of TrpSOH with 10% v/v di-*tert*-butylperoxide in the absence of O₂. g value = 2.01199.

A 30 mM sample of TrpSeO_x was then prepared in the same way, in benzene with di-*tert*-butyl peroxide, and allowed to decompose to TrpSeOH (in benzene) as described in Chapter 2 (~30 minutes) before irradiation and data collection. Unfortunately, no spectrum was observed for TrpSeO• under the same conditions used for the TrpSO• spectrum.

This may be because TrpSeO• is not sufficiently persistent on the time scale necessary to acquire the spectrum. It stands to reason that the selenenyl radical will be more reactive than the sulfinyl radical because the predicted SeO-H BDE is higher than the SO-H BDE (~81 kcal/mol vs. 71.9 kcal/mol). This is likely due to the longer Se-O bond, meaning the radical is less sterically protected by the triptycene moiety

and that the radical in TrpSeO• is less delocalized onto the Se atom than the radical in TrpSO• would be on the S atom.

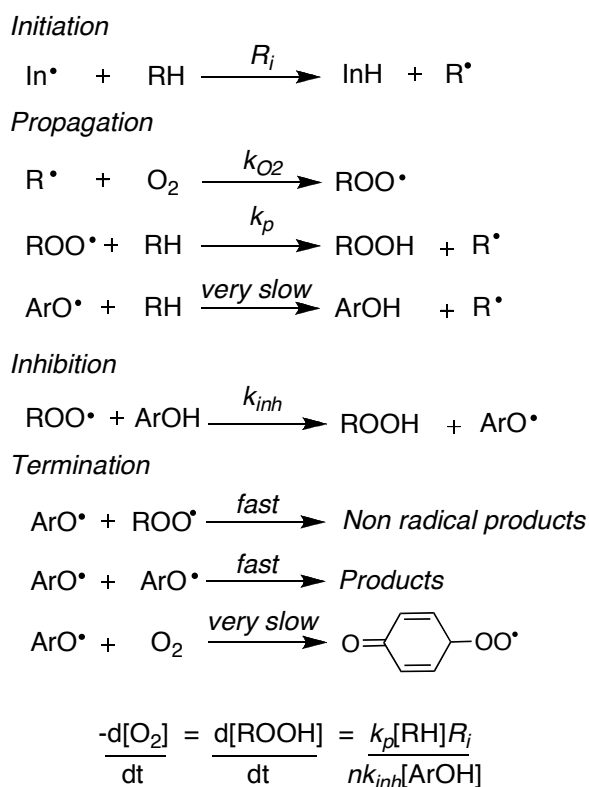
After attempts at obtaining EPR spectra, the sample of TrSeOH contained yellow precipitate, which by ¹H NMR appeared to contain selenoseleninate. Therefore, it is possible that once formed, the TrpSeO• is combining to produce selenoseleninate. This would not have been observed with TrpSO•, because its equivalent to selenoseleninate, the triptycenesulfinate, is too hindered given the shorter S-S bond length. This may explain why TrpSO• is so persistent and TrpSeO• is not.

If the TrpSeO• does not persist long enough, it may be helpful to use Laser Flash Photolysis (LFP) rather than a manually controlled lamp in order to minimize both the length of irradiation and the delay before the spectrum is acquired. Unfortunately, a time-resolved EPR instrument was not available for us to use for this experiment. It remains to be seen whether the lifetime of TrpSeO• is sufficiently long, and the rate of TrpSeO• combination sufficiently slow, to allow for equilibration with the BHT radical, a process which is diffusion controlled.

3.2.3 Antioxidant Activity

As described in Chapter 1, lipids readily undergo radical chain lipid peroxidation initiated by ROS which gives rise to lipid hydroperoxides. The efficiency of a *chain-breaking* antioxidant is measured by its ability to transfer a hydrogen atom to the chain propagating peroxy radicals, indicated by k_{inh} (scheme 3.2). The k_{inh} is measured by monitoring the inhibition of an autoxidation by the antioxidant of interest as compared to

the uninhibited autoxidation. Autoxidations can be monitored either by measuring either the disappearance of O₂ or the formation of peroxides as shown in the equation in Scheme 3.4, where d[O₂]/dt is the rate of O₂ consumption, d[ROOH]/dt is the rate of peroxide formation, k_p is the rate of propagation, R_i the rate of initiation, n the stoichiometric number for the antioxidant (the radical equivalents that can be trapped) and k_{inh} is the inhibition rate constant.



Scheme 3.3 Inhibition of radical autoxidation by phenolic antioxidant.

Sulfenic acids are known to be potent radical-trapping antioxidants, 2-propenesulfenic acid (derived from garlic's allicin), S-benzylphenylmethanethiosulfinate (isolated from *Peteveria alliaceae*, BPT) and the recently synthesized stable TrpSOH; all

show inhibition rate constants between $\sim 10^7$ - $10^8 \text{ mol}^{-1} \text{ s}^{-1}$.^{1,3,10} This raises the question of the antioxidant role of the equivalent TrpSeOH synthesized in Chapter 2.

Several methods exist to monitor autoxidations, these include iodometry, GC/HPLC analysis, enzymatic methods or fluorescence assays to monitor peroxide formation as oxidation occurs or using an oxygen uptake apparatus (OUA) to monitor consumption of molecular oxygen in the reaction system. While all allow for kinetic study of uninhibited and inhibited autoxidations, and determination of k_{inh} of an antioxidant in question, many also have some disadvantages.

Iodometric titration is tedious and air-sensitive. Analysis by GC or HPLC requires separation and analysis of each sample, which can be very lengthy over many time points. The OUA consists of a closed system with a pressure transducer between reaction and reference cells in order to measure the difference in pressure associated with consumption of O_2 by the autoxidation,¹¹ and is very sensitive and must be very carefully calibrated. It is therefore challenging to obtain reproducible results.

A more facile approach to studying autoxidations is to use fluorescent assays with probes that are “switched on” by lipid peroxides. Several of these dyes have been reported. They function through photoinduced electron transfer (PET) depicted in Figure 3.6 an electron from the donor’s HOMO quenches the fluorescence while in the “off” mode, but upon oxidation by a peroxide, the change in this HOMO’s energy prevents this electron transfer and allows fluorescence.

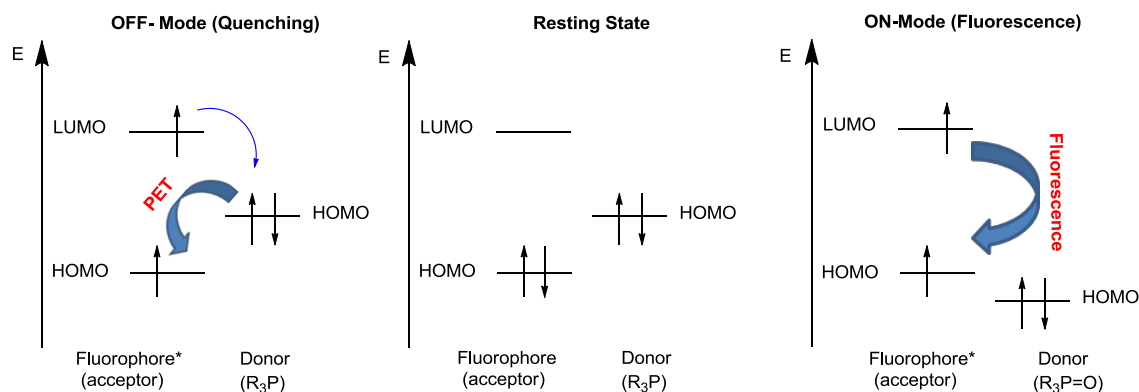
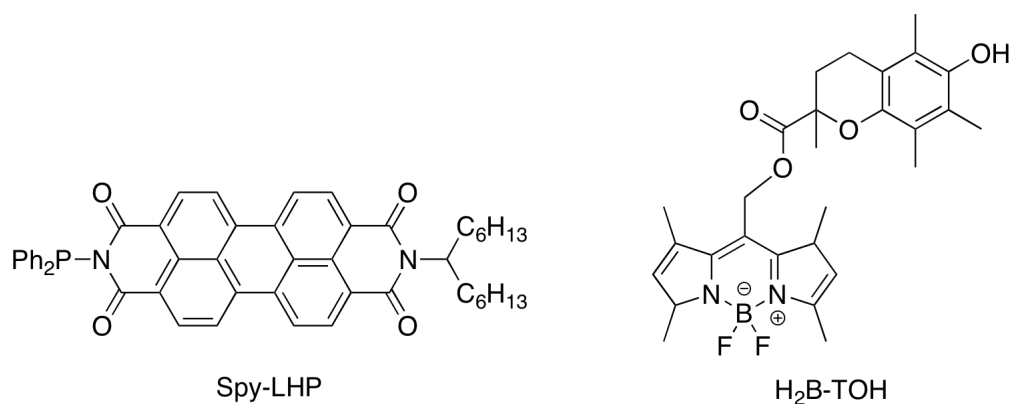
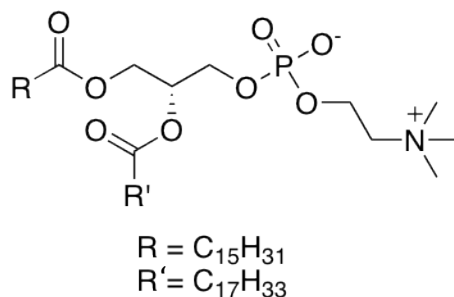


Figure 3.5 Illustration of energy diagrams of the orbitals involved in photoinduced electron transfer mechanism, the HOMO and LUMO of the fluorophore (* indicates excited state) and the HOMO of the donor quenched and fluorescent modes. Reprinted with permission from Schaferling, M.; Grogel, D. B. M.; Schreml, S. *Microchimica Acta* 2011, 174, 1. Copyright 2011 Springer.¹²

Recent examples of these fluorescent peroxide probes include Spy-LHP, a perylene-derived triphenyl phosphine-containing fluorescent dye that can be used for live-cell imaging of lipid peroxides.¹³ These fluorescent probes are effective for qualitative observation of lipid hydroperoxide formation in cells but are not sensitive and precise enough for quantitative measurements of the lipid hydroperoxide over the time course of an autoxidation experiment for the determination of k_{inh} .



Liposomes composed of a bilayer of phospholipids such as phosphocholine found in eggs, are used to simulate cell membranes in biological studies. Studies in lipid bilayers are important in the study of antioxidants because this where lipid peroxidation is especially problematic and thought to cause various cardiovascular and neurodegenerative diseases.¹⁴



Structure of L- α -Phosphocholine (eggPC)

Recent reports by Cosa *et al.* demonstrate the use of fluorogenic TOH analogues as probes for lipid peroxides in egg phosphatidylcholine liposomes. This methodology allowed the first k_{inh} α -TOH and PMHC in lipid bilayers, rather than homogeneous solvents. The fluorescent probes used in the liposomes contain a fluorescent moiety, BODIPY and the α -TOH analogue chromanol head, shown above, (H₂B-PMHC).¹⁵

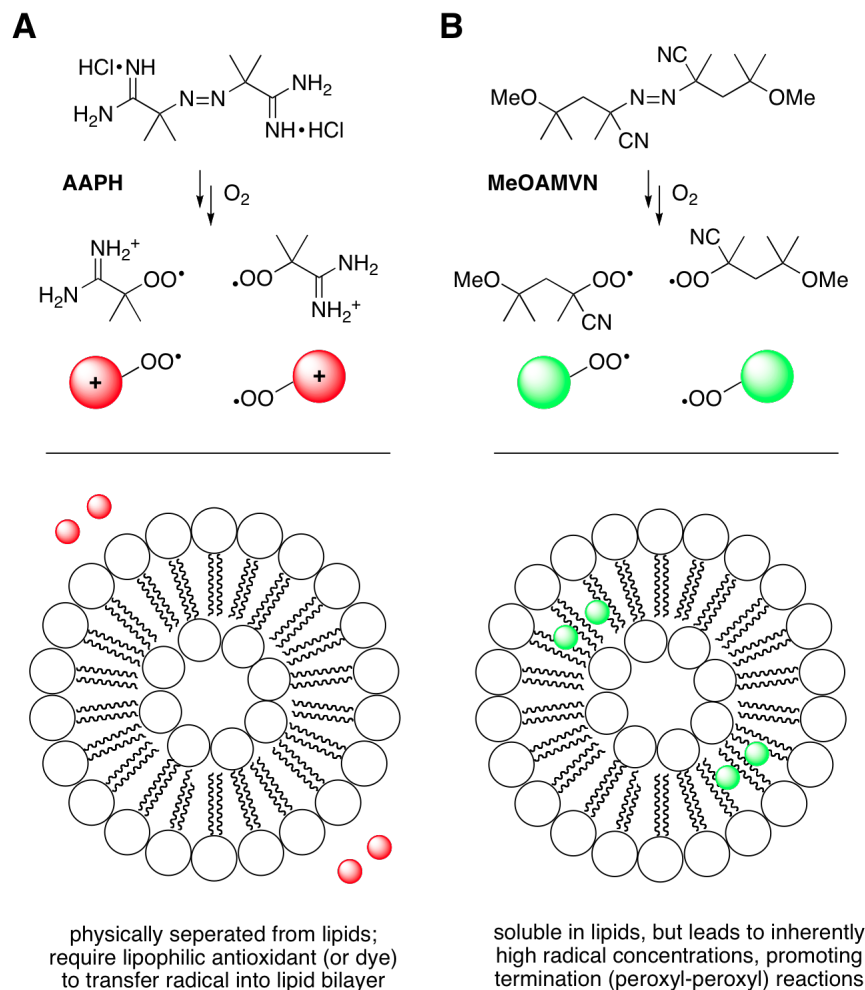


Figure 3.6 Illustration of liposomes bilayers made from egg phosphatidylcholine with hydrophilic (A) or hydrophobic (B) radical initiators.

Experiments were conducted using the same conditions as for TrpSeOH, liposomes were prepared from egg phosphatidylcholine in phosphate buffer (pH 7.4). Autoxidations were initiated either in the aqueous phase, using hydrophilic initiator 2,2'-azobis(2-amidinopropane)monohydrochloride (ABAP) or in the lipid bilayer, using hydrophobic initiator 2,2'-azobis(4-methoxy-2,4-dimethylvaleronitrile) (MeOAMVN) as illustrated in Figure 3.7.

Autoxidations were performed with varying concentrations of TrpSeOx, known to eliminate to TrpSeOH (see Chapter 2) or TrpSeEtPh, the precursor to 9-triptyceneselenoxide. It was expected that in the first case, TrpSeOx would be fully decomposed to TrpSeOH by the start of the experiment and that this species would demonstrate inhibition of the autoxidation. In the second case, we hypothesized that the selenide would be oxidized by the peroxide products of the lipid peroxidation to the selenoxide, which would decompose to give TrpSeOH, the hypothesized antioxidant. If this were to occur, the selenide would react more rapidly with peroxy radicals than the fluorescent probe H₂B-PMHC, forming selenoxide and preventing fluorescence of the probe. The subsequently formed TrpSeOH, would then also compete with H₂B-PMHC for reaction with peroxy radicals, also preventing fluorescence from being observed.

TrpSeOx was prepared immediately before the experiment, by oxidation of the selenide with *m*CPBA, and the reaction mixture was added directly to the liposome samples. Although a rapid and cold basic extraction is usually conducted after this oxidation in order to remove the *meta*-chlorobenzoic acid (*m*CBA) by-product, it was believed that the biphasic liposome system would act in lieu of this extraction by allowing the greasy triptycene compounds to penetrate the lipid bilayer while the benzoic acid remained in the aqueous phosphate buffer.

In recent studies by our group using TrpSOH as an antioxidant in these liposome systems, a well-defined inhibition period was observed in autoxidations with both radical initiators, ABAP and MeOAMVN (shown in Figure 3.11). The inhibition was found to be greater with TrpSOH than with the α -TOH analogue PMHC. Inspired by

these successful results, we hypothesized that inhibition of lipid peroxidation by TrpSeOH could also be observed in these liposomes using the H₂B-TOH, but no inhibition was observed. This shows that TrpSeOH is a less effective antioxidant than TrpSOH in these liposomes at pH 7.4 as it does not compete with H₂B-TOH for reaction with peroxy radicals under these conditions. However it does not necessarily demonstrate that TrpSeOH does not possess any antioxidant ability.

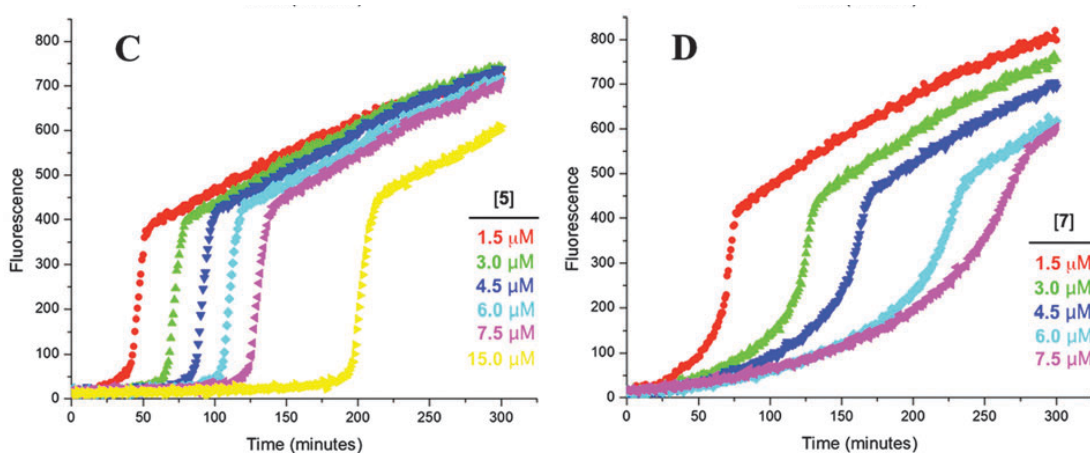


Figure 3.7 Fluorescence (at 520 nm) intensity–time profiles from MeOAMVN-mediated (0.2 mM) oxidations of egg phosphatidylcholine liposomes (1 mM) containing 0.15 mM H₂B-PMHC and increasing concentrations of 9-triptycenesulfenic acid (C) or PMHC (D). Reprinted with permission from Zheng, F.; Pratt, D.A., *Chem. Commun.*, **2013**, 49, 8181-8183. Copyright 2013 American Chemical Society.¹⁶

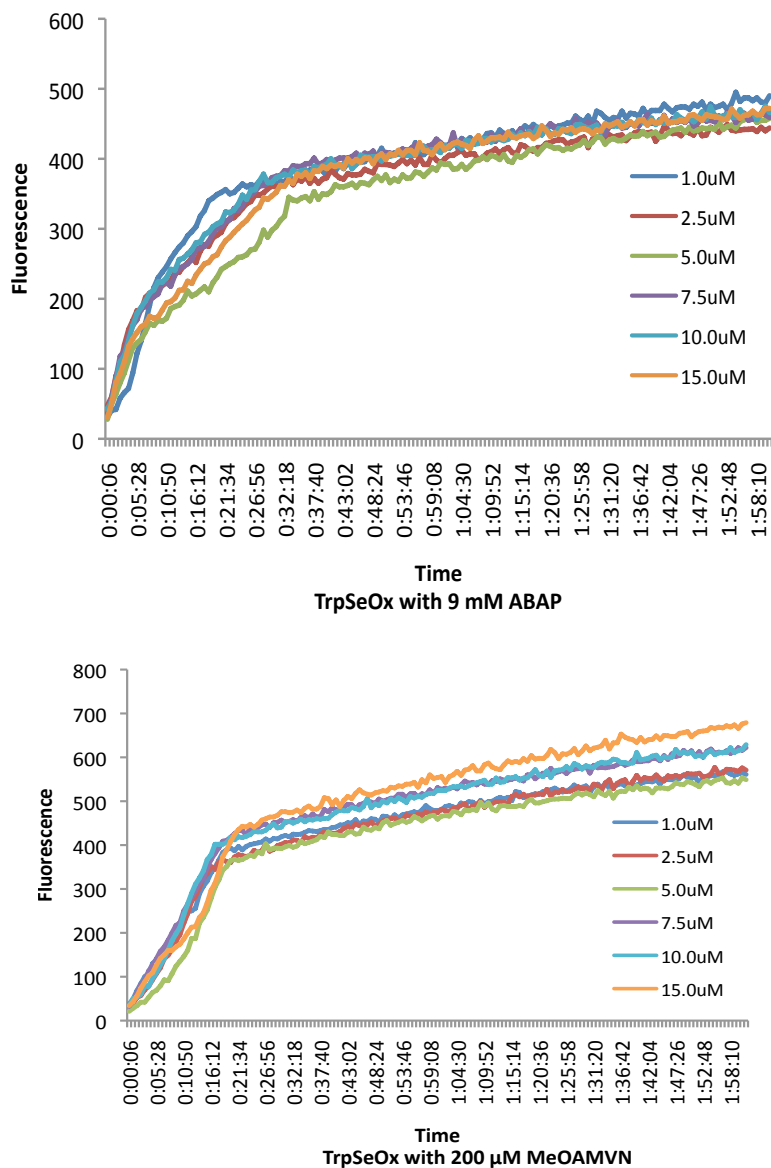


Figure 3.8 Fluorescence intensity–time profiles recorded in 1 mM egg phosphatidylcholine liposomes with increasing concentrations of TrpSeOx and ABAP (top), or MeOAMVN (bottom), showing no inhibition period.

No inhibition period of the autoxidation was observed at any concentration of the TrpSeOx with either the hydrophilic or hydrophobic initiating radicals (*cf* Figure 3.8). Under these experimental conditions, any inhibition of the autoxidation

depends on the effective generation *in situ* of TrpSeOH from TrpSeOx. It is possible that in the liposomes the elimination did not take place, or was not rapid enough to generate TrpSeOH that could compete with the fluorescent probe in reactions with lipid peroxides. It is also possible that the presence of *mCBA* was not as innocuous as expected. It is known that the condensation reaction of two TrpSeOH to form selenoseleninate is acid catalyzed, so if TrpSeOH were formed *in situ* but was exposed to *mCBA*, it may be lost without playing an antioxidant role. Another consideration is the pH of the buffer used in the liposome experiment, which has a pH of 7.4, because the pK_a of TrpSeOH has not been measured, it is unknown whether TrpSeOH may be deprotonated under these conditions, in which case it would not have an H-atom to donate to the lipid peroxy radicals it is intended to trap. Finally, it is also a distinct possibility that although TrpSeOH was formed and persistent under the experimental conditions, it simply did not demonstrate any antioxidant activity, if it is less efficient at reacting with peroxy radicals than the fluorogenic α -TOH analogue used as indicator, it would not register any inhibition.

The same result was observed when the selenide precursor was used as in the case of TrpSeOx: no inhibition (*cf.* Figure 3.9). Because no inhibition is observed in either case, it is impossible to determine whether the selenide doesn't show results because it is not converted to TrpSeOH under the experimental conditions, or whether we are simply seeing the same TrpSeOH result.

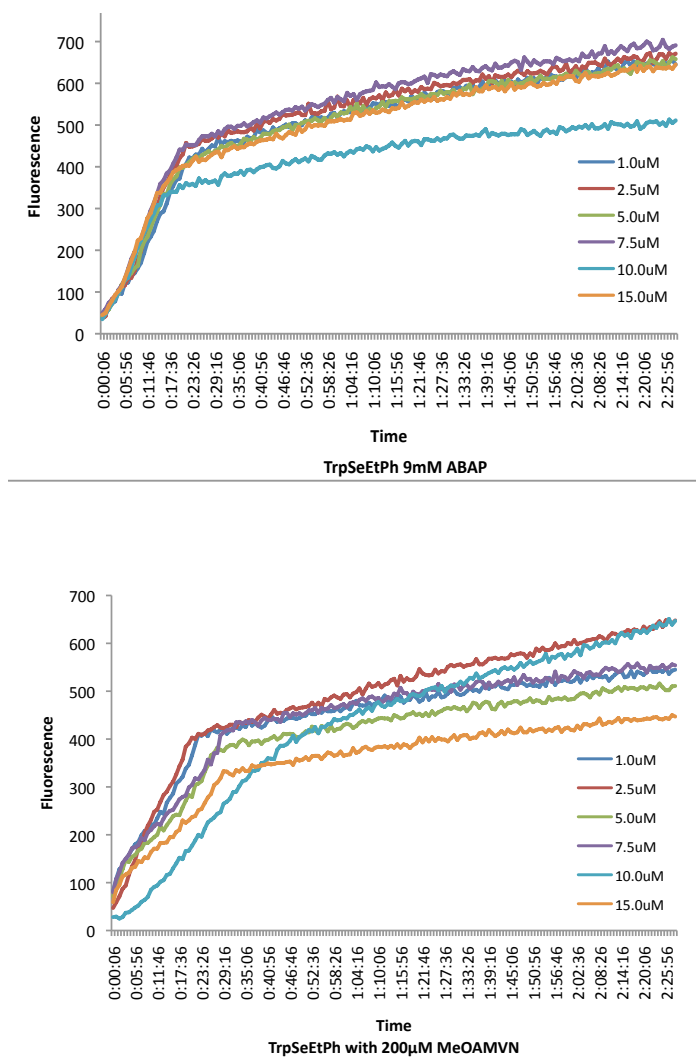


Figure 3.9 Fluorescence intensity–time profiles recorded in 1 mM egg phosphatidylcholine liposomes with increasing concentrations of TrpSeEtPh and ABAP (top), or MeOAMVN (bottom), showing no inhibition period.

Given the various problems and unknowns in these two cases of *in situ* generation of TrpSeOH, another approach was taken, this time preparing TrpSeOx exactly as reported in Chapter 2, and preparing a stock solution in MeCN where the *syn*-elimination proceeds with a known rate constant ($2.98 \times 10^{-4} \text{ s}^{-1}$) and the stock solution can be stirred at room temperature until it is converted to TrpSeOH as the

major product. Addition of this stock solution to the liposome samples eliminates uncertainty regarding the real concentration of TrpSeOH in the samples. However, as shown in Figure 3.10, even with accurate concentrations of authentic TrpSeOH in the autoxidations, no inhibition was observed.

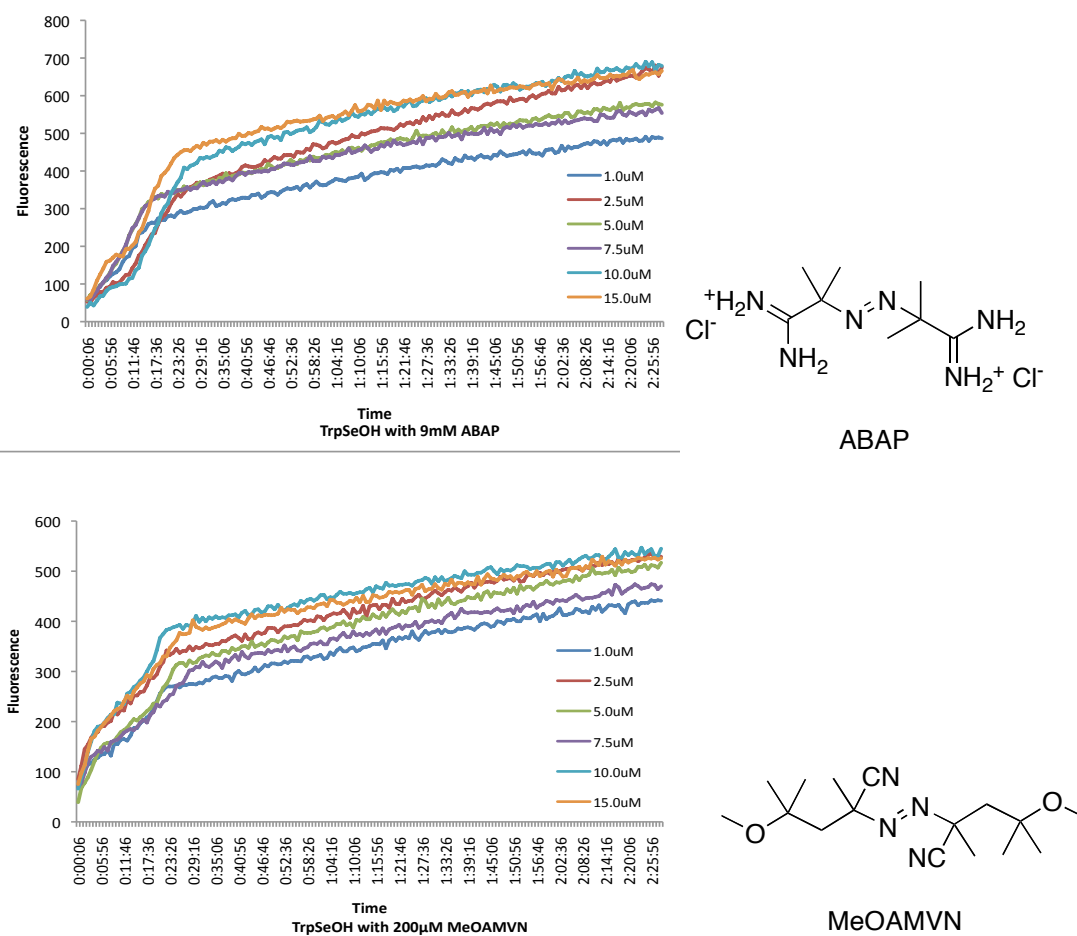
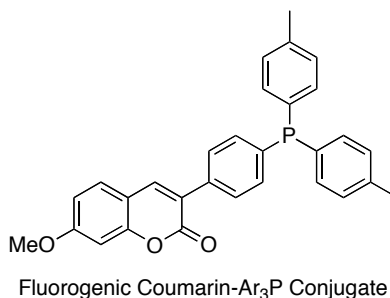


Figure 3.10 Fluorescence intensity–time profiles recorded in 1 mM egg phosphatidylcholine liposomes with increasing concentrations of TrpSeOH and ABAP (top), or MeOAMVN (bottom), showing no inhibition period.

An important experiment that may explain this disappointing result from the liposome studies and allow for observation of radical trapping by TrpSeOH is to perform

the inhibited autoxidation in a homogenous organic solvent. This would eliminate possible problems stemming from the complex reaction mixture, different phases, and slightly basic pH. Preliminary oxygen uptake experiments were conducted using styrene autoxidation with a model compound for TrpSeOH, *bis*-phenethylselenide as the antioxidant. However the instrument used was very challenging to equilibrate and results were so extremely diverse in three trials that further experimentation using this approach was aborted.

Fortunately, our group recently reported the synthesis of a fluorescent coumarin-triarylphosphine conjugate, activated by reaction with hydroperoxides that has been used to monitor 7-dehydrocholesterol and hexadecane autoxidations in organic solvents.¹⁷



Inhibited autoxidations using TrpSeOH could be monitored using this method, affording a more simple system in comparison to the liposomes, and thus increasing the precision of the results and a greater likelihood of observing any antioxidant activity that may be exhibited by TrpSeOH.

3.3 Conclusions

The reactivity of TrpSeOH and the method for its generation *in situ* from TrpSeOx before experiments made the studies in this chapter challenging and none yielded the desired results. The voltammograms did not show reversible oxidation and

did not allow for determination of E° , however a preliminary E_{pa} was observed at 0.7 V vs NHE for TrpSeOH and 0.2 V vs NHE for TrpSeO⁻. No EPR spectra could be observed for TrpSeOH and thus the experimental SeO-H BDE could not be determined. The experimental conditions may not have been fast enough to observe the compound during its short lifetime and further EPR studies should be carried out using a laser as the photon source and a faster acquisition time. However if the TrpSeO• is too short lived, it may not be possible to use REqEPR to determine the SeO-H BDE. Lastly, no inhibition occurred by TrpSeOH in lipid peroxidations in liposomes, which may be due to poor hydrogen trapping by TrpSeOH or due to the inability of TrpSeOH to reach the autoxidation occurring within the liposome. A novel fluorescent coumarin-triarylphosphine conjugate will allow autoxidations studies to take place in organic solvents and may provide a better environment to observe radical trapping by TrpSeOH. Although these studies are made difficult by the instability of TrpSeOH, preliminary results have demonstrated that it can, under the right conditions, be used in experiments.

Note: Following the initial submission of this thesis, collaborators at the University of Bologna in Italy conducted further EPR and inhibited autoxidation experiments using TrpSeOH, yielding valuable results that contribute to our understanding of TrpSeO• persistence, the O-H BDE of TrpSeOH, and antioxidant activity of TrpSeOH. Valgimigli was able to observe the TrpSeO• radical by EPR using continuous photolysis and shorter acquisition time. The selenenyl radical was not found to be persistent, however it did have life times long enough to equilibrate with 2,4,6-tri-*tert*-butylphenoxy radical and determine a preliminary O-H BDE of 80.3 ± 0.7 Kcal/mol. Given this result, TrpSeOH

should exhibit antioxidant properties. Valgimigli conducted inhibited styrene autoxidations and did observe inhibition by TrpSeOH and calculated its inhibition rate constant of $1.7 \times 10^5 \text{ M}^{-1}\text{s}^{-1}$.¹⁸

As discussed in a note at the end of Chapter 2, the method for isolation of pure TrpSeOH was achieved after the initial submission of this thesis. With pure TrpSeOH, inhibited autoxidations experiments in liposomes can be conducted using the exact method that was used for TrpSOH without depending on the *in situ* decomposition of the selenoxide to TrpSeOH to observe inhibition. Furthermore, because TrpSeOH has shown antioxidant properties in styrene autoxidations, it will likely act as an antioxidant in the liposome experiments as well.

3.4 Experimental Procedures

Electrochemistry. Cyclic voltametry was performed using a BASi potentiostat with a glassy-carbon working electrode, a platinum counter electrode and Ag/AgNO₃ (0.005 M) reference electrode. Samples were measured in dry/argon purged acetonitrile using Bu₄N•PF₆ (0.1 M) as an electrolyte at 25°C. Cyclic voltammograms were obtained using a scan rate of 100 mV/s. All sets of experiments were immediately preceded by a verification of the voltammetric properties of the ferrocene/ferrocenium⁺ couple, which was used as a reference (400 mV vs. NHE).¹⁹

Electron Paramagnetic Resonance. EPR attempts were performed at 25°C in a JOEL JES-FA100 spectrometer. A solution of TrpSeOH (30 mM) in benzene, containing 10% v/v di-*tert*-butyl peroxide, oxygen was removed by sparging with

argon. Sample was irradiated by short (10-30s) beam of focused light of a Luzchem LUZ-XE Xenon 175 W lamp in the cavity of the spectrometer. Results were compared to a sample of TrpSOH prepared in the same way.

Liposome preparation. 137 mg of eggPC was weighed into a dry vial and dissolved with a minimal amount of chloroform. The solvent was evaporated with a stream of argon while rotating the sample vial to create a thin film on the vial wall. The film was left under vacuum to remove excess solvent. After 1 h the aliquot of eggPC was hydrated with 9 mL of a pH 7.4, 10 mM PBS solution 150 mM in NaCl, yielding a 20 mM lipid suspension. The lipid suspensions were subjected to ten freeze–thaw–sonication–vortex cycles, where each cycle involved storing the vials with the solutions in dry ice for 4 min and then thawing at 37 °C for 4 min, followed by 4 min sonication. After the third cycle, the lipid suspensions were extruded 15 times using an Avanti mini-extruder with one 100 nm polycarbonate membrane. Liposomes roughly 100 nm in diameter and each containing ca. 100 000 eggPC lipids was thus obtained.

Lipid autoxidation in liposomes. Stock solutions were prepared in MeCN: (A) 130.7 μM H₂B-TOH, (B) 100 μM TrpSeOx, (C) 400 μM TrpSeOx, (D) 100 μM TrpSeEtPh and (E) 400 μM TrpSeEtPh. H₂B-TOH concentration was determined by measuring the absorption at $\lambda_{max} = 517$ nm in MeCN and using its molar extinction coefficient of 65 000 $\text{M}^{-1} \text{cm}^{-1}$. Four series of six 64.3 μL aliquots of 20 mM eggPC (24 aliquots in total) were placed in microcentrifuge tubes and further diluted with 100 μL of the PBS solution utilized in lipid hydration, to yield 7.8 mM lipid suspensions. To each of

the 6 aliquots in two series of eggPC were added increasing amounts of TrpSeOx (8, 20 μ L of Stock B, 10, 15, 20, 30 μ L Stock C) and to each of the 6 aliquots of the two other series of egg PC were added increasing amounts of TrpSeEtPh (8, 20 μ L of Stock D, 10, 15, 20, 30 μ L Stock E). The solutions were subsequently diluted with the PBS solution, to yield 1.2 mL of solutions 1.07 mM in lipids and 1, 2.5, 5, 7.5, 10, or 15 μ M in TrpSeOx or TrpSeEtPh. From each of the lipid suspensions, aliquots of 280 μ L were loaded into the wells of a microplate reader tray. The solutions were left equilibrating at 37 °C for 15 min, after which 20 μ L of free-radical initiator was added to each of the wells. The initiator solutions utilized were either 0.135 M in ABAP in a pH 7.4 PBS solution, or 3.0 mM in MeOAMVN in MeCN. The final solutions were 1 mM in lipids, 10 nM in liposomes, 0.1 μ M in H₂B-TOH, and 9 mM in ABAP or 200 μ M in MeOAMVN.

3.5 References

¹ McGrath, A.J.; Garrett, G.E.; Valgimigli, L.; Pratt, D.A., *J. Am. Chem. Soc.* **2010**, 132, 16759-16761.

² McGrath, A., Synthesis, Redox Chemistry and Antioxidant Activity of Sulfenic Acids, Master's Thesis, Queen's University, 2010.

³ Vaidya, V.; Ingold, K.U.; Pratt, D.A., *Angew. Chem. Intl. Ed.* **2009**, 48, 157-160.

⁴ Chenier, J.H.B.; Howard, J.A. *Can. J. Chem.* **1975**, 53, 623-627.

⁵ Claus Jacob, C.; Giles, G.I.; Giles, N.M.; Sies, H., *Angew. Chem. Intl. Ed.* **2003**, 42, 4742-4758.

⁶ Pavlishchuck, V.V.; Addison, A.W., *Inorg. Chim. Acta* **2000**, 298, 97-102.

- ⁷ Lucarini, M.; Pedulli, G.F.; Cipollone, M., *J. Org. Chem.*, **1994**, 59, 5063–5070.
- ⁸ Lucarini, M.; Pedrielli, P., Pedulli, G.F.; Cabiddu, S.; Fattuoni, C., *J. Org. Chem.* **1996**, 61, 9259-9263.
- ⁹ Wijtman, M.; Pratt, D.A.; Valgimigli, L.; DiLabio, G.A.; Pedulli, G.F.; Porter, N.A., *Chem.- Eur. J.* **2003**, 9: 4997–5010.
- ¹⁰ Lynett, P.T.; Butts, K.; Vaidya, V.; Garrett, G.E.; Pratt, D.A., *Org. Biomol. Chem.*, **2011**, 9, 3320-3330.
- ¹¹ Valgimigli, L.; Pratt, D.A., Antioxidants in Chemistry and Biology. *Encyclopedia of Radicals in Chemistry, Biology and Materials*; Wiley: New York, 2012; Vol.56, p. 1623-1677.
- ¹² Schaferling, M.; Grogel, D. B. M.; Schreml, S. *Microchimica Acta* **2011**, 174, 1.
- ¹³ Soh, N.; Ariyoshi, T.; Fukaminato, T.; Nakajima, H.; Nakano, K.; Imato, T., *Org. Biomol. Chem.* **2007**, 23, 3721-3876
- ¹⁴ Negre-Salavayre, A.; Auge, N.; Alaya, V.; Basaga, H.; Boada, J.; Brenke, R.; Capple, S.; Cohen, G.; Feher, J.; Grune, T.; Lengyel, G.; Mann, G.E.; Pamplona, R.; Poli, G.; Portero-Otin, M.; Riah, Y.; Salavayre, R.; Sasson, S.; Serrano, J.; Shamn, O.; Siems, W.; Siow, R.C.M.; Wiswedel, I.; Zarkovic, K.; Zarkovic, N. *Free Rad. Res.*, **2010**, 44, 1125-1171.
- ¹⁵ Krumova, K.; Friedland, S.; Cosa, G., *J. Am. Chem. Soc.* **2012**, 134, 10102-10113.
- ¹⁶ Zheng, F.; Pratt, D.A., *Chem. Commun.*, **2013**, 49, 8181-8183.
- ¹⁷ Hanthorn, J. J.; Haidasz, E.; Gebhardt, P.; Pratt, D. A. *Chem. Commun.* **2012**, 48, 10141–10143.
- ¹⁸ Zielinski, Z.; Presseau, N.; Amorati, R.; Valgimigli, L.; Pratt, D.A., *J. Am. Chem. Soc.* **2014**, 136, 1570–1578

¹⁹ Pavlishchuk, V. V.; Addison, A. W; *Inorg. Chim. Acta* **2000**, 298, 97–102

CHAPTER 4

PRELIMINARY STUDIES OF THIOL OXIDATION

THAT REVEAL THE INTERMEDIACY OF SULFENIC ACID

4.1 Introduction

Reactive oxygen species, including H_2O_2 , are generated *in vivo* as discussed in Chapter 1. When they overwhelm an organism's capacity to reduce them, ROS lead to oxidative stress, which is believed to contribute to neurodegenerative and cardiovascular diseases as well as diabetes and cancer pathologies.¹ Aside from these harmful effects, H_2O_2 is also shown to be a crucial second messenger in redox cell signalling,^{2,3} and plays a role in modulating enzyme activity including regulation of those enzymes which aid in controlling the concentration of ROS in the cell, *eg.* glutathione peroxidase (GPx, see Chapter 1).⁴

Sulfenic acids are believed to be key intermediates in these redox-signalling pathways. Protein-cysteine thiols are easily oxidized by H_2O_2 to cysteine-sulfenic acids, which react with other thiols, such as other protein cysteines or glutathione to form disulfide bonds that are an important post-translational modification and can regulate protein function. Disulfide bond formation, especially in the case of glutathione, is also a part of the cell's defence against oxidative damage. Through the oxidation of thiols to disulfides, a reversible process, the cell is protected from oxidative damage that would be irreversible and damaging such as the oxidation of sulfenic acid to sulfinic and sulfonic acid (Figure 4.1).⁵

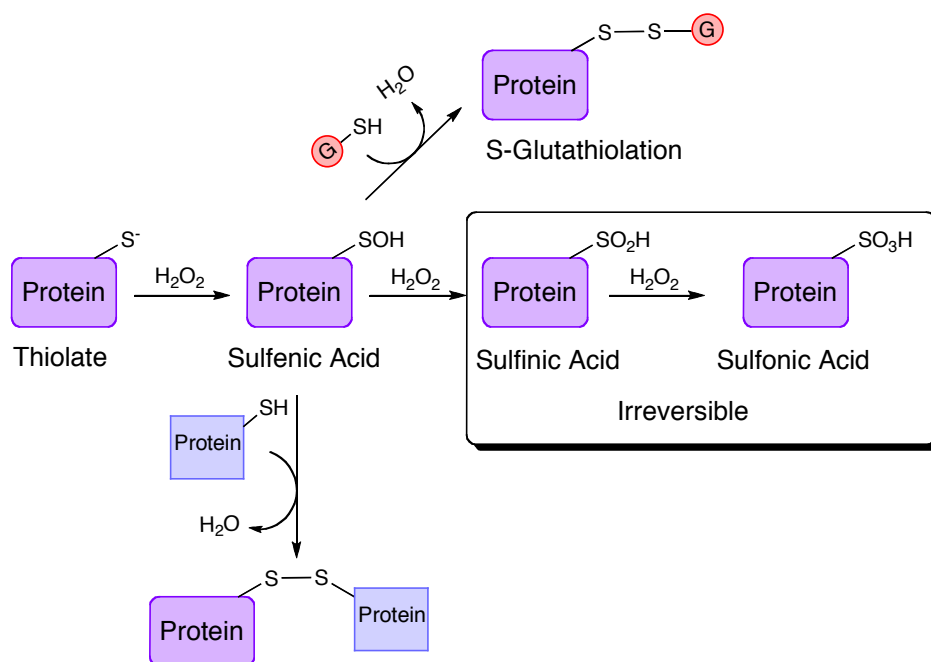


Figure 4.1 Possible reaction pathways for oxidation of protein cysteine thiols in vivo. Adapted with permission from Paulsen, C. E.; Carroll, K.S., ACS Chem. Biol., 2010, 5, 1, 47-62. Copyright 2010 American Chemical Society.⁵

Because it is the product of thiol oxidation by H_2O_2 , sulfenic acid can be used as an indicator of ROS in cells, and there has been interest in finding methods to quantify sulfenic acids *in vivo* as a means to better understand redox signalling and the role of sulfenic acid in these pathways. Probes that react selectively with sulfenic acids have been used to recognize cysteine-sulfenic acid. Among them are either affinity or fluorescent probes that employ a nucleophilic dimedone-like groups that give rise to a thioether product that can then be identified as illustrated in Figure 4.2.⁶

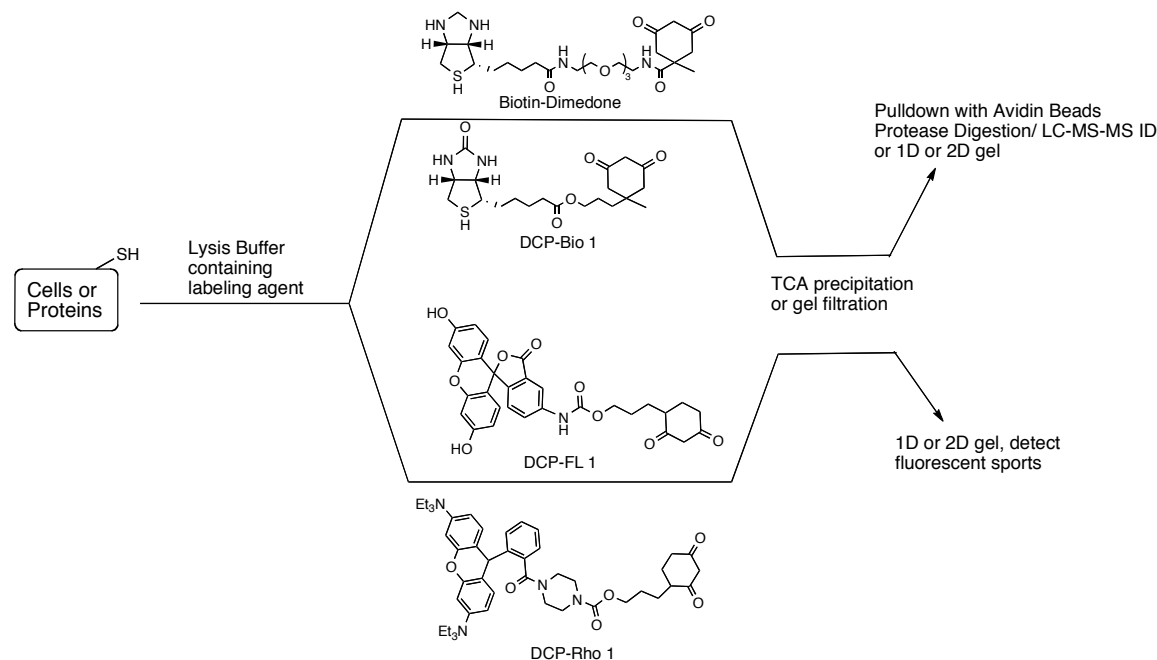
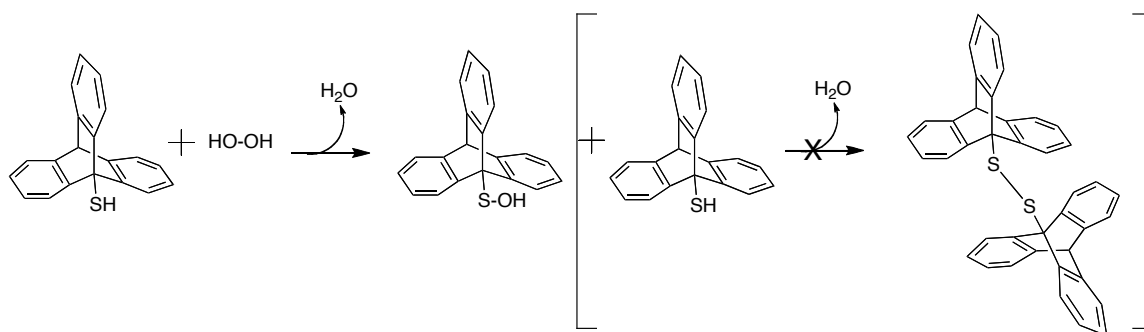


Figure 4.2 Strategies for detecting sulfenic acids in proteins using either dimedone-based affinity probes or fluorescently tagged reagents. Reproduced from Seo, Y.H.; Carroll, K.S., *Proc. Natl. Acad. Sci.*, **2009**, 61, 16163-16168. Copyright 2009 The National Academy of Science.⁶

Due to their important role in oxidative stress and cell signalling, sulfenic acids are important research targets, especially as it concerns their production by oxidation of thiols. Previous reports studying the kinetics and mechanism of the oxidation of cysteine, and other small thiols such as glutathione and *N*-acetylcysteine have shown only disulfides as the products.^{7,8,9} Reports by Ashby *et al.* have allowed some study of sulfenic acid reactivity by generating it *in situ* from reaction cysteine thiosulfinate and cysteine thiol. Attempts by the same group at generating sulfenic acid by hydrolysis of thiosulfinate or disulfide demonstrated that these reactions are too slow to observe accumulation of the sulfenic acid given.¹⁰ The direct oxidation of thiols to sulfenic acids have not been observed, given the high reaction rate with thiols in the system.

In previous work, our group has demonstrated that a sulfenic acid substituted with a triptycene moiety permitted the determination of a variety of thermodynamic and kinetic parameters associated with the one-electron (radical) reactivity of sulfenic acids.¹¹ As such, we felt that this system would also be the ideal substrate for direct studies of the two-electron oxidation of thiols to sulfenic acids – particularly in light of the fact that thiosulfonates and disulfides derived from 9-triptycenesulfenic acids had never been prepared despite extensive efforts. Indeed, crude computational studies of the triptycene disulfide (*cf.* Figure 4.3) reveal that the large triptycene groups impose a bond angle of 180° on the disulfide linkage, where the optimal angle should be 85° as shown for dimethyl disulfide.¹² The aromatic hydrogens on the bulky triptycene groups are also too close together given the length of the disulfide bond. Therefore, the triptycene-sulfur compounds provide an ideal system to study the oxidation of thiol to sulfenic acid, which does not allow reaction of sulfenic acid with thiol to form the disulfides that are observed in previous studies of this reaction.



Scheme 4.4 Possible reaction of TrpSOH and TrpSH to 1,2-di-9-triptycenedisulfide

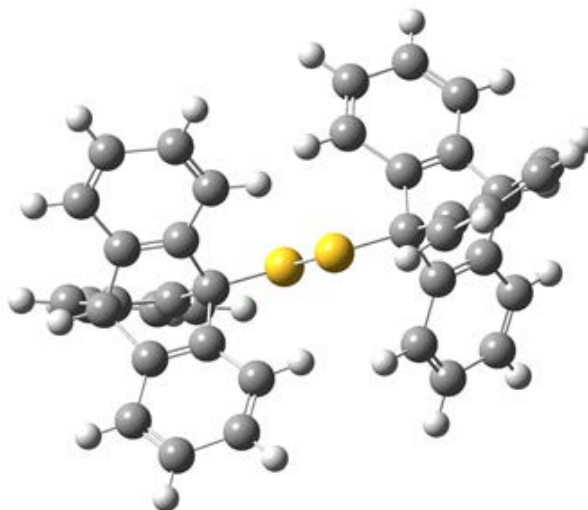


Figure 4.3 AM1 energy minimized structure of *bis*-triptycenedisulfide showing C-S-S-C bond angle of 180° and adverse interaction of peri hydrogens.

4.2 Results and Discussion

4.2.1 Preliminary Data on The Oxidation of 9-Triptycenethiol

Our group has previously attempted studying the direct oxidation of 9-triptycenethiol (TrpSH) with hydrogen peroxide (performed by undergraduate student Jazmin Bansagi, Figure 4.4). In this preliminary experiment, 9-triptycenethiol was oxidized using urea-H₂O₂ complex in deuterated methanol, and the conversion of the thiol to the sulfenic acid could be clearly observed by ¹H NMR via its characteristic bridgehead proton resonance give these initial results demonstrated that TrpSH did not react fully despite an excess of peroxide, and that the triptycenesulfenic acid (TrpSOH), which was initially formed was further oxidized to triptycenesulfonic acid (TrpSO₃H). It should be noted that it was later noticed that TrpSH was insoluble in methanol (the solvent used for this NMR

experiment) at the purported concentration of 50 mM, which could account for why the reaction did not go to completion.

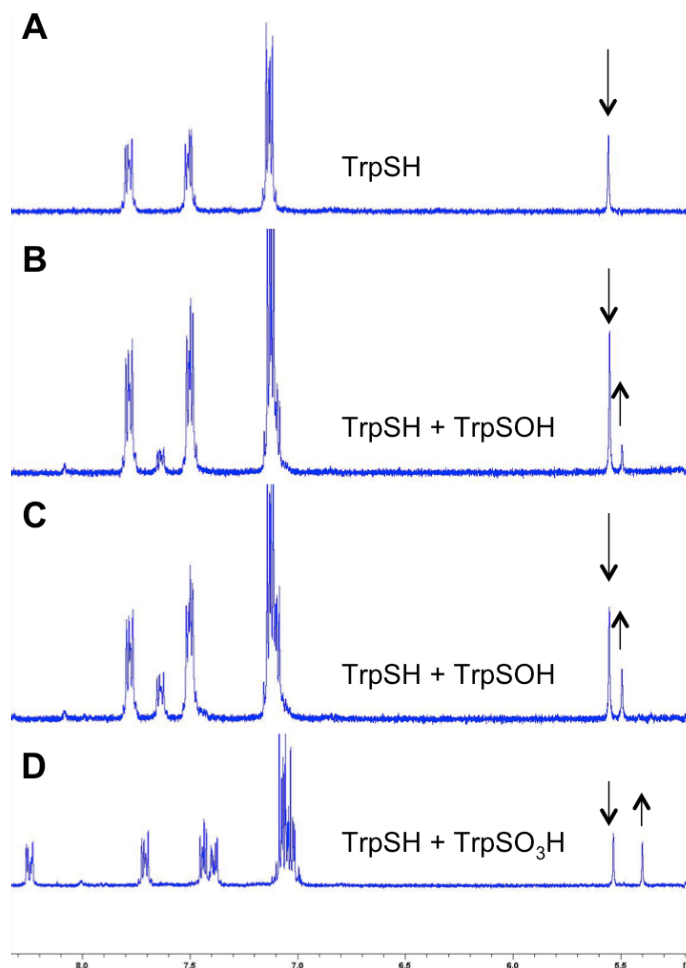


Figure 4.4 ^1H NMR (300 MHz) of thiol oxidation (50 mM) by H_2O_2 -urea complex (50 mM) in d_3 -MeOH at 25°C. Decay of TrpSH and growth of TrpSOH and TrpSO₃H is monitored by their respective bridgehead protons at time zero (A), 30 minutes (B), 5 hours (C) and 3 days (D).

Because TrpSOH was not soluble in methanol at concentrations required for convenient observation by NMR, a different method of study was required and HPLC was chosen to observe the process and better understand the direct reaction of TrpSH to TrpSOH, and the relative rates at which this process competes with the

further oxidation of TrpSOH to sulfinic (TrpSO₂H) and sulfonic (TrpSO₃H) acids. Initially a new solvent system was sought out to replace methanol that would not cause precipitation of TrpSH during experiments, and thus give accurate results and more liberty of concentration range for the kinetic experiments. Several solvents and solvent combinations were tested. Because the interest in the reaction of thiols to form sulfenic acids stems from their biological role, we endeavoured to find a solvent that could mimic biological aqueous conditions to a certain extent, while still being able to accommodate the three aromatic rings of the triptycene compound. Based on observations in the preliminary kinetic studies, a protic solvent is necessary in the reaction with H₂O₂, in order for the reaction to remain unimolecular in H₂O₂, as is the case for the reaction of phosphines with peroxides.¹³ Therefore, solvents offering an alcohol group but with increased hydrophobicity as compared to methanol were tested first, *ie.* amyl alcohol and ethylene glycol, but the solubility of TrpSH was not improved. Solvent combinations consisting of 50/50 mixtures of a lower polarity solvent and a protic solvent were also tested, *i.e.* acetonitrile/water, glyme/methanol and DCM/methanol. The last two mixtures, glyme/methanol and DCM/methanol offered solubility up to 25 mM at 37°C.

The DCM/methanol mixture was quickly eliminated because H₂O₂ (30% in water) that was being used for the oxidation caused the TrpSH to precipitate and the urea-H₂O₂ complex that could have substituted the aqueous solution of hydrogen peroxide was insoluble in the solvent mixture. The glyme/methanol mixture was chosen for the continuation of the oxidation study, and showed no solubility concerns with addition of H₂O₂ 30% in water.

The oxidation of thiol was monitored using HPLC and with UV detection. Using a normal phase silica column and 4% *iso*-propylalcohol in hexanes as the mobile phase, TrpSH and TrpSOH could be easily separated and quantified by comparison of peak area to the internal standard, phenol, as the reaction progressed over time.

No reaction or loss of thiol was observed when a 25 mM solution of TrpSH in glyme/methanol (1:1) was subjected to 1 or 10 equivalents of urea-H₂O₂ or H₂O₂ (30% in water) at 25°C, nor was any change observed with 10 equivalents of *tert*-butyl peroxide, or when the reaction was heated to 37°C. This lack of reaction in the presence of excess strong oxidant was especially concerning given the kinetic observations made by preliminary NMR study of the reaction of TrpSH, at much lower concentration in methanol and at lower temperature, with urea-H₂O₂ complex.

Many cysteine thiols (as well as selenocysteine selenols) exist as anions in their resting states at physiological pH and are more easily oxidized by H₂O₂. Previous studies have also indicated that the thiolate ion is the species that is oxidized by H₂O₂, not the thiol.^{7,14} Therefore, considering the possibility that trace amounts of base were unknowingly present in the preliminary NMR studies, a reaction of TrpSH with H₂O₂ was conducted in the presence of 10 mol% Et₃N. TrpSH was completely consumed in a matter of minutes, by the time the first HPLC injection could be completed and the data collected. This confirms that the reaction is not particularly facile at neutral pH, but requires base catalysis, and prompted us to explore the use of basic buffers in methanol as a reaction medium.

4.2.2 Oxidation in Basic Methanol Buffers

The pH of non-aqueous solvents can be measured using pH meters with standard aqueous electrodes by taking into consideration the error in pH measurement that comes from the liquid-junction potentials between the solvent in question and the aqueous electrode.¹⁵ This pH meter error is known for methanol, and so to facilitate the buffering of the reaction mixture, the solvent mixture of glyme/methanol was abandoned in favour of methanol despite the lower TrpSH solubility.

The pH reading given by a standard pH meter for a methanol solution, $s_w\text{pH}$ by IUPAC nomenclature,¹⁶ is corrected by addition of 2.24 pH units to give the $s_s\text{pH}$, or the accurate pH in methanol. With this knowledge in hand, different bases were used as buffers with trifluoromethanesulfonic acid in methanol (20 mM in base), each offering a different range of pH above methanol neutrality ($s_s\text{pH}$ 8.4)¹⁷; triethylamine (Et₃N, 10.10 – 11.3) and 2,2,6,6-tetramethylpiperidine (TMP, 11.5 – 12.1),¹⁷ and the reaction of TrpSH observed once again by HPLC and UV-vis spectrophotometry.

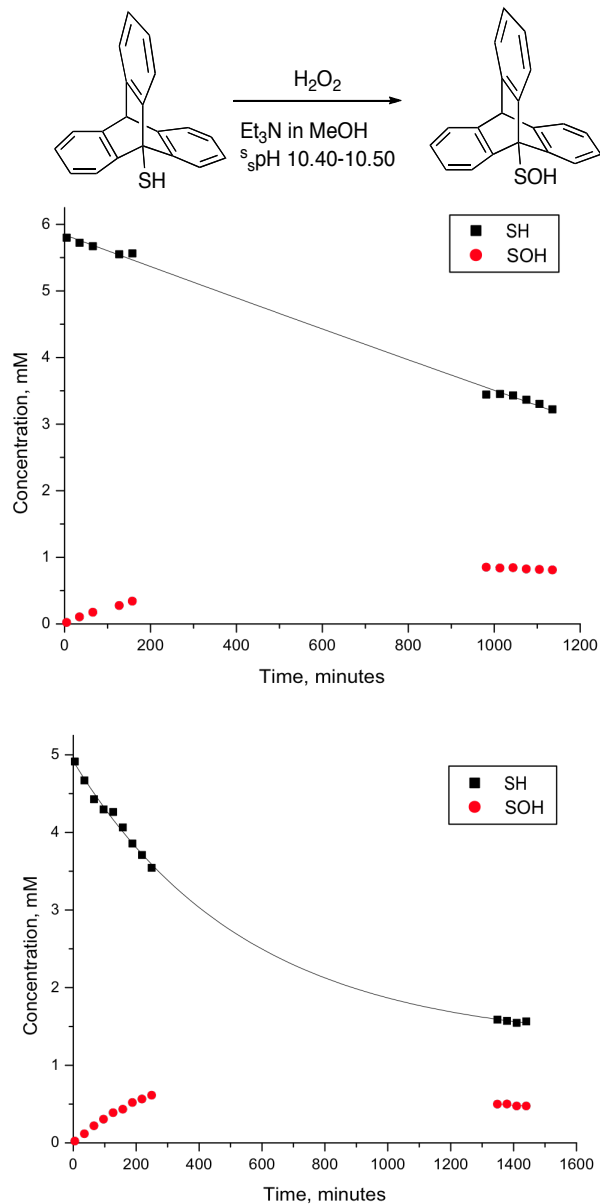


Figure 4.5 Reaction of TrpSH with 2 equivalents (top) and 10 equivalents (bottom) of H₂O₂ (30% in water) in MeOH containing 20 mM Et₃N buffer at 25°C over the course of a day. Initial rate for reaction with 2 equivalents (top) $d[\text{TrpSH}]/dt = 2.7 \times 10^{-5} \text{ mM/s}$ and $d[\text{TrpSOH}]/dt = 3.4 \times 10^{-5} \times 10 \text{ mM/s}$. Initial rate for reaction with 10 equivalents (bottom) $d[\text{TrpSH}]/dt = 8.9 \times 10^{-5} \text{ mM/s}$ and $d[\text{TrpSOH}]/dt = 4.0 \times 10^{-5} \times 10 \text{ mM/s}$.

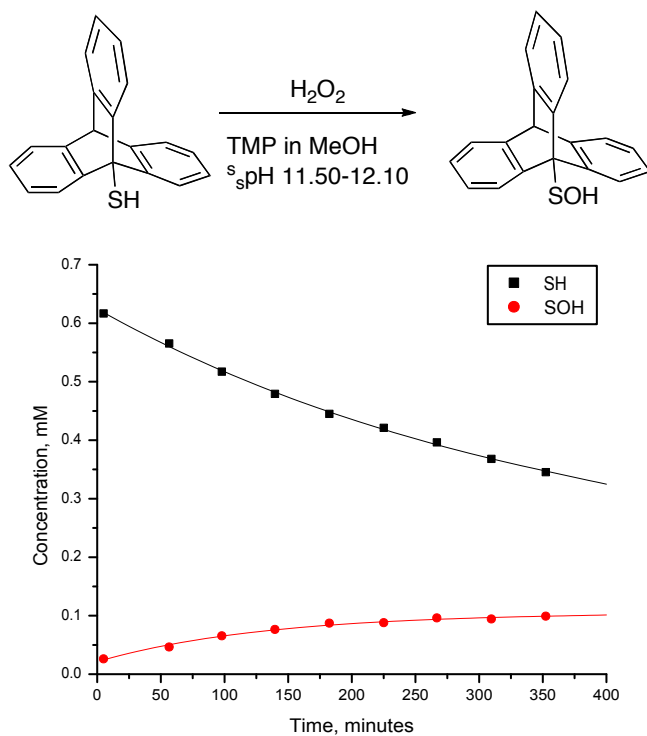


Figure 4.6 Reaction of TrpSH with 2 equivalents of H_2O_2 (30% in water) MeOH containing 20 mM TMP at 25°C over a period of 5 hours.

Interestingly, in these thiol oxidations (Figure 4.5 and 4.6), even in the case of excess peroxide, TrpSH did not react completely and the two compounds appeared to trend towards an equilibrium with *ca.* 20% TrpSOH to 80% TrpSH in the final concentration that was maintained over the course of a day.

In the reaction of TrpSH with 2 equivalents of H_2O_2 in $Et_3N/MeOH$ buffer, (Figure 4.5 - top) the initial rates of TrpSH decay and TrpSOH growth are comparable, suggesting that one does correspond to the other. That of TrpSOH is a little greater, (which cannot truly occur as it comes from TrpSH), but this may be experimental error, as it was only carried out once. The mass balance contradicts this simple reaction as it indicates that other products must also be formed because

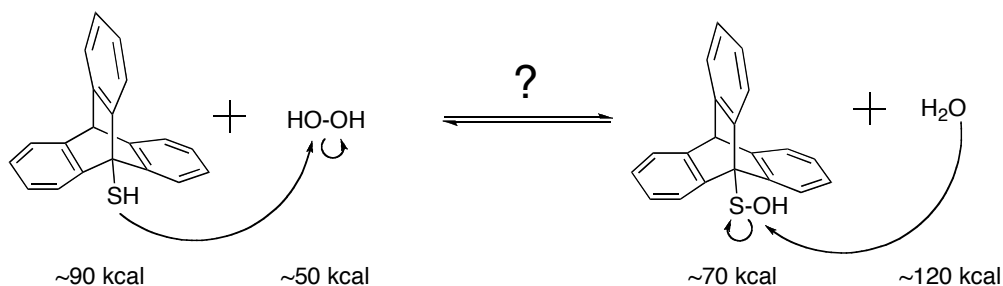
the final concentration of the two thio-triptycene species is approximately 4.5 mM (3.5 mM TrpSH + 1 mM TrpSOH) – noticeably less than the initial concentration of approximately 6 mM.

A mass imbalance is also observed in the reaction of TrpSH with 10 equivalents of H₂O₂ in Et₃N/MeOH buffer (Figure 4.5 – bottom), with only a total final concentration of approximately 2 mM from a starting concentration of TrpSH of 5 mM. In this reaction the initial rate of TrpSH decay is greater than in the previous oxidation, consistent with the increase in H₂O₂ from 2 equivalents to 10 equivalents, suggesting that the reaction may approach first order in H₂O₂. However, the initial rate of TrpSH decay is twice the initial rate of TrpSOH growth, suggesting, as does the mass imbalance, that TrpSOH is participating in other chemistry.

The reaction of TrpSH with 2 equivalents of H₂O₂ in TMP/MeOH buffer (Figure 4.6) is consistent with the above conclusions. It, too, shows a mass imbalance of the final TrpSH and TrpSOH concentrations as compared to the initial concentration of TrpSH.

The ratio between TrpSH and TrpSOH in the final mixture is consistent between experiments performed at ^spH ~10.40 and ~12.10 and with two different oxidants, (H₂O₂ and peroxy carbonate). This may have been explained by the equilibrium shown in Scheme 4.1, however, the final product ratio is the same when 2 or 10 equivalents of oxidant were used. Furthermore, upon examining the approximate BDEs at play, the reverse reaction, that is the nucleophilic attack of

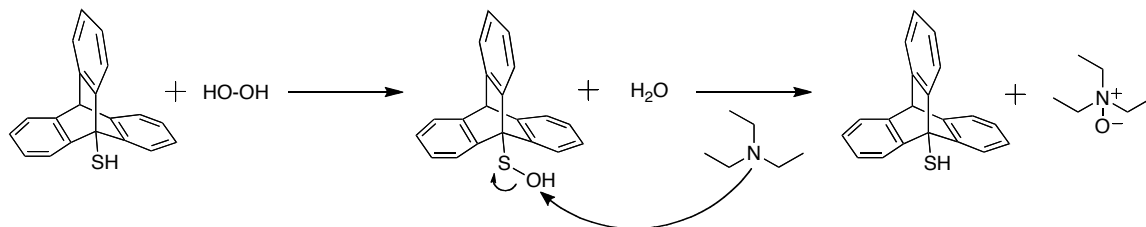
water on TrpSOH would be endothermic by *ca.* 50 kcal/mol, making an equilibrium between TrpSH and TrpSOH very unlikely.



Scheme 4.1 Unlikely equilibrium between triptycenesulfenic acid and hydrogen peroxide, and triptycenesulfenic acid and water. Bond strengths of S-H, O-O, S-O and O-H bonds needing to be broken for the equilibrium

An equilibrium between thiols and sulfenic acids has not been previously reported but other systems have not allowed for the identification of sulfenic acid as a product, because other systems do not offer the steric hindrance of the triptycene that blocks formation of the disulfide when sulfenic acids are in the presence of thiols. Thus it is possible that if this purported equilibrium exists, it has not been observed previously.

Given the highly unlikely explanation that the thiol oxidation to sulfenic acid is in fact in equilibrium, it was hypothesized that the observed equilibrium could be a result of the reaction of the strong amine bases with the product TrpSOH. The amine bases, Et₃N and TMP, used to buffer the solution, are in large excess to the triptycene compounds and may react with TrpSOH to yield TrpSH as shown in Scheme 4.2. This could explain why the reaction never appears to go to completion.



Scheme 4.2 Possible mechanism of amine base reaction with sulfenic acid

In order to investigate whether this is the case, the reaction of TrpSOH and Et₃N or TMP (Figures 4.7 and 4.8 respectively) was carried out in order to see if TrpSH would be formed under these reaction conditions.

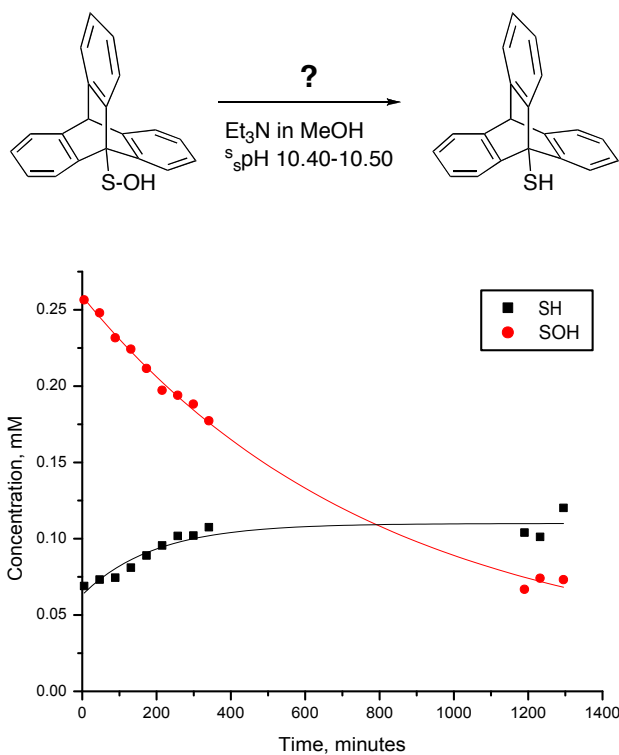


Figure 4.7 Reaction of TrpSOH with Et₃N (20 mM) in MeOH at 25 °C. Initial rate for TrpSOH decay = 3.96×10^{-6} mM/s and for TrpSH growth = $2.05 \times 10^{-6} \times 10$ mM/s.

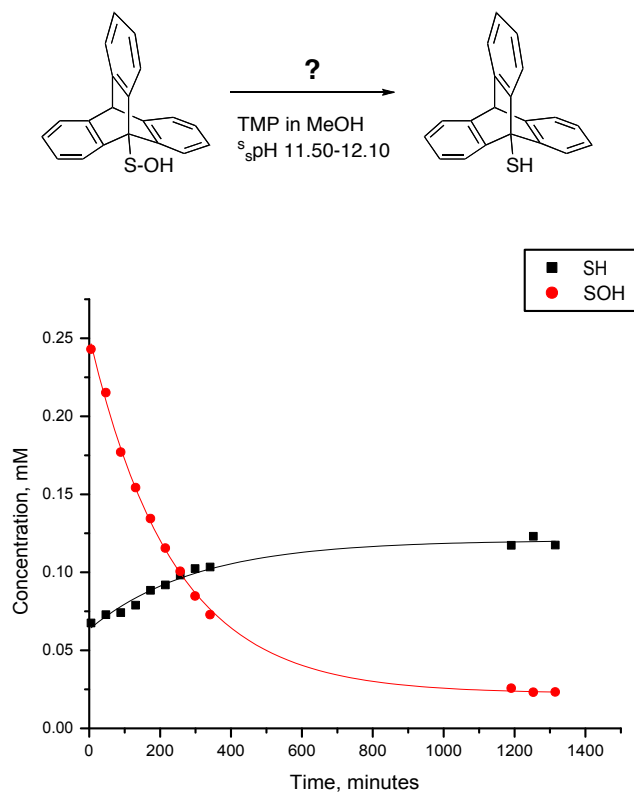


Figure 4.8 Reaction of sulfenic acid with TMP (20 mM) in MeOH at 25 °C. Initial rate for TrpSOH decay = 8.36×10^{-6} mM/s and for TrpSH growth = $1.94 \times 10^{-6} \times 10$ mM/s.

In the reaction of TrpSOH with Et_3N in methanol TrpSH formation from TrpSOH is observed, which supports the hypothesis of amine attack on the sulfenic acid. However it is unlikely that this is the only transformation involved, comparing the mass balance and initial rates suggest that TrpSOH is also undergoing another reaction the product of which is not TrpSH. There is significantly less TrpSH product at the end of the reaction ($C_f = \sim 0.125$ mM) than there is starting material, TrpSOH ($C_i = \sim 0.25$ mM). The initial rates for these two reactions also suggest that TrpSOH is being consumed by a different (or additional) mechanism than the one indicated in Figure 4.2, leading only to TrpSH. In the reaction of TrpSOH with Et_3N

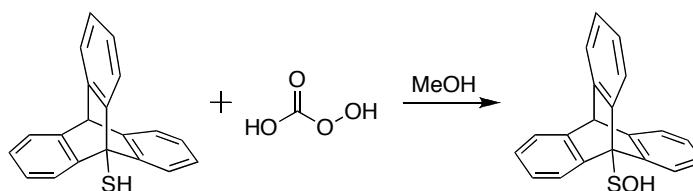
(Figure 4.7) TrpSOH is consumed approximately twice as fast as TrpSH is appearing, and in the reaction with TMP (Figure 4.8) this difference is increased to a four-fold faster decay of TrpSOH than growth of TrpSH. This is especially contradictory to the proposed mechanism of nucleophilic amine attack on sulfenic acid given that TMP is much more hindered than Et₃N. If it were able to react with TrpSOH it would be expected to do so much more slowly than Et₃N.

Unfortunately, in these experiments, TrpSH was already present in low concentration from the start of the reaction. Given that the TrpSOH starting material was pure by NMR, this may be explained by a reaction occurring with the TrpSOH while the experiment was prepared, before addition of the amine, or by an impurity co-eluting with TrpSH on the HPLC. Given that the peak associated to TrpSH did show growth over the time course of the experiment, some is being formed from TrpSOH, regardless of the pathway.

These results do not support the equilibrium between TrpSH and TrpSOH illustrated in scheme 4.1, nor can they be explained entirely by the nucleophilic amine mechanism shown in scheme 4.2, because TrpSOH is depleted faster than TrpSH is formed, and because a larger quantity of TrpSOH is consumed than TrpSH is generated. Therefore, there must be another mechanism involved in the consumption of TrpSOH. Sulfenic acids can disproportionate to disulfide, sulfinic acid and water, it may be worth investigating whether in the thio-triptycene that are too sterically hindered to form disulfides, thiol is the product of disproportionation. It is also possible that TrpSOH is being oxidized to TrpSO₂H and TrpSO₃H, subsequently acting as a reductant. The excess aminebase in solution will

deprotonate the TrpSH to TrpS⁻, a strong reductant that may be giving rise to O₂^{•-}. Although no H₂O₂ was added to the reaction, it may be formed *in situ* and explain the loss of TrpSOH to further oxidized species.

In order to provide further insight into the role of the amine in the unexpected reaction profiles shown above, we elected to replace the amine base with a carbonate base, which would be expected to be less nucleophilic than the amine. Peroxycarbonate, which exists in equilibrium with carbonate and H₂O₂,¹⁸ was used both as the oxidant and for base catalysis, to further investigate the possibility that the reaction with the amine-base is the source of the observed equilibrium. This reaction (*cf.* Figure 4.9) gave the same equilibrium trend towards 80% TrpSH and 20% TrpSOH. As was proposed for the other oxidations in Figure 4.5 – 4.8, this experiment demonstrates that TrpSOH must be undergoing a subsequent reaction. The concentration of TrpSOH is decreasing near the end of the reaction, the initial rates show that TrpSH is consumed almost four times faster than TrpSOH is formed, and the concentration of the final products does not account for all the starting material.



Scheme 4.3 Reaction of peroxycarbonate with TrpSH

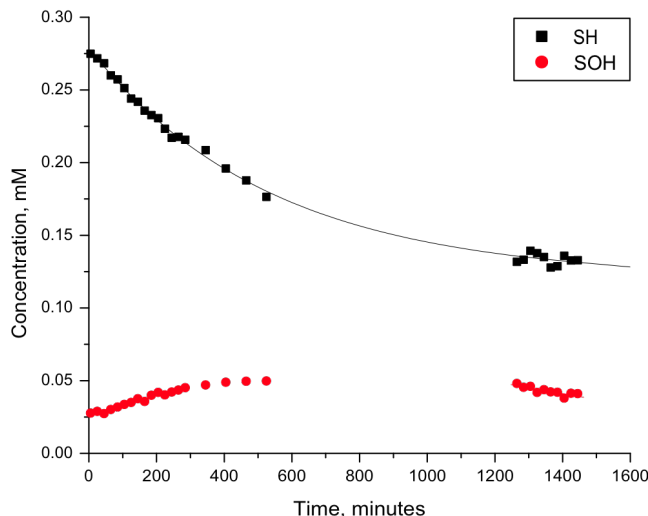


Figure 4.9 Reaction of TrpSH with 10 equivalents of peroxy carbonate ($\text{H}_2\text{O}_2 + \text{NaHCO}_3$) in MeOH. Initial rate for TrpSH decay = 3.15×10^{-6} mM/s and for TrpSOH growth = 8.14×10^{-7} x 10 mM/s.

The results presented in Figures 4.5 - 4.9 and discussed above are consistent with the possibility that TrpSOH undergoes further chemistry that is not observed by the HPLC conditions, because the concentration of TrpSOH levels out over time, and even begins to decrease at the end of the longer oxidation experiments. It is plausible that this subsequent chemistry is the oxidation of TrpSOH to TrpSO₂H and/or TrpSO₃H. This could occur by reaction of TrpSOH with the H₂O₂ in solution, meant for oxidation of TrpSH. In this case, the oxidant could be consumed by the newly formed TrpSOH before all the TrpSH has been oxidized. The concentrations of TrpSH and TrpSOH continue to slowly decrease even once all the oxidant is consumed. The other possible, if less likely, conclusion is that there is an impurity in the system that co-elutes with the thiol, and has a very similar UV-Vis spectrum, giving the illusion of an equilibrium. In order to further examine this system, an

analytical approach is needed to identify the higher oxidation states that may be involved, TrpSO₂H and TrpSO₃H, or any co-eluting species.

4.2.3 Reaction Profiles Monitored by LC/MS

The initial observation of thiol oxidation by H₂O₂ was conducted by normal phase HPLC with UV detection as described above. A significant limitation to this method was the inability to observe all of the potential products of the reaction. Attempts were made to analyze a standard of TrpSO₃H on HPLC, but it was not observed. This is likely because this acidic species was remaining on the polar normal phase column, despite attempts using various, increasingly polar, mobile phases. Therefore, formation of sulfonic acid (and presumably also sulfinic acid, although no standard was available to verify), which could result from the oxidation of sulfenic acid once it is formed, could not be monitored using the HPLC conditions. Hence, we continued our study of thiol oxidation using reverse phase LC/MS in an attempt to achieve both better separation of potential reaction products, and enable their identification by their mass spectra. The separation of TrpSH and the three products of the oxidation (TrpSOH, TrpSO₂H, and TrpSO₃H) is shown in Standard curves were established for TrpSH, TrpSOH and TrpSO₃H relative to the internal standard, phenol, and are presented in Figures 4.10, 4.11 and 4.12 respectively. (MS detection (ESI⁻) at m/z of 285, 301, and 333.

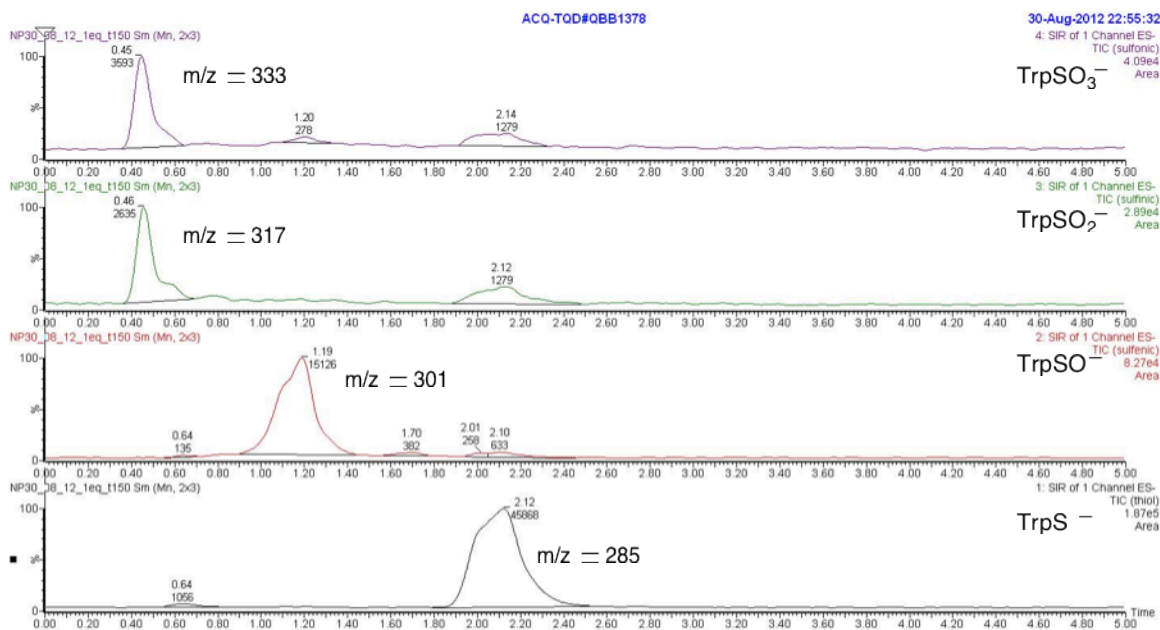


Figure 4.10 Mass spectral chromatograms of the products of a TrpSH oxidation: TrpSO₃H (top), TrpSO₂H (2nd from top), TrpSOH (3rd from top), and starting material TrpSH (bottom) from LC/MS analysis with 20% H₂O/MeOH mobile phase, flow rate 0.2 mL/min, Acquity C₁₈ 1.7µm 2.1 x 50 mm column and MS detection (ESI⁻) at m/z of 333, 317, 301, and 285.

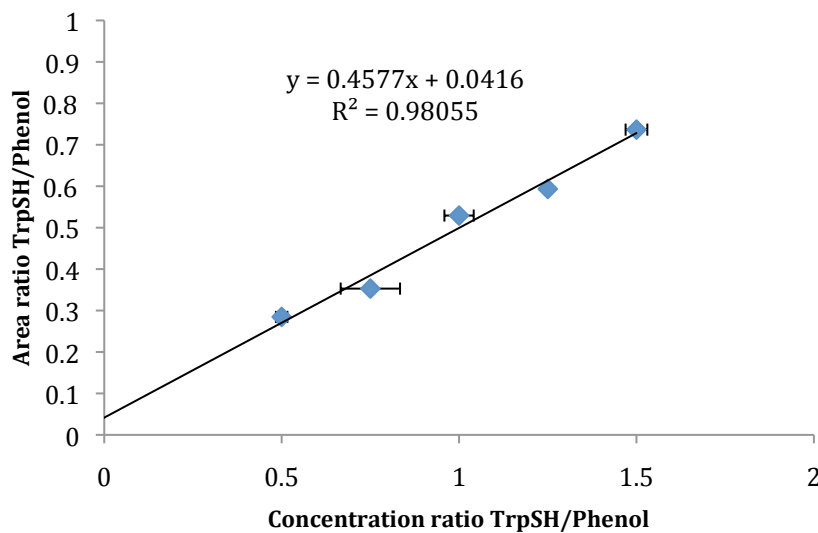


Figure 4.11 Standard curve for TrpSH using the internal standard phenol, for TrpSH sample concentrations from 10 to 30 µM.

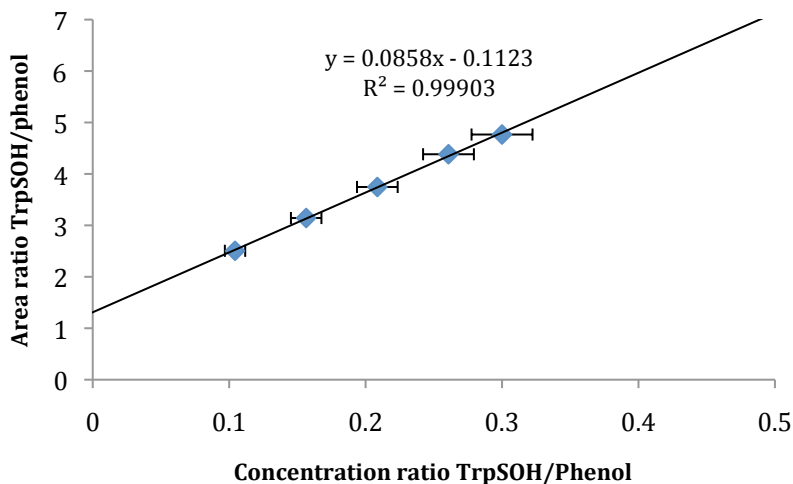


Figure 4.12 Standard curve TrpSOH using the internal standard phenol, or TrpSOH sample concentrations from 10 to 30 μM .

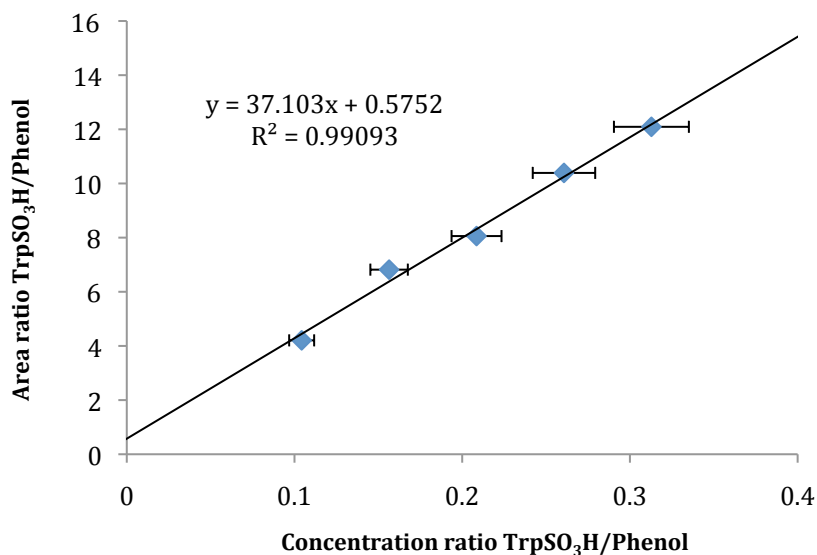


Figure 4.13 Standard curves for TrpSO₃H using the internal standard phenol, for TrpSO₃H sample concentrations from 10 to 30 μM .

The oxidations were performed in the same way as was done for the HPLC experiments, in methanol, with 10 equivalents of peroxy carbonate as oxidant and base catalyst. It was immediately apparent that the HPLC results had been misleading, as peaks corresponding to both TrpSO₂H and TrpSO₃H are almost

immediately observed and TrpSH is consumed entirely within a few hours, as illustrated in the reaction plot (Figure 4.14) below.

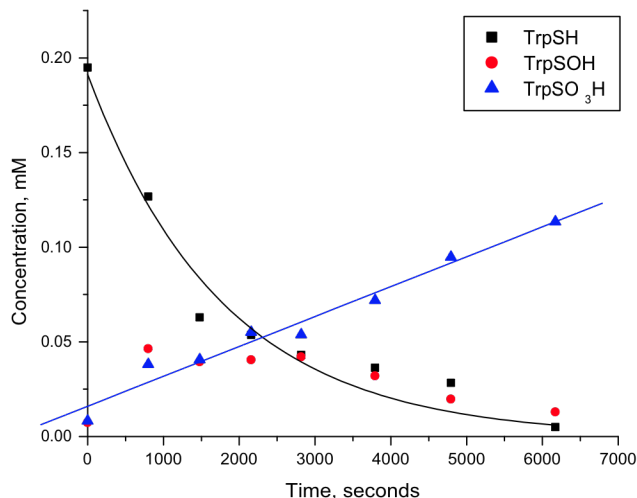


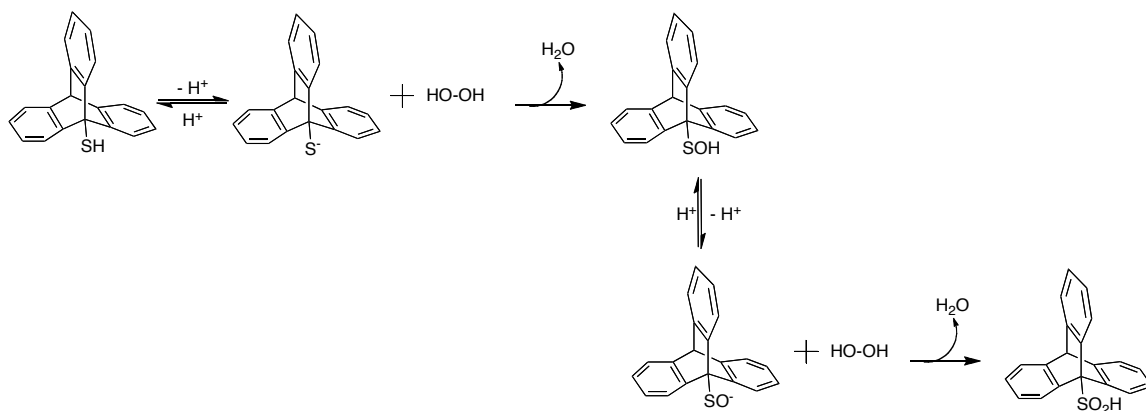
Figure 4.14 Reaction of TrpSH with 10 equivalents of peroxy carbonate ($\text{H}_2\text{O}_2 + \text{K}_2\text{CO}_3$) in MeOH showing decay of TrpSH and growth of TrpSOH and TrpSO₃H. TrpSO₂H was also produced but could not be plotted because no authentic material has been synthesised in order to generate a standard curve.

These results suggest that the reason for an apparent equilibrium in the HPLC results is simply that the TrpSOH is being further oxidized, at once limiting the concentration of TrpSOH and depleting the oxidant that could otherwise oxidize the TrpSH to completion. In Figure 4.14, only three of the four involved triptycene compounds is represented, no authentic sample of TrpSO₂H has been made and therefore no standard curve could be made to allow us to plot its growth. However, TrpSO₂H was formed in the reaction with comparable peak areas to TrpSO₃H and is likely the reason that in Figure 4.14, the mass of TrpSH starting material is greater than the total mass of final products. Therefore, in continuing these studies, it is

important to synthesize and standardize an authentic sample of TrpSO₂H in order to obtain accurate results.

Together, the results of the different oxidations presented above demonstrate that TrpSOH is being further oxidized, to TrpSO₂H and TrpSO₃H. This explains why the concentration of TrpSOH was never very high, and it didn't correspond to the starting concentration of TrpSH. This shows that TrpSOH is more easily oxidizable than TrpSH. Once formed from TrpSH oxidation, TrpSOH reacts with H₂O₂, depleting the oxidant that would otherwise oxidize the TrpSH to completion, explaining why TrpSH often remained in the final mixture. While it may be counterintuitive that TrpSOH be more readily oxidizable than TrpSH, this would explain why it is so difficult to observe TrpSOH as the intermediate in oxidations of thiols. Because the oxidation occurs in a basic solution, it is likely that a pH sensitive pre-equilibrium is at play (TrpSH/TrpS⁻ and TrpSOH/TrpSO⁻) and is important in the competition for H₂O₂. The greater oxidizability of TrpSOH is likely due to a higher concentration of the anion in the case of TrpSOH/TrpSO⁻ relative to TrpSH/TrpS⁻ (Scheme 4.4).

The TrpSO₂H that is formed by oxidation of TrpSOH is also oxidizable by H₂O₂, further depleting the oxidant available for reaction with TrpSH. However, in LC/MS traces, TrpSO₂H seemed to accumulate more than TrpSOH; this might indicate that it is less oxidizable than TrpSOH, which would make sense, but thus far this remains an assumption based on the unstandardized results for TrpSO₂H.



Scheme 4.4 Reaction of deprotonated triptycene thiol and sulfenic acid with H₂O₂

4.3 Conclusions

The results obtained by UPLC/MS studies of thiol oxidation mixtures disprove the possibility of an equilibrium between triptycenethiol and triptycenesulfenic acid, and demonstrate that the triptycene system is in fact an ideal system to study the direct oxidation of thiol to sulfenic acid without formation of a disulfide. The observation of triptycenesulfinic and sulfonic acids means that under the right conditions this system can further be used to study the stepwise oxidation from thiol to sulfenic acid, sulfenic acid to sulfinic acid and lastly from sulfinic acid to sulfonic acid.

The goal of this study was to isolate the oxidation reaction of thiol to sulfenic acid, however other products are formed during the reaction. In all the oxidations analyzed by LC/MS, TrpSO₂H and TrpSO₃H were observed before TrpSH had fully reacted. This suggests that the TrpSOH is more easily oxidizable than TrpSH and so reacts with H₂O₂ once it is formed. Further study of this reaction is needed in order to establish a reaction system that will allow characterization of the direct oxidation

of thiols to sulfenic acids. The greater oxidizability of the TrpSOH as compared to the TrpSH must also be confirmed by direct oxidation of TrpSOH and comparison to direct oxidation of TrpSH.

Given that sulfinic and sulfonic acids were also observed as playing a role in this scope of oxidation reactions, the kinetics of these subsequent oxidation reactions should also be studied independently of the thiol oxidations. This would require synthesis and isolation of pure TrpSO₂H as a starting material for the oxidation to TrpSO₃H.

4.4 Experimental Procedures

9-Triptycenethiol. To a solution of TfOH (0.138 mL, 1.80 mmol) and TFA (0.138 mL, 1.56 mmol) in toluene (90 mL, 0.01 M) was added 9-(*tert*-butylthio)-triptycene (300 mg, 0.876 mmol), the reaction mixture was stirred overnight at 80°C and concentrated *in vacuo*. The crude product was purified by silica gel chromatography using hexanes as the eluent to afford triptycenethiol as a white solid (195 mg, 77%) ¹H NMR (400 MHz, CDCl₃) δ ppm 2.40 (s, 1H), 5.43 (s, 1H), 7.04-7.06 (m, 6H), 7.38-7.40 (m, 3H), 7.68-7.70 (m, 3H) ¹³C NMR (100 MHz, CDCl₃) δ ppm 53.9, 59.2, 122.1, 123.5, 126.0, 145.2, 145.8 HRMS (EI⁺) calculated (M) 286.0738, observed 286.0791.

9-Triptycenesulfenic acid. *N.B. Reaction carried out by undergraduate student Andrew Ingold by the following procedure:* To an ice cooled solution of 9-(*tert*-butylthio)-triptycene (0.5 g, 1.46 mmol) in CH₂Cl₂ (34 mL, 0.043 M) in a dry round bottom flask under argon, was added a 0.086M solution of 77% mCPBA in

CH₂Cl₂ (165 mg, 0.95 mmol) dropwise. The reaction was stirred at room temperature overnight under argon and was concentrated *in vacuo* and purified by a very long column using hexanes as the eluent and then 1% EtOAc/Hex and slowly increasing to 5% EtOAc/Hex to afford 9-triptycenesulfenic acid as a white powder (243 mg, 55%) ¹H NMR (400 MHz, CDCl₃) δ ppm 3.09 (br s, 1H), 5.42 (s, 1H), 7.03-7.08 (m, 6H), 7.42-7.48 (m, 6H). The spectral characteristics are in good agreement with those presented in the literature.¹¹

9-Triptycenesulfonic acid. *N.B.* Reaction carried out by undergraduate student Jazmin Bansagi by the following procedure: To a solution of 9-triptycenesulfenic acid (40 mg, 0.1323 mmol) in methanol (2.5 mL, 0.053 M) was added hydrogen peroxide as a 30% solution in water (15 ul, 0.1323 mmol). The reaction mixture was stirred at room temperature for 3 days and concentrated *in vacuo* to yield 9-triptycenesulfonic acid as a white solid (30 mg, 68%). ¹H NMR (400 MHz, *d*₃-MeOH) δ ppm 5.40 (s, 1H), 7.02-7.05 (m, 6H), 7.38-7.40 (m, 3H), 8.24-8.26 (m, 3H) ¹³C NMR (100 MHz, *d*₃-MeOH) δ ppm 55.7, 68.8, 123.8, 125.5, 126.2, 126.5, 143.9, 148.0 HRMS (ESI⁻) calculated (M) 334.39, observed (M²⁻) 333.92.

Basic methanol buffers. Buffer solutions were prepared by addition of amine base [Et₃N (28 μL, 0.20 mmol) or TMP (34 μL, 0.20 mmol)] in methanol (10 mL, 0.02 M) and the pH adjusted with trifluoromethanesulfonic acid to the desired ^s_wpH, as read on the meter, and converted by addition of 2.24 pH units to the desired ^s_spH in methanol. Triethylamine: ^s_spH = 10.10-11.3, TMP: ^s_spH = 12.00-12.10.¹⁷

Thiol oxidation reactions in amine buffers. A stock solution of TrpSH (2.0 mM) was prepared in methanol buffer. Hydrogen peroxide (3.6 μ L, 0.04 mmol) was added to a solution of TrpSH (1.0 mL of the stock solution, 0.02 mmol) in methanol buffer (9 mL, 0.2 mM). Samples of the reaction were analyzed by HPLC (4% *i*-PrOH/ hexanes mobile phase, with a flow rate of 1.0 mL/min, Sun-Fire Silica, 5 μ m 4.6 x 150 mm column) with UV detection at 225 nm.

Thiol oxidations with peroxy carbonate. A stock solution of TrpSH (1.0 mM) was prepared in methanol. Potassium carbonate (3.3 mg, 0.02 mmol) and H₂O₂ (2.0 μ L, 0.02 mmol) were added to a solution of TrpSH (2.0 mL of the stock solution, 0.002 mmol) in methanol buffer (8 mL, 0.2 mM). Samples for analysis were made up of aliquots (100 μ L) of the reaction, 890 μ L MeOH and 10 μ L phenol stock solution (1.2 mM). Samples were analyzed by HPLC (4% *i*-PrOH/ hexanes mobile phase, with a flow rate of 1.0 mL/min, Sun-Fire Silica, 5 μ m 4.6 x 150 mm column) with UV detection at 225 nm or by UPLC (20% H₂O/MeOH mobile phase, flow rate 0.2 mL/min, Acquity C₁₈ 1.7 μ m 2.1 x 50 mm column) with MS detection (ESI⁻) at *m/z* of 285, 301, 317 and 333.

4.5 References

¹ Negre-Salavayre, A.; Auge, N.; Alaya, V.; Basaga, H.; Boada, J.; Brenke, R.; Capple, S.; Cohen, G.; Feher, J.; Grune, T.; Lengyel, G.; Mann, G.E.; Pamplona, R.; Poli, G.; Portero-

- Otin, M.; Riah, Y.; Salavayre, R.; Sasson, S.; Serrano, J.; Shamn, O.; Siems, W.; Siow, R.C.M.; Wiswedel, I.; Zarkovic, K.; Zarkovic, N. *Free Rad. Res.*, **2010**, 44, 1125-1171.
- ² Rhee, S.G., *Science*, **2006**, 312, 1882-1883.
- ³ Paulsen, C.E.; Carroll, K.S., *ACS Chem. Biol.*, **2010**, 5, 47-62.
- ⁴ Wood, Z.A.; Poole, L.B.; Karplus, P.A. *Science*, **2003**, 300, 650-653.
- ⁵ Paulsen, C. E.; Carroll, K.S., *ACS Chem. Biol.*, **2010**, 5, 1, 47-62.
- ⁶ Seo, Y.H.; Carroll, K.S., *Proc. Natl. Acad. Sci USA*, **2009**, 61, 16163-16168.
- ⁷ Luo, D.; Smith, S.W.; Anderson, B.D. *J. Pharm. Sci.* **2005**, 93, 304-316.
- ⁸ Regino, C.A.S.; Richardson, D.E., *Inorg. Chim. Acta*, **2007**, 360, 3971-3977.
- ⁹ Winterbourn, C.C., Metodiewa, D. *Free Radic. Biol. Med.*, **1999**, 27, 322-328.
- ¹⁰ Nagy, P.; Lemma, K.; Ashby, M.T. *J. Org. Chem.*, **2007**, 72, 8838-8846.
- ¹¹ McGrath, A.J.; Garrett, G.E.; Valgimigli, L.; Pratt, D.A. *J. Am. Chem. Soc.* **2010**, 132, 16759-16761.
- ¹² Honda, M.; Tajima, M, *J. Mol. Struct.*, **1986**, 136, 93-98.
- ¹³ Hiatt, R.; Smythe, R. J.; McColeman, C. *Can. J. Chem.*, **1971**, 49, 1707-1711.
- ¹⁴ Barton, J.P.; Packer, J.E.; Sims, R.J. *J. Chem. Soc. Perkin II*, **1973**, 1547-1549.
- ¹⁵ De Ligny, C.L.; Rehbach, M. *Rec. Trav. Chim. Pays-Bas*, **1960**, 79, 727-730.
- ¹⁶ Inczédy, J.; Lengyel. T.; Ure, A.M. *Compendium of Analytical Nomenclature. Definitive Rules* 1997 3rd ed; Blackwell: Oxford, UK, 1998.
- ¹⁷ Mohamed, M.F.; Sánchez-Lombardo, I.; Neverov, A.A.; Brown, R.S., *Org. Biomol. Chem.*, **2012**, 10, 631-639.
- ¹⁸ Flangan, J.; Jones, D.P.; Griffith, W.P.; Skapski, A.C.; West, A.P., *J. Chem. Soc., Chem. Commun.*, **1986**, 20-21.